Cooperative Communication Systems Using Distributed Convolutional-Based Coding

Mohamed Mustafa Mohamed Elfituri

- Distributed space-time coding
- Decode-and-forward
- Amplify-and-forward
- Channel estimation
- Relay channels

Cooperative Communication Systems Using Distributed Convolutional–Based Coding

Mohamed Mustafa Mohamed Elfituri

To My Parents

for Their Love and Patience

Acknowledgments

Numerous people supported and helped me during the development of my book. A few words mention here cannot adequately capture all my appreciation.

First and foremost, I would like to dedicate this book to my parents, who, from the day I came to the world, have provided me tremendous support and constant encouragement. Their love and support are always the greatest inspiration to me, and without these, it would not have been possible for me to complete this work.

I would like also to thank my wife and my kids for their love, encouragement, and care during my difficult time.

Finally, I would like to thank all my friends who encouraged me throughout my work in College of Electrical and Electronics Technology.

Introduction

Whenever size, power, or other constraints preclude the use of multiple-input multiple-output (MIMO) systems, wireless systems cannot benefit from the well-known advantages of space-time coding (STC) methods. Also the complexity (multiple radio-frequency (RF) front ends at both the transmitter and the receiver), channel estimation, and spatial correlation in centralized MIMO systems degrade the performance. In situations like these, the alternative would be to resort to cooperative communications via multiple relay nodes. When these nodes work cooperatively, they form a virtual MIMO system. The destination receives multiple versions of the same message from the source and one or more relays, and combines these to create diversity. There are two main cooperative diversity techniques for transmission between a pair of nodes through a multiple relay nodes: decode-and-forward (DF) and amplify-and-forward (AF) modes. In the DF mode, the signal received from the source node is demodulated and decoded before retransmission. In the AF mode, the relay node simply amplifies and retransmits the signal received from the source node. No demodulation or decoding of the received signal is performed in this case.

In uncoded cooperative communication networks, the diversity of the system degrades significantly. This diversity degradation is attributed to the errors made at the relay nodes. Consequently, if better reliability is achieved at the relay nodes, the diversity may improve, or even may be preserved, as compared to the error-free case.

In this book, we present a coding scheme suitable for cooperative networks where the source and relays share their antennas to create a virtual transmit array to transmit towards their destination. We focus on the problem of coding for the relay channels. While the relays may use several forwarding strategies, including

AF and DF, we focus on coded DF relaying. We derive upper bounded expressions for the bit error rate (BER) assuming M−ary phase shift keying (M−PSK) transmission and show that the proposed scheme achieves large coding gains and full diversity relative to the coded non-cooperative case for a wide range of signal-to-noise ratio (SNR) of interest.

To improve the detection reliability further, we consider antenna/relay selection on the performance of cooperative networks in conjunction with the distributed coding scheme proposed. For simplicity, we assume that there is one relay that is equipped with n_R antennas and only the best antenna is selected. For this scenario, assuming DF and AF relaying, we derive upper bounds on the BER for M−PSK transmission. Our analytical results show that the proposed scheme achieves full diversity for the entire range of BER of interest, unlike the case without antenna selection.

In the last part of the book, we consider the same system considered in the ideal case but now with system imperfections. In particular, we consider the case when the channel state information is estimated at all nodes involved in the transmission process. We derive upper bounds on the performance with imperfect channel estimation. Our results show that there is performance degradation due to the presence of channel estimation error. However, the observations made in the case of ideal channel state information still hold for the non-ideal case.

In Chapter I, we introduce the definition of wireless systems, fading, and diversity.

Chapter II presents some background material and a review of previous work in cooperative communication. First, we begin with a brief description on the uncoded DF and AF single-relay channels and introduce three different time-division multiple-access (TDMA)-based protocols, as well as the corresponding channel and signal models. We also review several important coded

cooperation schemes, and previous works which lead to the development of the new scheme. Later, we present simulation results for these three protocols and coded cooperation using binary phase shift keying (BPSK) transmission. Finally, we present a review of existing works in antenna selection and channel estimation.

In Chapter III, we introduce the proposed distributed coded cooperation scheme for relay channels. Assuming M -PSK transmission, we analyze the performance of the proposed distributed coded cooperation scheme and show that it achieves large coding gains and full diversity relative to the coded non-cooperative case. Also, we investigate the outage probability of the achievable rate of the DF relay channels in a Rayleigh fading environment. Finally, we derive expressions for the BER upper bound and the outage probability in the case of error-free and erroneous relaying.

Chapter IV considers antenna/relay selection in conjunction with the distributed coding scheme introduced in Chapter III in an effort to improve the detection reliability at the relay nodes. We show that performing antenna selection preserves the diversity order of the system for a wider range of SNR, which translates to significant coding gains over systems without antenna selection. Our analytical results show that the proposed scheme achieves full diversity for the entire range of bit error rate of interest, unlike the case without antenna selection.

In Chapter V, we study a channel estimation strategy for the distributed coding scheme, described in Chapter III. We also use Alamouti scheme for the distributed space-time coding cooperation in the second frame. Finally, we derived expressions for the BER upper bound in the case of error-free and erroneous relaying with imperfect channel estimation.

Contents

Contents

1

Wireless Systems

The increasing demand for high data rates in wireless communications due to emerging new technologies makes wireless communications an exciting and challenging field. The spectrum or bandwidth available to the service provider is often limited and the allotment of new spectrum by the federal government is often slow in coming. Also, the power requirements are that devices should use as little power as possible to conserve battery life and keep the products small. Thus, the designers for wireless systems face a two-part challenge, increase data rates and improve performance while incurring little or no increase in bandwidth or power. The wireless channel is by its nature random and unpredictable, and in general error rates are poorer over a wireless channel than over a wired channel.

1.1 Wireless Channel

The wireless channel contains objects and particles which scatter the transmitted signal. These scattered signals take different paths with different path lengths and thus arrive at the receiver out of phase and create interference. These scatters introduce a variety of impairments in the wireless channel such as fading, delay spread and attenuation. This results in severe attenuation of the signal, referred to as deep fade. This instantaneous decrease of the signal-to-noise ratio (SNR) results in error bursts which significantly degrade the performance.

1.2 Fading

Fading can be classified as long term fading and short term fading. Long term fading is due to shadowing and the relative distance between the source and destination. It is also referred to as path loss. Short term fading is due to the multipath propagation of the transmitted signal due to reflections from various objects. When the delay differences between the multipath components are small

as compared to the symbol interval, these components can add constructively or destructively at the receiver depending upon the carrier frequency and delay differences. Multipath fading can be controlled by techniques like diversity and channel coding.

1.3 Channel Coding

Channel coding is a technique to overcome transmission errors over a noisy channel. Here redundancy is introduced at the transmitter and utilized at the receiver for error correction. Channel coding is effective in correcting independent random symbols. However when the fading is correlated, channel coding is not an effective technique, in this scenario interleaving is used. In this method, at the transmitter, the coded signals are first interleaved to reduce the effect of correlation. Interleaving is effective in combating the correlated fading at the cost of increased delay and extra hardware.

1.4 Diversity

Diversity is one of the techniques to combat channel fading [1]-[4]. Diversity makes use of more than one independently faded version of the transmitted signal to improve the overall reception. This is because if several copies of the original signal are sent through different paths, they encounter different channel characteristic and therefore the probability that all the paths will experience deep fading at the same instant is greatly reduced. Diversity can be achieved using the following technique:

Frequency diversity: Here the message is transmitted simultaneously over several frequency slots. This form of diversity is effective when the transmission bandwidth is large enough such that different sub-bands will experience different

amounts of fading.

Temporal Diversity: Here the message is transmitted over several time slots. This form of diversity is effective when the fading is time selective. The time slots must be separated such that the channel fading experienced by each transmission is independent of the channel fading experienced by other transmissions. Therefore this form of diversity introduces a significant delay in processing. Temporal diversity can be achieved through techniques like interleaving, forward error correction and automatic repeat request (ARQ) protocols.

Spatial diversity: Here the message is transmitted using multiple transmitting and/or receiving antennas. The requirement for using spatial diversity is that the separation between adjacent antennas should be large enough that signals from different antennas undergo independent fading.

1.5 Multiple-Input Multiple-Output (MIMO)

In most wireless systems, antenna diversity is a practical, effective, and hence, a widely applied diversity technique [5]. It is shown in [6], [7] that a system with multiple antennas on both ends of the communication link (referred to as multiple-input multiple-output (MIMO)) improves the received signal reliability through diversity [8]-[10]. In these systems, each pair of transmitter and receiver antennas provides an independent path from the transmitter to the receiver. By proper encoding, multiple independent faded replicas of a signal are obtained at the receiver side, hence, creating spatial diversity. Furthermore, it is possible to have much higher spectral efficiency in MIMO systems compared to single-input single-output (SISO) systems through spatial multiplexing.

A typical MIMO system is depicted in Figure 1.1. As shown in the figure, the transmitter is equipped with M transmit antennas and the receiver is equipped

with N receive antennas. The channel between the mth transmit antenna and the nth receive antenna can be represented by the random propagation coefficient h_{mn}. To send information to the receiver, at every transmission time, the transmitter feeds signals s_1, s_2, ..., s_M to its M antennas respectively. The antennas then send the signals simultaneously to the receiver. Every receive antenna obtains a signal that is a superposition of the signals from every transmit antenna sent through the fading channels.
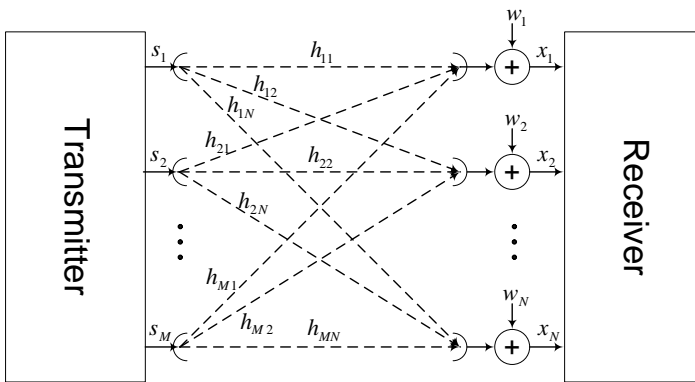
Figure 1.1   Centralized MIMO system.

Information theoretic investigations over the past decade have shown that very high capacity can be obtained by employing multiple antenna elements at both the transmitter and the receiver of a wireless system [6], [8]. These investigations have led to the development of a novel multiple transmit-receive architecture called bell labs layered space-time architecture (BLAST) [6]. Using BLAST, it was shown that rates close to the channel capacity can be attained. Another approach that uses multiple transmit antennas and (optionally) multiple receive antennas is space-time coding (STC), which was introduced in [1], [9], [11], [12] to provide reliable communications over fading channels. This concept of STC combines coding, modulation, and spatial diversity into a two-dimensional coded modulation technique. Examples of STCs include space-time block codes (STBC)

[11], and space-time trellis codes (STTC) [12]. STTCs are known to provide full diversity and coding gain at the cost of a complex receiver. On the other hand, STBCs offer only diversity gain (compared to single-antenna schemes) and not coding gain. The design of STBCs is based on the so-called diversity criterion derived by Tarokh et al. in their earlier paper on STTCs.

The down side of MIMO technology, however, is the associated complexity. For instance, for every antenna employed, it is required to employ a radio frequency (RF) chain, which is bulky and costly. Also, the power consumption is relatively high due to the complex circuitry. In addition, the overhead required for training can be significant especially when the underlying channel changes relatively fast. In light of these constraints, MIMO technology is deemed not practical for certain applications where power consumption and/or physical size are an issue. Such applications include cellular networks where it is not practical to mount multiple antennas along with their associated circuitry on a small mobile phone while keeping its size small and its cost affordable. Another example is wireless sensor networks, where the nodes are battery-operated and thus prolonging the battery life as much as possible is a crucial requirement.

As an alternative to using collocated antennas as in MIMO systems, one can achieve the same spatial diversity gain through cooperative diversity [13]-[17]. In cooperative communications, multiple nodes in a wireless network cooperate among themselves to form a virtual antenna array. Using cooperation, it is possible to exploit the spatial diversity of the traditional MIMO techniques without each node necessarily having multiple antennas. The destination receives multiple versions of the message from the source and one or more relays and combines these to obtain a more reliable estimate of the transmitted signal. These cooperative techniques utilize the broadcast nature of wireless signals by observing that a source signal intended for a particular destination can be

overheard at neighboring nodes. These nodes, called relays, partners, or helpers process the signals they overhear and transmit towards the destination. At any given time, any node can be a source, relay, or destination. The function of the relay node is to assist in the transmission of the source information to the destination node.

Owing to its significant advantages, cooperative communications has recently emerged as a strong candidate for the underlying technology for most future wire- less applications, including 4G cellular networks, wireless sensor networks (IEEE 802.15.4), and fixed broadband wireless systems (WiMax, IEEE 802.16j). Among these advantages are 1) the great flexibility in the network configurations whereby the number of cooperating nodes can be changed according to a specified system performance criterion; 2) the relaying strategy can be adapted to fit various scenarios; 3) adaptive modulation and coding can be employed to achieve certain performance objectives; 4) the coverage is expected to be better since users will always find relaying nodes close by even if they are at the far end of their cell; and 5) a consequence of this is an increased user capacity since the user transmitted power can be better controlled which in turn controls the level of multiple access interference at the access point. In Figure 1.2, we depict an example of a virtual MIMO system where there is one source, L relays, and one destination node. The fading coefficients are denoted by h_{SD}, h_{SR_m} and $h_{R_m D}$ $m=1, 2, ..., L$. Other forms of virtual MIMO systems are also possible, including those that have multi-hop stages.

With all these great advantages of cooperative communications, there are challenges that must be tackled for such technology to be brought to a successful deployment, including the sensitivity of the overall performance to the detection reliability at the relays, and determining the relaying framework that would yield

the best performance. In terms of the end-to-end performance of cooperative communication networks, it has been demonstrated that it significantly depends on the detection reliability at the relay nodes [15]-[17]. In the ideal situation where detection at the relays is perfect, the diversity of the system is maintained, that is, as if the relay node is collocated with the transmitting source node [15]-[17]. However, with imperfect detection, the diversity degrades. The severity of this degradation depends on the detection reliability level at the relay nodes. From what we have seen, the diversity starts degrading when the source-relay link is worse in terms of reliability than the source-destination link and/or the relay-destination link. One immediate solution that comes to mind to improve the detection reliability at the relay nodes is to use coding in conjunction with decode-and-forward (DF) relaying. This has been investigated before but in a different context. In particular, all coded cooperation schemes have assumed ideal detection at the relay nodes, which is idealistic. This motivates us to develop coded cooperation schemes under practical situations. In particular, we will develop efficient ways of achieving useful cooperation while reducing the impact of error propagation.
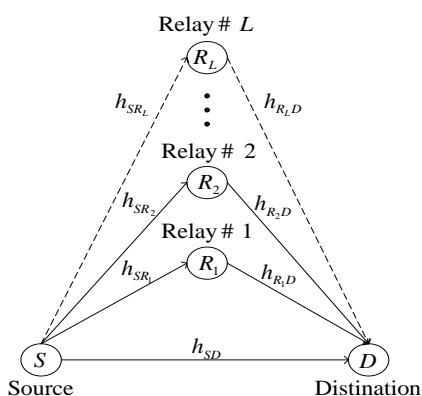
Figure 1.2 *Distributed MIMO system using relay nodes.*

Multiple antennas are considered at the relay and destination nodes are

considered in [18]-[20]. In [18] a system with five-node network with two sources, two relays and one common destination is considered. The source and relay nodes are equipped with a single antenna while the destination node is equipped with multiple antennas. Also, perfect source-relay channels are assumed in [18]. Also in [19], a two-hop system is investigated with one source, one destination and multiple relays with multiple antennas. Threshold-based MRC and threshold-based selection combining (SC) of this multiple antenna system are studied in [19]. In [20], the authors considered cooperative relaying system with multiple sources, one relay and one destination. The relay and destination nodes are equipped with multiple antennas while the source is equipped with a single antenna.

2

Cooperative Systems

This chapter summarizes recent works that relate to the problems studied in this book. Our objective is to make the reader aware of the many considerations involved, highlight the particular scenarios that we study throughout the book, and encourage further work in the area.

2.1 Relaying Protocols

In cooperative diversity, nodes can cooperate with each other to provide spatial diversity gain at the destination. In this case, at any given time, any node can be a source, relay, or destination. The function of the relay node is to assist in the transmission of the source information to the destination node. To ensure diversity gains, this relay is chosen in such a way that its link to the destination is independent from that of the source. Within the framework of cooperative diversity, there are two main cooperative diversity techniques for transmission between a pair of nodes through a multiple relay nodes: AF [21] and DF [15], [12] modes. In the AF mode, the relay terminal simply amplifies and retransmits the signal received from the source terminal (the signal received at the relay terminal is corrupted by fading and additive noise). No demodulation or decoding of the received signal is performed in this case. On the other hand, in the DF mode, the signal received from the source node is demodulated and decoded before retransmission.

Most of the previous research on un-coded cooperative diversity adopts AF protocols [23]-[29]. However, for AF, when the instantaneous channel state information (CSI) is not available to the receivers, satisfying the relay power constraints greatly complicates the demodulation as well as analysis [24]. Obviously, the DF protocols require more processing than AF, as the signals have to be decoded and then re-encoded at the relay transmission. However, if signals

are correctly decoded at relays, performances are better than those of AF protocols, as noise is deleted. In addition, the DF can be extended to combine coding techniques and might be easier to incorporate into network protocols [26]-[29].

Relay channels are central to our study of cooperative diversity. Many of the initial works performed in this area have focused on additive white Gaussian noise (AWGN) channels, and examined the performance in terms of the well-known Shannon capacity [30]. The classical relay channel models a class of three terminal communication channels, originally introduced and examined in [31], [32], and subsequently studied by a number of authors, primarily from the information theory community. In general, the distinctive property of relay channels is that certain terminals, i.e., relay nodes, receive, process, and re-transmit some information bearing signal of interest to a certain destination in order to improve the performance of the system.

Cover and El Gamal [33] examined certain non-faded relay channels, and developed lower and upper bounds on the channel capacity via random coding. Generally these lower and upper bounds do not coincide, except in the class of degraded relay channels [33]. These lower bounds on capacity, i.e., achievable rates, are obtained via three structurally different random coding schemes, referred to in [33] as facilitation, cooperation, and observation.

Many configurations arise for cooperative diversity in wireless settings. In what follows, we denote the source, relay, destination nodes by $S, R,$ and D, respectively. Figure 2.1 depicts a number of these configurations. For example, the classical relay channel in Figure 2.1(a) reduces to direct transmission when the relay is removed, and cascade transmission when the destination cannot receive (or ignores) the source transmission. Figure 2.1(b) represents the parallel relay channel without direct transmission. The configurations in Figure 2.1(c)-(e)

represent a classical multiple-access channel, broadcast channel, and interference channel, respectively.
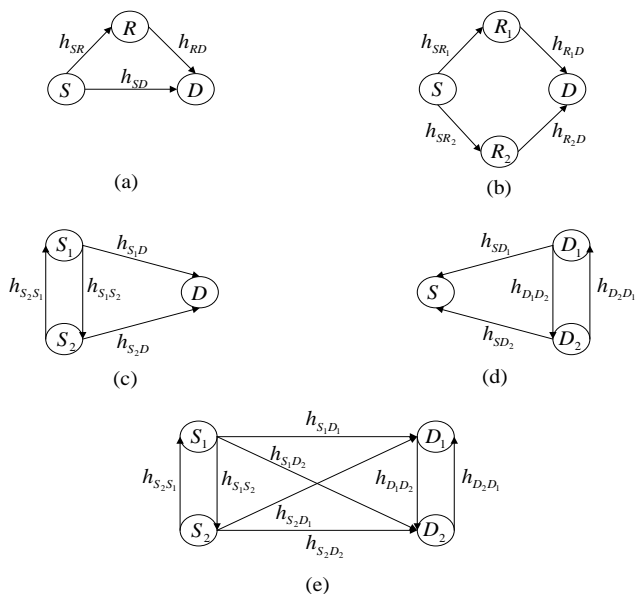
Figure 2.1 *Various relaying configurations that arise in wireless networks: Classical relay channel, (b) parallel relay channel, (c) multiple-access channel with relaying, (d) broadcast channel with relaying, (e) interference channel with relaying.*

Of the remaining configurations depicted in Figure 2.1, only parallel relay channels (see Figure 2.1(b)) and multiple-access channels with relaying (see Figure 2.1(c)) have received attention in the literature. Schein and Gallager [34] introduced the parallel relay channel model in an attempt to make the classical relay channel symmetric.

Most of the work that has been done in the area of cooperative networks considered three main types of TDMA-based transmission protocols. These protocols are termed Protocols I, II and III and they were proposed in [15]-[17], respectively. Protocols I, II and III convert the spatially distributed antenna system into effective MIMO, single-input multiple-output (SIMO) and

multiple-input single-output (MISO), respectively. We should mention that Protocol II has been the most popular due to its simplicity and performance. All of the previous works assume that transmission takes place in a half-duplex fashion (the nodes cannot transmit and receive simultaneously) in all relays over two separate time slots. Since our work will use these transmission protocols, in the following, we shall briefly describe the details of these three protocols in the un-coded DF and AF modes.

2.1.1 System Model

Protocol I. In the AF mode, the source node transmits the signal to both the destination and relay nodes during the first time slot (see Figure 2.2(a)). The signals received at the destination and the relay nodes in the first time slot are given by

$$y_{SD}(t_1) = \sqrt{E_{SD}}\, h_{SD} s_1 + n_{SD}(t_1), \tag{2.1}$$

$$y_{SR}(t_1) = \sqrt{E_{SR}}\, h_{SR} s_1 + n_{SR}(t_1), \tag{2.2}$$

where s_1 is the symbol transmitted in the first time slot t_1; E_{SD}, and E_{SR} represent the transmitted signal energy for the corresponding link; h_{SD}, and h_{SR} are the complex fading channel coefficients with unit-power gain; $n_{SD}(t)$, and $n_{SR}(t)$ are AWGN samples with zero mean and variance $N_0/2$ per dimension.
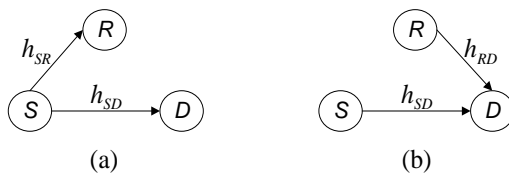

Figure 2.2   Protocol I: (a) the first time slot, (b) the second time slot.

In the second time slot, both the relay, and the source nodes transmit the signal

to the destination node (see Figure 2.2 (b)). The signals received at the destination in the second time slot are then given by

$$y_{SD}(t_2) = \sqrt{E_{SD}} h_{SD} s_2 + n_{SD}(t_2), \tag{2.3}$$

$$y_{RD}(t_2) = h_{RD} A_{RD} y_{SR}(t_1) + n_{RD}(t_2),$$

$$= h_{RD} A_{RD} \left(\sqrt{E_{SR}} h_{SR} s_1 + n_{SR}(t_1) \right) + n_{RD}(t_2), \tag{2.4}$$

where s_2 is the symbol transmitted in the second time slot t_2; h_{RD} is the complex fading channel coefficient with unit-power gain; $n_{RD}(t_2)$ is AWGN samples with zero mean and variance $N_0/2$ per dimension; A_{RD} is the amplification factor at the relay node. One choice for the amplification gain was given in [25] to be

$$A_{RD}^2 = \frac{E_{RD}}{E_{SR} |h_{SR}|^2 + \frac{N_0}{2}}, \tag{2.5}$$

where E_{RD} is the transmitted signal energy from the relay node. One can rewrite (2.4) as

$$y_{RD}(t_2) = h_{RD} A_{RD} \sqrt{E_{SR}} h_{SR} s_1 + n_{SRD}, \tag{2.6}$$

where $n_{SRD} = h_{RD} A_{RD} n_{SR}(t_1) + n_{RD}(t_2)$. The signals received at the destination node over two time slots are then given by

$$y_{D_1} = y_{SD}(t_1) = \sqrt{E_{SD}} h_{SD} s_1 + n_{SD}(t_1), \tag{2.7}$$

$$y_{D_2} = y_{SD}(t_2) + y_{RD}(t_2) = \sqrt{E_{SD}} h_{SD} s_2 + n_{SD}(t_2) + h_{RD} A_{RD} y_{SR}(t_1) + n_{RD}(t_2)$$

$$= \sqrt{E_{SD}} h_{SD} s_2 + n_{SD}(t_2) + h_{RD} A_{RD} \left(\sqrt{E_{SR}} h_{SR} s_1 + n_{SR}(t_1) \right) + n_{RD}(t_2)$$

$$= h_{RD} A_{RD} \sqrt{E_{SR}} h_{SR} s_1 + \sqrt{E_{SD}} h_{SD} s_2 + n_D, \tag{2.8}$$

where $n_D = n_{SD}(t_2) + h_{RD} A_{RD} n_{SR}(t_1) + n_{RD}(t_2)$. Protocol I in the AF mode can now be summarized as

$$Y_{P_{I-AF}} = H_{P_{I-AF}} S + N_{P_{I-AF}}, \tag{2.9}$$

where $Y_{P_{I-AF}} = [y_{D_1} \quad y_{D_2}]^T$ is the received signal vector; the superscript $(\cdot)^T$ stands for transpose; $N_{P_{I-AF}} = [n_{SD}(t_1) \quad n_D]^T$ is the noise vector; $S = [s_1 \quad s_2]^T$ is transmitted signal vector; $H_{P_{I-AF}}$ is the complex fading channel matrix given by

$$H_{P_{I-AF}} = \begin{bmatrix} \sqrt{E_{SD}}h_{SD} & 0 \\ h_{RD}A_{RD}\sqrt{E_{SR}}h_{SR} & \sqrt{E_{SD}}h_{SD} \end{bmatrix}. \tag{2.10}$$

In the DF mode, the source node transmits the signals to both the destination and the relay nodes during the first time slot. The signals received at the destination node and the relay nodes in the first time slot are given by (2.1) and (2.2), respectively. Different from the AF mode, in the DF mode, the relay node demodulates and decodes the received signal during the first time slot. Assuming that the signal is decoded correctly and retransmitted, we obtain

$$y_{RD}(t_2) = \sqrt{E_{RD}}h_{RD}s_1 + n_{RD}(t_2). \tag{2.11}$$

Similar to the AF mode, Protocol I in the DF mode can now be summarized as

$$Y_{P_{I-DF}} = H_{P_{I-DF}}S + N_{P_{I-DF}}, \tag{2.12}$$

where $Y_{P_{I-DF}} = [y_{D_1} \quad y_{D_2}]^T$ is the received signal vector; $N_{P_{I-DF}} = [n_{SD}(t_1) \quad (n_{SD}(t_2) + n_{RD}(t_2))]^T$ is the noise vector; $S = [s_1 \quad s_2]^T$ is transmitted signal vector; $H_{P_{I-DF}}$ is the complex fading channel matrix given by

$$H_{P_{I-DF}} = \begin{bmatrix} \sqrt{E_{SD}}h_{SD} & 0 \\ \sqrt{E_{RD}}h_{RD} & \sqrt{E_{SD}}h_{SD} \end{bmatrix}. \tag{2.13}$$

The spectral efficiency of Protocol I is given by

$$\text{H} = \frac{R_b}{B} = \frac{R_s k \log_2 M}{R_s p} = \frac{k \log_2 M}{p} = \frac{2 \log_2 M}{2} = \log_2 M \ \text{ bits/s/Hz} \tag{2.14}$$

where k is the number of symbols of the source node, p is the number of

transmission periods to transmit symbols, R_b is the bit rate, R_S is the symbol rate, M is the constellation size, and B is the bandwidth.

Protocol II. In this protocol, in the first time slot, the source node sends a message to both the relay and the destination nodes (see Figure 2.3(a)). In the second time slot, the relay node sends to the destination node (see Figure 2.3(b)).

In the AF mode, the received signal at the destination node for Protocol II can be written as

$$Y_{P_{II-AF}} = H_{P_{II-AF}} s_1 + N_{P_{II-AF}}, \qquad (2.15)$$

where $Y_{P_{II-AF}} = [y_{D_1} \quad y_{D_2}]^T$ is the received signal vector; $N_{P_{II-AF}} = [n_{SD}(t_1) \quad (n_D - n_{SD}(t_2))]^T$ is the effective noise vector; s_1 is transmitted signal; $H_{P_{II-AF}}$ is the first column of $H_{P_{I-AF}}$ in (2.10).

Figure 2.3 *Protocol II: (a) the first time slot, (b) the second time slot.*

In the DF mode, the received signal at the destination node for Protocol II can be rewritten from (2.12) as

$$Y_{P_{II-DF}} = H_{P_{II-DF}} s_1 + N_{P_{II-DF}}, \qquad (2.16)$$

where $Y_{P_{II-DF}} = [y_{D_1} \quad y_{D_2}]^T$ is the received signal vector; $N_{P_{II-DF}} = [n_{SD}(t_1) \quad n_{RD}(t_2)]^T$ is the effective noise vector; $H_{P_{II-DF}}$ is the first column of $H_{P_{I-DF}}$ in (2.13).

The spectral efficiency of Protocol I is given by

$$\text{H} = \frac{R_b}{B} = \frac{R_s k \log_2 M}{R_s p} = \frac{k \log_2 M}{p} = \frac{\log_2 M}{2} \text{ bits/s/Hz} \qquad (2.17)$$

Protocol III. The source node in this protocol sends a message to the relay node in the first time slot (see Figure 2.4(a)). Both the source and the relay nodes send to the destination node in the second time slot (see Figure 2.4(b)).
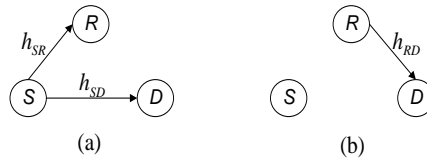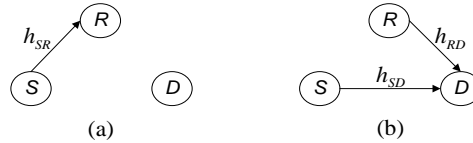

Figure 2.4 *Protocol III: (a) the first time slot, (b) the second time slot.*

In the AF mode, the received signal at the destination node for Protocol III can be written as

$$y_{P_{III-AF}} = H_{P_{III-AF}} S + n_{P_{III-AF}}, \qquad (2.18)$$

Where $y_{P_{III-AF}}$ is the received signal; $n_{P_{III-AF}} = n_D$ is the effective noise; $S = [s_1 \quad s_2]^T$ is transmitted signal vector; $H_{P_{III-AF}}$ is the second row of $H_{P_{I-AF}}$ in (2.10).

In the DF mode, the received signal at the destination node for Protocol III can be rewritten from (2.12) as

$$y_{P_{III-DF}} = H_{P_{III-DF}} S + n_{P_{III-DF}}, \qquad (2.19)$$

where $y_{P_{III-DF}}$ is the received signal; $n_{P_{III-DF}} = n_{SD}(t_2) + n_{RD}(t_2)$ is the effective noise; $S = [s_1 \quad s_2]^T$ is transmitted signal vector; $H_{P_{III-DF}}$ is the second row of $H_{P_{I-DF}}$ in (2.13).

The spectral efficiency of Protocol III is given by

$$\text{H} = \frac{R_b}{B} = \frac{R_s k \log_2 M}{R_s p} = \frac{k \log_2 M}{p} = \frac{2 \log_2 M}{2} = \log_2 M \text{ bits/s/Hz} \qquad (2.20)$$

2.1.2 Simulation Results

Here, we present simulation results for Protocols I, II, and III using BPSK transmission. In all scenarios we assume that there is one relay node. In all of these results, the transmission links (source to relay, source to destination, and relay to destination) are modeled as a quasi-static flat fading channels where the fading coefficients are fixed within a frame and change independently from one frame to another, the receiver has perfect knowledge of the channel coefficients, and the transmitted frame size is equal to 130 symbols. Also we consider equal transmitted energies for the different links, i.e., $E_{SD}=E_{SR}=E_{RD}=E_b$.

Figure 2.5 shows the BER comparisons for Protocols I, II, and III, all operating in the DF mode with error-free recovery at the relay. This assumption, however, seems to be too optimistic and can only be justified under special conditions (i.e., large SNR or un-faded channel between the source and relay). For Figure 2.5, we can see that at the BER of 5×10^{-4}, Protocol II is better by about 11 dB and 14 dB than Protocol I and III, respectively. Also we note that Protocol II achieves full diversity, which is two in this case, while Protocols I and III do not achieve full diversity.

Figure 2.6 shows BER comparisons for Protocols I, II, and III, all operating in the DF mode, considering the effect of channel errors at the relay. From this figure, it can be observed that at the BER of 5×10^{-4}, Protocol II gains about 2 dB and 5 dB relative to Protocol I and III, respectively. Also we note that Protocols I, II, and III do not achieve full diversity.

In Figure 2.7 we perform BER comparisons for Protocols I, II, and III, all operating in the AF mode. From this figure, Protocol II at the BER of 5×10^{-4} is superior by about 9 dB and 14 dB to Protocols I and III, respectively. Also, we

note that Protocol II achieves full diversity, which is two in this case, while Protocols I and III do not achieve full diversity.
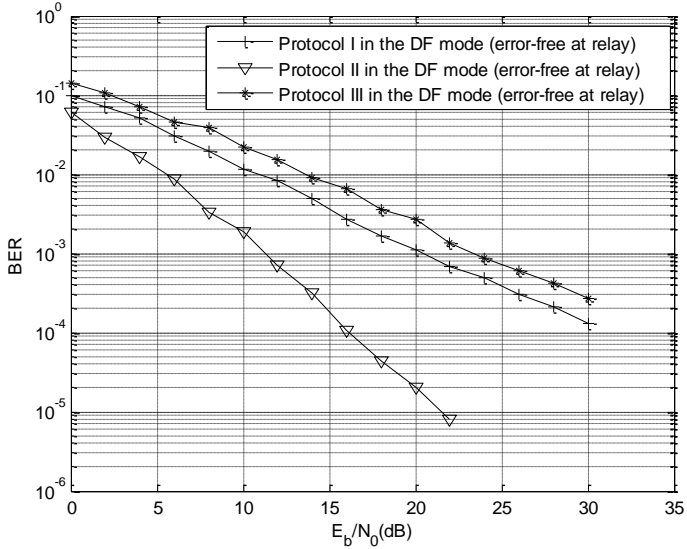
Figure 2.5   *BER comparisons for Protocols I, II, and III in the DF mode (error-free at relay).*
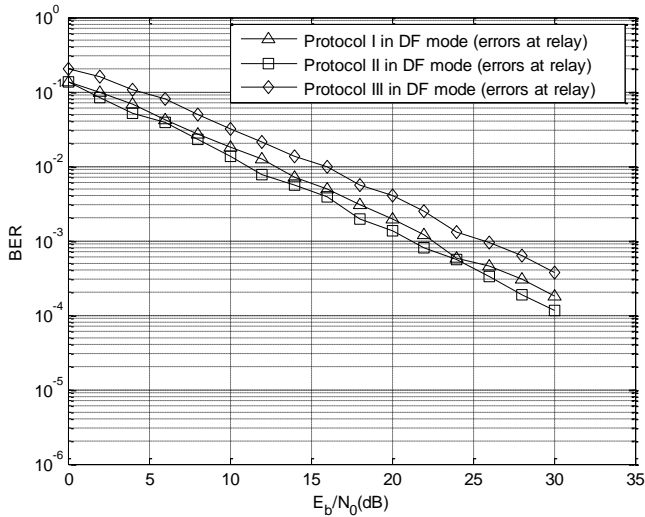
Figure 2.6   *BER comparisons for Protocols I, II, and III in the DF mode (errors at relay).*
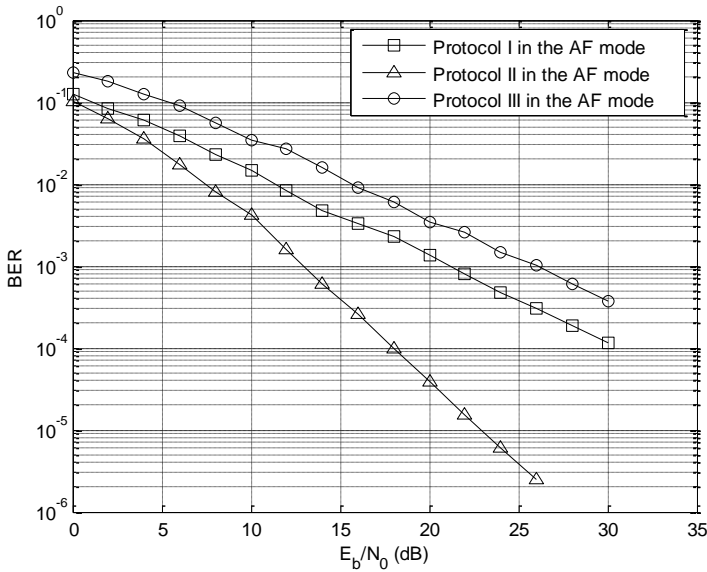
Figure 2.7 *BER comparisons for Protocols I, II, and III in the AF mode.*

2.2 Coded Cooperation

In the previous section, we have seen that the performance of un-coded multi-relay systems when the nodes operate in the DF mode degrades. This was shown via simulations. Based on the results we have obtained so far, it is clear that the diversity of multi-relay systems is very sensitive to the decoded errors at the relays. This suggests that improving the reliability of detection at the relays should improve the diversity.

Coded cooperative communication has been a very active research topic in recent years. In [13], [14], Sendonaris et al. demonstrated that cooperation among users not only leads to higher data rates, but also to decrease sensitivity to channel variations. They have also shown that spatial diversity can be obtained using the partnering user, even if the inter-user channel is noisy. Laneman et al. [16] developed several cooperative protocols which can achieve full diversity.

The goal was to minimize the outage probability. Recently, channel coding for cooperative systems has been studied in [35]-[37].

For instance, Hunter and Nosratinia [35] used rate-compatible punctured convolutional (RCPC) codes for the partnering users and cyclic redundancy check (CRC) at the partner to arrive at an efficient coding scheme for cooperation. Along the same lines, Stefanov and Erkip [37] provided a frame-error rate (FER) analysis to show that coded cooperation can achieve full diversity. They illustrated that when different users experience independent fades, the block-fading channel model is appropriate for coded cooperation, and the framework in [38] can be used for code design. Liu et al. [36] considered punctured turbo codes for cooperation with a strict decoding delay constraint, and analyzed the FER behavior. Some recent work includes cooperative STC, where the partnering nodes may have multiple antennas [39].

In [22], the authors considered space-time coded cooperation schemes for multi- relay channels. The first scheme is a repetition-based cooperative diversity scheme where the destination receives separate signals from each of the relays during the second phase on orthogonal sub-channels. The second one is a space-time-coded cooperative diversity scheme, in which relays utilize a suitable space-time code in the second phase and therefore can transmit simultaneously on the same sub-channel.

In [35], [37], [39]-[41], the authors proposed cooperative diversity with classical DF. The key idea is that each user transmits its own bits in the first frame. Each user also receives and decodes the partner's transmission. If the user successfully decodes the partner's code word, determined by checking the CRC bits, the user computes and transmits additional parity bits for the partner's data in the second frame. In [42], [43], the authors considered cooperative diversity with superposition modulation. In the superposition modulated cooperative

transmission system, a node transmits its own signal superimposed on other node's signal to the destination node.

The schemes that we consider most related to our work are the ones proposed in [35], [37], [39]-[41]. In light of this, coded cooperation in essence splits each code- word into two partitions, each of them is transmitted in a distributed manner to ensure large coding gains relative to conventional coding schemes (i.e., non-cooperative systems). In addition to the coding advantage, coded cooperation is based on incremental redundancy and thus allows a more flexible bandwidth allocation between the source and relay nodes, as compared to repetition coding.

In the following, we shall briefly describe the details of Schemes I, II that are related to our work. Scheme I is the one proposed in [35], [40], [41] and Scheme II is the one proposed in [37], [39].

2.2.1   System Model

Scheme I. In this scheme, the users segment their source data into blocks which are augmented with a CRC code, for a total of K bits per source block (including the CRC bits). Each block is then encoded with a forward error-correcting code, so that, for an overall rate R code, we have $N = K/R$ total code bits per block. Figure 2.8 illustrates the general coded cooperation frame work.

The two users cooperate by dividing the transmission of their N-bit code words into two successive time segments, or frames. In the first frame, each user transmits a rate $R_1 > R$ code word with $N_1 = K/R_1$ bits. This it is a valid (albeit weaker) code word which can be decoded to obtain the original information. Each user also receives and decodes the partner's transmission. If the user successfully decodes the partner's rate R_1 code word, determined by

checking the CRC bits, the user computes and transmits N_2 additional parity bits for the partner's data in the second frame, where $N_1 + N_2 = N$. These additional parity bits are selected such that they can be combined with the first frame code word to produce a more powerful rate R code word. If the user does not successfully decode the partner, N_2 additional parity bits for the user's own data are transmitted. Each user always transmits a total of N bits per source block over the two frames, and the users only transmit in their own multiple access channels.
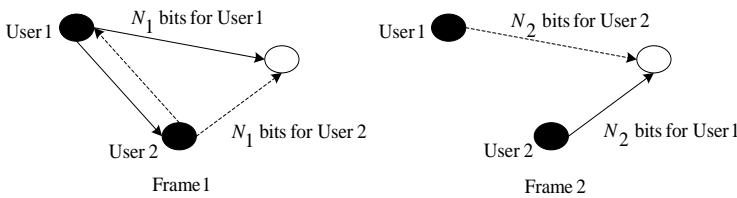
Figure 2.8 *Cooperative transmission scheme.*

In general, various channel coding methods can be used within this coded cooperation framework. For example, the overall code may be a block or convolutional code, or a combination of both. The code bits for the two frames may be partitioned through puncturing, product codes, or other forms of concatenation. In this scheme, the overall rate R code is selected from a given RCPC code family (e.g., the mother code). The code word for the first frame is obtained by applying the puncturing matrix corresponding to rate R_1, and the additional parity bits transmitted in the second frame are those punctured from the first frame. Figure 2.9 illustrates a user's implementation of coded cooperation using RCPC codes.
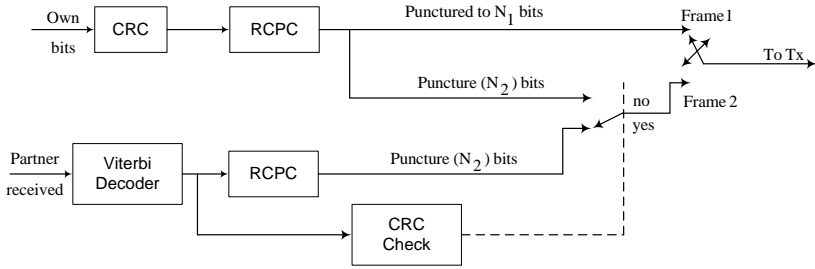
Figure 2.9 *A user's implementation of coded cooperation with RCPC codes.*

The users transmit on orthogonal channels (e.g., TDMA, code-division multiple- access (CDMA), or frequency-division multiple-access (FDMA)), which allows the destination, and other users in the cooperative case, to separately detect each user. In scheme I, BPSK modulation is assumed, for which the baseband-equivalent discrete- time signal transmitted by user $i \in \{1,2\}$ and received by user $j \in \{0,1,2\}$ ($j \neq i$, and $j = 0$ denotes the destination) is given by

$$r_{ij}(t) = h_{ij}(t)\sqrt{E_{ij}} x_i(t) + n_j(t), \qquad (2.21)$$

where E_{ij} is the transmitted energy per bit for user i, $x_i(t) \in \{-1, +1\}$ is the BPSK modulated code bit at time t, $h_{ij}(t)$ is modeled as complex Gaussian distributed with zero mean and unit variance, representing the fading channels between users i and j, and $n_j(t)$ accounts for noise and other additive interference at the receiver. For slow (quasi-static) fading, the fading coefficients remain constant ($h_{ij}(t) = h_{ij}$) over the transmission of each source frame. The noise term $n_j(t)$ is modeled as independent, zero-mean AWGN with variance $N_0/2$ per dimension.

The instantaneous received SNR for the channel between users i and j is defined as

$$\gamma_{i,j}(t) = \frac{|h_{i,j}(t)|^2 E_{i,j}}{N_0} \qquad (2.22)$$

For $|h_{i,j}(t)|$ Rayleigh distributed, $\gamma_{i,j}(t)$ has an exponential distribution with mean

$$\bar{\gamma}_{i,j} = E[\gamma_{i,j}(t)] = E\left[\frac{|h_{i,j}(t)|^2 E_{i,j}}{N_0}\right] = \frac{E_{i,j}}{N_0} E\left[|h_{i,j}(t)|^2\right] \qquad (2.23)$$

where $E[\cdot]$ denotes the expectation operator; $|h_{i,j}|^2$ is constant over t for a given channel.

Scheme II. In this scheme, the cooperative system is shown in Figure 2.10. For each node, the information bits are encoded by a channel encoder. The coded symbols are properly multiplexed for cooperation. The multiplexed symbols are passed through a serial-to-parallel converter, and are mapped to a particular signal constellation. When node S_i, transmits, the output of the modulator at each discrete time slot t is the signal $x_i(t)$.
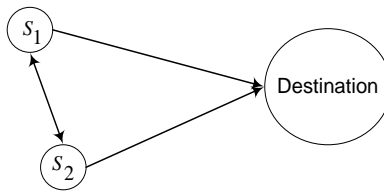

Figure 2.10 *Cooperative system.*

The received signal at the destination at time t due to transmission from S_i is given by

$$y_{i,j}(t) = h_{i,j}(t)\sqrt{E_{i,j}}\,x_i(t) + z_j(t), \qquad (2.24)$$

where the noise samples, zj (t), are modeled as independent realizations of a zero-mean complex Gaussian random variable with variance $N_0/2$ per dimension.

Using time division, each user has a separate time slot consisting of coded symbols (see Figure 2.11(a)). For the cooperative scheme, each user divides its own time slot into two equal segments, as shown in Figure 2.11(b). Along with channel coding for error correction, the users also perform a CRC for error detection. To optimize the performance of coded cooperative system, S_1 can transmit any portion of coded bits. For simplicity, S_1 uses the first segment of its time slot to transmit half of its coded symbols. These symbols are obtained by multiplexing the original coded symbol stream. Both the destination and the partner receive these coded symbols. Note that for the rate $1/4$ convolutional code, the effective code rate that the partner observes is $1/2$. If S_2 can successfully decode (as indicated by the CRC), it re-encodes the information bits to get the additional coded symbols which were not originally transmitted by S_1. These coded symbols are transmitted by S_2 for S_1 in the second segment of S_1's time slot. Hence, the destination observes half of the coded symbols through the S_1 destination link, the remaining half through the S_2 destination link.
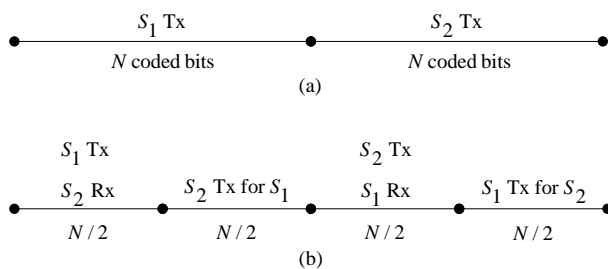
Figure 2.11   *Time-division channel allocations. (a) Orthogonal direct transmission. (b) Orthogonal cooperative diversity transmission.*

These links were assumed to have independent quasi-static fading, leading to an overall block-fading channel from the perspective of the destination. This provides additional diversity, obtained through the partner's link toward the destination.

If S_2 cannot receive the source's information correctly, using one bit of information, it notifies S_1 that there was a failure in decoding, and S_1 continues transmission. As far as the destination is concerned, it does not matter whether the second segment of coded bits comes from S_1 or its partner. It is assumed that the destination estimates the channel attenuation every N/2 symbols, hence, the decoding algorithm remains unchanged. Note that by coded cooperation, S_1 does not decrease its information rate. Finally, S_1 and S_2 change roles for the time slot of S_2. Since the inter-user channel from S_1 to S_2 has the same average quality with S_2 to S_1 channel, with cooperation, both nodes continue to meet their individual average power constraints.

2.2.2   Simulation Results

Here, we present our simulation results for Schemes I, II that are related to our work. In all of these results, we assume that the cooperative node operates in the DF mode. For simplicity, BPSK modulation is assumed. The different sub-channels between the source, relay, and destination are assumed to be independent flat Rayleigh fading channels. Also, we consider a quasi-static fading channel where the channel coefficients are fixed for the duration of the frame and change independently from one frame to another. In all simulations, the transmitted frame size is equal to 130 coded bits, and equal transmitted energies in both schemes for the different links is considered, i.e., $\gamma_{1,0} = \gamma_{2,0} = E_b/N_0$ but from user to destination node, $\gamma_{1,2} = \gamma_{2,1}$, can be different.

The convolutional code used is of constraint length four and generator polynomials $(13, 15, 15, 17)_{octal}$ [44]. When the relay cooperates with the source node, the source transmits the code words corresponding to rate 1/2, $(13, 15)_{octal}$

convolutional code to the relay and destination nodes in the first frame. The relay node receives this codeword and decoding is performed to obtain an estimate of the source information bits. In the second frame, both the relay and source nodes transmit the code words corresponding to rate 1/2, $(15, 17)_{octal}$ convolutional code to the destination node.

Figure 2.12 shows a comparison of the BER performance of Schemes I and II for one relay channel operating in the DF mode when the effect of channel errors at relay is considered (i.e., $\bar{\gamma}_{1,2} = \bar{\gamma}_{2,1} = 8\ dB$). We also include in the same figure the performance of these schemes with perfect detection at the relay. To maintain the same average power, the source and relay nodes divide their power according to the ratio 1/2. As shown from these results, the performance of Scheme II is 0.5 dB better than Scheme I. The 0.5-dB penalty incurred is due to the use of RCPC code. Also, the diversity gain achieved using one relay is evident from these results.
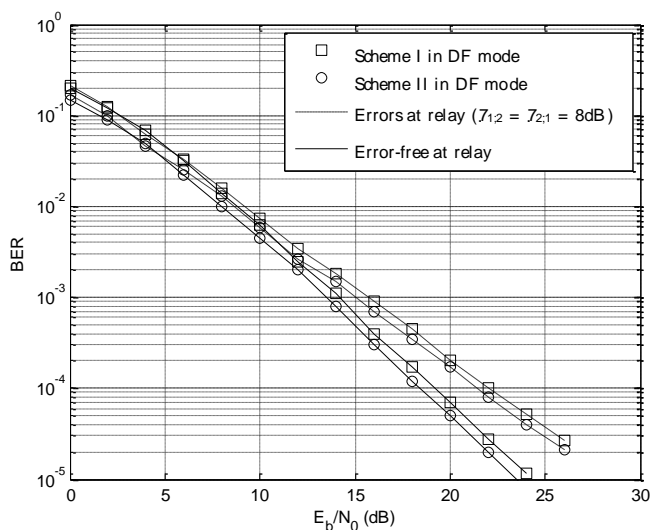

Figure 2.12 BER comparisons for Schemes I, II in the DF mode with error-free detection at relay node, and $\bar{\gamma}_{1,2} = \bar{\gamma}_{2,1} = 8\ dB$ with relay errors.

2.3   Antenna/Relay Selection

Antenna selection has been considered before for centralized MIMO systems where it was shown that impressive diversity and coding gains can be achieved [45]-[49]. The idea behind antenna selection is to use only a subset of the available antennas. The consequence of this is that, while taking advantage of the benefits of the available antennas, the number of RF chains is reduced to the number of selected antennas, which results in complexity reduction. A natural extension of antenna selection is relay selection, whereby the relay that enjoys the best reliability is selected. To accomplish this, the source will have to know the reliability of the available nodes through some feedback to decide on what relay to use for relaying. It is also possible to select multiple relays for cooperation.

In [45], the authors studied the impact of antenna selection at the receiver on the diversity order and coding gain provided by the underlying STC. It was shown that, for full-rank STTC codes and quasi-static fading channels, the diversity order of the underlying STTC code is maintained. A comprehensive performance analysis of STBCs with receive antenna selection was presented in [46]. They showed that the diversity order with antenna selection is maintained as that of the full complexity system. The performance of a serial concatenated scheme comprising a convolutional code and a STBC separated by an inter leaver was studied in [47]. They showed that the use of antenna selection at the receiver side only affects the SNR coding gain, but not the overall diversity order. This phenomena was evident for both the fast and block flat fading channel models.

In [48], algorithms for exact channel knowledge and statistical channel knowledge selection with the antenna sets selected to minimize the probability of error were presented. They showed that when exact channel knowledge is available, the selection algorithm chooses the antenna subsets that minimizes the

instantaneous probability of error and maximizes the SNR. The combination of transmit antenna selection with STBC scheme was considered in [49]. They showed that if all the transmit antenna were used, then this scheme achieves a full diversity order with simple decoding complexity.

In Chapter 4, we consider antenna/relay selection for coded cooperative networks in an effort to improve their end-to-end performance by improving the detection reliability at the relay nodes. Considering DF and AF relaying, we analyze the impact of antenna/relay selection on the performance of cooperative networks in conjunction with the distributed coding scheme introduced in Chapter 3. Specifically, we derive upper bounded expressions for the bit error rate assuming M -PSK transmission. Our analytical results show that the maximum diversity order of the system is maintained for the entire range of BER of interest, unlike the case without antenna/relay selection. Several numerical and simulation results are presented to demonstrate the efficacy of the proposed scheme.

2.4   Channel Estimation

Coherent reception requires the receiver to acquire channel knowledge to compensate for the channel induced distortions. The process of acquiring the channel knowledge is called channel estimation and is an integral part of most communication systems. Apart from the knowledge of channel statistics, the channel estimator also requires knowledge of the instantaneous channel values to track the channel fading and compensate it. Typically, known symbols called "pilot" symbols are multiplexed along with the data to aid the receiver in channel estimation [50]-[58].

STC modulation with multiple transmits and/or multiple receive antennas and orthogonal pilot sequence insertion was proposed in [50]. In this scheme, the

transmitter inserts periodic orthogonal pilot sequences in each one of the simultaneously transmitted blocks. Each block is then pulse-shaped and transmitted from a different antenna. Since the signal at each receive antenna is a linear superposition of the transmitted signals, the receiver uses orthogonal pilot sequences to estimate the different fading channels. The receiver then uses an appropriately designed interpolation filter to interpolate those estimates and obtain accurate CSI. The problem of training sequence design for multiple-antenna transmissions over quasi-static frequency-selective channels was addressed in [51]. In [51] various methods to identify good training sequences for systems employing multiple transmit antennas over frequency-selective channels were studied.

In [52], multiple-antenna wireless communication links with training-based schemes were addressed. They showed that if optimization over the training and data powers is allowed, then the optimal number of training symbols is always equal to the number of transmit antennas. They also showed that if the training and data powers are instead required to be equal, then the optimal number of symbols can be larger than the number of antennas. In [53], the authors proposed linear dispersion space-time codes in wireless relay networks. It was shown that the source and relay nodes do not have any channel information but the destination has knowledge of both the source to relay channel and relay to the destination channel.

In [54], it is assumed that the relays do not have any channel information, while the destination has only a partial-channel knowledge, by which mean that destination knows only the relay-to-destination channel. In [55], the authors considered pilot symbol aided channel estimation for AF relay based cooperation diversity systems. They investigated the impact of the underlying channel on the pilot insertion strategy and estimator design. In [56], a proposed coherent distributed space-time coding in AF relay networks using training and channel estimation scheme was proposed. It was shown that the relay nodes do not

perform any channel estimation using the training symbols transmitted by the source but instead simply amplify and forward the received training symbols.

The training based channel estimation for AF based relay networks was proposed in [57]. The overall channel from source to destination is estimated at the destination only while the relays amplify and retransmit the information to the destination. In [57], both the least square (LS) and the minimum mean square error (MMSE) channel estimation approaches were considered. In [58], a differential transmission scheme for wireless relay networks using the ideas of distributed space-time coding and differential space-time coding was proposed. The authors showed that compared to coherent distributed space-time coding, distributed differential space-time coding performs 3 dB worse.

In the above works [53]-[57], it has been shown that the source and relay nodes do not have any channel information but the destination has a full/partial channel knowledge. Also the proposed schemes assumed AF relaying but not DF relaying. To this end, we will show in Chapter 5 that the source, relay, and destination nodes do not have any channel information. So in Chapter 5 we propose to use the same coding scheme introduced in Chapter 3 with an imperfect channel estimation and distributed space-time coding cooperation using Alamouti scheme.

3

Convolutional-Based Distributed
Coded Cooperation for
Relay Channels

In this chapter, we consider a distributed coded cooperation scheme where the source and relays share their antennas to create a virtual transmit array to transmit towards their destination. While the relays may use several forwarding strategies, including AF and DF, we focus on coded DF relaying. It is assumed that the source is equipped with two encoders, where the output of the first encoder is referred to as the first frame (of length N_1 bits) and the output of the second encoder is referred to as the second frame (of length N_2 bits). Each relay is equipped with an encoder similar to the second encoder at the source. The cooperation scheme under consideration may be summarized as follows. In the first phase, using the first encoder, the source node sends the first frame to the relays and destination node. If a relay successfully decodes the received frame, i.e., the corresponding CRC checks, then the relay encodes the message before transmission. Otherwise, that relay keeps silent. In the second phase, the source and relay nodes (whose CRCs check) transmit the second frame on orthogonal channels (e.g., TDMA, CDMA, or FDMA) to the destination, and the received replicas are combined using maximal-ratio combiner (MRC). The information bits are detected via a Viterbi decoder for the two frames ($N = N_1 + N_2$ bits). Assuming M -PSK transmission, we analyze the performance of the above distributed coded cooperation scheme and show that it achieves large coding gain and full diversity relative to the coded non-cooperative case. We remark that perfect synchronization is assumed, as is the case in most papers published on this topic.

3.1   Proposed Coding Scheme

The model of the proposed convolutional encoded transmission system is shown in Figure 3.1. In this model, instead of using a centralized convolutionally coded system at the source node, one can design a distributed coding scheme at

both the source and relay nodes where the encoding process is divided over two frame transmissions. To improve the overall performance through diversity, the coded cooperation operates by sending two code words via *L+1* independent fading path, where *L* is the number of relay nodes that can be used for cooperation. In what follows, we denote the source, m^{th} relay, destination nodes by *S*, R_m, and *D*, respectively. Consider the relay channels shown in Figure 3.2 where data is sent from *S* to *D* with the assistance of R_m. All nodes are equipped with single antenna transmitters and receivers. Throughout the book, we assume that a node cannot transmit and receive simultaneously.
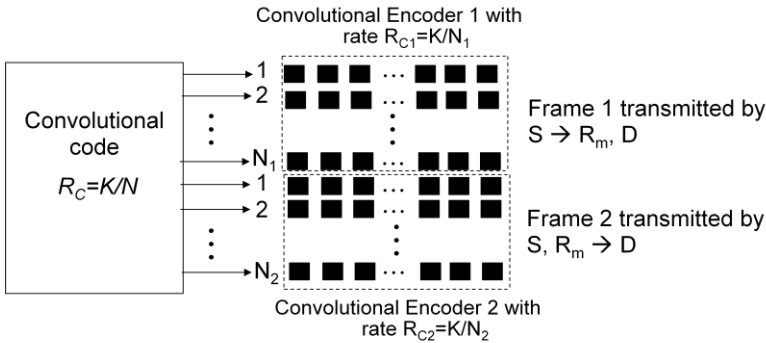

Figure 3.1 *Convolutional code designed for distributed coded cooperation.*
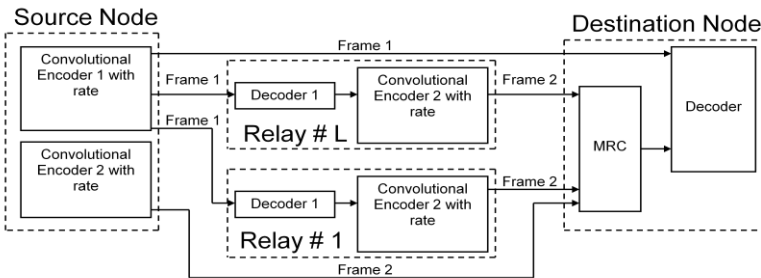

Figure 3.2 *Proposed distributed coded cooperation scheme.*

Let $b = [b_1, b_2, \cdots, b_K]$ be the information sequence at the input of the

convolutional encoder at the source, and let $C = [c_1, c_2, \cdots, c_N]$ be the corresponding code-word. The coded bits are then mapped into a modulated signal word. The coded bits are then mapped into a modulated signal $x = [x_1, x_2, \cdots, x_n]$ the code rate in this case is $R_c = K/n$ where $n = \frac{N}{\log_2 M}$, M is the constellation size. According to our coding scheme, codeword C is partitioned into two sub-code words, namely, C_1 and C_2, of lengths N_1 and N_2, respectively, where $N_1 + N_2 = N$. Hence, the modulated signal x is partitioned into two modulated signals, namely, x_1 and x_2, of lengths n_1 and n_2, respectively, where $n_1 + n_2 = n$.

In the first phase, the source broadcasts the first frame to the relays and destination node using convolutional encoder I with rate $R_{C_1} = {K}/{n_1}$. If the relays correctly decode the message they received from the source, they re-encode it with convolutional encoder II with rate $R_{C_2} = {K}/{n_2}$. In the second phase, the source and those relays whose CRC checks transmit the second frame to the destination. The received copies of the second frame are combined using MRC and the information bits are detected via a Viterbi decoder based on the two frames $N_1 + N_2 = N$. We assume that all sub-channels are independent, orthogonal, and quasi-static fading. We consider two different convolutional codes, whose generator polynomials in octal form are generally given by $(c_1, c_2, c_3, c_4)_{\text{octal}}$. In this context, it is implied that encoder I employs $(c_1, c_2)_{\text{octal}}$ and encoder II employs $(c_3, c_4)_{\text{octal}}$.

During the first frame transmission, the signals received at the relay and the destination nodes at time *t* are given by

$$r_{SR_m}(t_1) = \sqrt{R_{C_1} E_{SR_m}} h_{SR_m}(t) x(t) + n_{SR_m}(t), \qquad (3.1)$$

$$r_{SD}(t_1) = \sqrt{R_{C_1} E_{SD}} h_{SD}(t) x(t) + n_{SD}(t), \qquad (3.2)$$

where $x(t)$ is the output of the source modulator at time slot t $(t = 1, 2, \cdots, n_1)$, $m = 1, 2, \cdots, L$, L is the number of relay channels, $h_{SR_m}(t)$ and $h_{SD}(t)$ are modeled as complex Gaussian distributed with zero mean and unit variance, representing the fading channels from S to R_m and from S to D, E_{SR_m} and E_{SD} are the transmitted signal energies for the corresponding link, $n_{SR_m}(t)$ and $n_{SD}(t)$ represent the complex AWGN on the $S - R_m$ and $S - D$ links, respectively, with zero mean and one-dimensional variance $N_0/2$.

Now let L' denote the number of relays used for cooperation in the second phase, i.e., they decode the received message correctly. Accordingly, the received signals at the destination node at time t are given by

$$r_{R_m D}(t) = \sqrt{R_{C_2} \frac{E_{R_m D}}{(L'+1)}} h_{R_m D}(t) \hat{x}(t) + n_{R_m D}(t), \qquad (3.3)$$

$$r_{SD}(t) = \sqrt{R_{C_2} \frac{E_{SD}}{(L'+1)}} h_{SD}(t) x(t) + n_{SD}(t), \qquad (3.4)$$

where $\hat{x}(t)$ is the output of the relay modulators at time slot t $(t = n_1 + 1, n_1 + 2, \cdots, n_1 + n_2)$, $m = 1, 2, \cdots, L'$, $h_{R_m D}(t)$ is the complex fading coefficient of the $R_m - D$ link, $E_{R_m D}$ is the transmitted signal energy for the $R_m - D$ link, $n_{R_m D}(t)$ is the AWGN with zero mean and variance N_0, $\frac{1}{(L'+1)}$ is a ratio used to maintain the same average power in the second frame. For example, when $L' = 0$, the relay nodes do not transmit. That is, the relay nodes transmit with energy $\frac{E_{R_m D}}{(L'+1)}$ and the source node transmits with energy $\frac{E_{SD}}{(L'+1)}$. Note that the coefficients in (3.3) and (3.4) are functions of L', which assumes that power control is used. In the absence of power control, L' is replaced by L and consequently the results obtained will serve as upper bounds. However, at

sufficiently high SNR, the difference will be small.

In the following analysis, we consider the performance of our coding scheme over slow fading channels where the fading coefficients remain constant over the transmission of each frame interval, (i.e., $h_{SR_m}(t) = h_{SR_m}$, $h_{SD}(t) = h_{SD}$, and $h_{R_m D}(t) = h_{R_m D}$).

3.2 Upper Bound on the Probability of Bit Error

In this section, we evaluate the performance of our proposed scheme for L-relay channels in terms of the average BER at the destination. In our analysis, we consider M-PSK modulation. We first consider error-free recovery at the relays. Note that this assumption is optimistic and can only be justified under special conditions (i.e., high SNR or un-faded channel between the source and relays), however, it can serve as a lower bound on the BER performance. Then we consider the effect of channel errors at the relays. Only those relays who correctly decode the message they received from the source node using CRC code, re-encode it with a different code and send it to the destination node, which is more realistic to apply. The instantaneous received SNR for non-cooperative transmission from S to D,

$$\gamma_D(t) = 2R_C \frac{E_{SD}}{N_0} |h_{SD}(t)|^2 = 2R_C \gamma_{SD}(t),$$

and the average SNR

$$\bar{\gamma}_D(t) = 2R_C \frac{E_{SD}}{N_0} E[|h_{SD}(t)|^2] = 2R_C \bar{\gamma}_{SD}(t).$$

The end-to-end conditional pairwise error probability for a coded system is the probability of detecting an erroneous codeword $\hat{x} = [\hat{x}_1, \hat{x}_2, \cdots, \hat{x}_n]$ when in fact $x = [x_1, x_2, \cdots, x_n]$ is transmitted. Therefore, for non-cooperative transmission,

the conditional pairwise error probability from S to D is given by

$$P(x \to \hat{x}|\gamma_{SD}(t)) =$$

$$Q\left(\sqrt{\frac{2g_{PSK}R_C E_{SD}}{N_0}\sum_{t\in\eta}|h_{SD}(t)|^2}\right) = Q\left(\sqrt{2g_{PSK}R_C\sum_{t\in\eta}\gamma_{SD}(t)}\right), \qquad (3.5)$$

where $g_{PSK} = \sin^2(\pi/M)$, $Q(\cdot)$ is the Gaussian Q-function, η is the set of all t for which $\hat{x}(t) \neq x(t)$, the cardinality of η is equal to the Hamming distance d between code-words x and $\hat{x}$, $\gamma_{SD}(t) = \frac{E_{SD}}{N_0}|h_{SD}(t)|^2$, and R_C is the code rate. Under slow fading, $h_{SD}(t) = h_{SD}$ for all t and consequently (3.5) can be written as

$$P(d|\gamma_{SD}) = Q\left(\sqrt{2g_{PSK}R_C d\gamma_{SD}}\right). \qquad (3.6)$$

In what follows, we derive an upper bound on the probability of bit error for the coded L-relay channels.

3.2.1 Distributed Coded Cooperation with Error-Free Relays

Under the assumption of free errors at the relay nodes, the instantaneous received SNR for the channel from S to D for the first frame is given by

$$\gamma_D(t) = 2R_{C_1}\frac{E_{SD}}{N_0}|h_{SD}(t)|^2 = 2R_{C_1}\gamma_{SD}(t), \quad t = 1,2,\cdots,n_1, \qquad (3.7)$$

and the instantaneous received SNR for the channels from S to D and R_m to D for the second frame is given by

$$\gamma_D(t) = \frac{2R_{C_1}}{(L+1)}\left(\frac{E_{SD}}{N_0}|h_{SD}(t)|^2 + \sum_{m=1}^{L}\frac{E_{R_m D}}{N_0}\left|h_{R_m D}(t)\right|^2\right)$$

$$\gamma_D(t) = \frac{2R_{C_1}}{(L+1)}\left(\gamma_{SD}(t) + \sum_{m=1}^{L}\gamma_{R_m D}(t)\right), t = n_1+1, n_1+2, \cdots, n_1+n_2, \quad (3.8)$$

where $\gamma_{R_m D}(t) = \frac{E_{R_m D}}{N_0}\left|h_{R_m D}(t)\right|^2$. To maintain the same average power in the

second frame, the relay and source nodes split their powers according to the ratio $1/(L + 1)$.

When the fading coefficients h_{SD}, and $h_{R_m D}$ are constant over the codeword, the conditional pair-wise error probability is given by

$$P(d|\gamma_{SD}, \gamma_{R_1 D}, \cdots, \gamma_{R_L D}) = Q\left(\sqrt{2g_{PSK}\left(R_{C_1}d_1\gamma_{SD} + \frac{R_{C_2}d_2}{(L+1)}\left(\gamma_{SD} + \sum_{m=1}^{L}\gamma_{R_m D}\right)\right)}\right), (3.9)$$

where η_i is equal to the Hamming distance d_i for the two frames, $i = 1, 2$, and $d_1 + d_2 = d$.

Using Craig's formula for Q(x) [59]

$$Q(x) = \frac{1}{\pi}\int_0^{\frac{(M-1)\pi}{M}} exp\left(-\frac{x^2}{2\sin^2\theta}\right)d\theta. \qquad (3.10)$$

we can rewrite (3.9) as

$$P(d|\gamma_{SD}, \gamma_{R_1 D}, \cdots, \gamma_{R_L D}) =$$
$$\frac{1}{\pi}\int_0^{\frac{(M-1)\pi}{M}} exp\left(\frac{-g_{PSK}\left(R_{C_1}d_1 + \frac{R_{C_2}d_2}{(L+1)}\right)\gamma_{SD}}{\sin^2\theta}\right)\prod_{m=1}^{L} exp\left(\frac{-g_{PSK}R_{C_2}d_2\gamma_{R_m D}}{(L+1)\sin^2\theta}\right)d\theta. \qquad (3.11)$$

The average pairwise error probability is then given by

$$P(d) = \frac{1}{\pi}\int_0^{\frac{(M-1)\pi}{M}}\int_0^{\infty} exp\left(\frac{-g_{PSK}\left(R_{C_1}d_1 + \frac{R_{C_2}d_2}{(L+1)}\right)\gamma_{SD}}{\sin^2\theta}\right)p_{\gamma_{SD}}(\gamma_{SD})d\gamma_{SD}$$

$$\prod_{m=1}^{L}\int_0^{\infty} exp\left(\frac{-g_{PSK}R_{C_2}d_2\gamma_{R_m D}}{(L+1)\sin^2\theta}\right)p_{\gamma_{R_m D}}(\gamma_{R_m D})d\gamma_{R_m D}d\theta, \qquad (3.12)$$

where average $p_{\gamma}(\gamma) = \frac{1}{\bar{\gamma}}exp(\frac{-\gamma}{\bar{\gamma}})$ is a chi-sequare probability density function (PDF), and $\bar{\gamma}$ is the average SNR per information bit.

Given the moment generating function (MGF) of γ [60]

$$\psi_\gamma(-s) = \int_0^\infty exp(-s\gamma)p_\gamma(\gamma)d\gamma = \frac{1}{1+s\bar{\gamma}}. \tag{3.13}$$

One can show that (3.12) can be expressed as

$$P(d) = \frac{1}{\pi} \int_0^{\frac{(M-1)\pi}{M}} \left(1 + \frac{g_{PSK}\left(R_{C_1}d_1 + \frac{R_{C_2}d_2}{(L+1)}\right)\bar{\gamma}_{SD}}{\sin^2\theta} \right)^{-1}$$

$$\cdot \prod_{m=1}^{L} \left(1 + \frac{g_{PSK}\,R_{C_2}d_2\bar{\gamma}_{R_mD}}{(L+1)\sin^2\theta} \right)^{-1} d\theta, \tag{3.14}$$

where $\bar{\gamma}_{SD} = \frac{E_{SD}}{N_0}E[|h_{SD}|^2]$, and $\bar{\gamma}_{R_mD} = \frac{E_{R_mD}}{N_0}E\left[|h_{R_mD}|^2\right]$ are the average SNRs. If we assume $\bar{\gamma}_{SD}$, and $\bar{\gamma}_{R_mD}$ to be large, then (3.14) can be written as

$$P(d) \approx \left(\sin\frac{\pi}{M}\right)^{-2L-2} \left(\frac{R_{C_2}d_2}{(L+1)}\right)^{-L} \left(R_{C_1}d_1 + \frac{R_{C_2}d_2}{(L+1)}\right)^{-1} (\bar{\gamma}_{SD})^{-1}$$

$$\cdot \prod_{m=1}^{L}(\bar{\gamma}_{R_mD})^{-1} \frac{1}{\pi}\int_0^{\frac{(M-1)\pi}{M}}(\sin\theta)^{2L+2}d\theta, \tag{3.15}$$

which suggests that the diversity order achieved is $L+1$ when the channels from S to the L relays are error-free. Having obtained the pairwise error probability in (3.15), the BER probability can be upper bounded assuming Gray mapping as [60]

$$P_b(e) \le \frac{1}{\log_2 M}\frac{1}{k_c}\sum_{d=d_f}^{\infty} c(d)P(d), \tag{3.16}$$

Where k_c is the number of information bits encoded into a trellis transition, $c(d)$ is the sum of bit errors for error events of distance d, and d_f is the free Hamming distance of the code.

3.2.2 Distributed Coded Cooperation with Errors at Relays

In this section, we consider the more realistic case in which some of the relays may fail to correctly decode the message they received from the source, that is, when their CRC does not check. Obviously, the number of cooperating relays ranges from zero to L. Let Ω denote the set of indices of the cooperating relays, i.e.,

$$\Omega = \{j_1, j_2, \cdots, j_{L'}\} \subset \{1, 2, \cdots, L\}. \tag{3.17}$$

Note that the cardinality of Ω is $L^{'}$.

Assuming that γ_{SD}, γ_{SR_1}, $\cdots$, γ_{SR_L}, γ_{R_1D}, $\cdots$, γ_{R_LD} are all mutually independent, the expression for the conditional pairwise error probability can be decomposed into three parts. The first part corresponds to the case of no cooperation; the second part corresponds to the case when some of the relays cooperate ($L^{'}$ of them); and the third part corresponds to the case of error-free relaying, i.e., all relays cooperate. As such, the conditional pairwise error probability can be expressed as

$$P\big(d|\gamma_{SD}, \gamma_{SR_1}, \cdots, \gamma_{SR_L}, \gamma_{R_1D}, \cdots, \gamma_{R_LD}\big) = Q\left(\sqrt{2g_{PSK}\big(R_{C_1}d_1 + R_{C_2}d_2\big)\gamma_{SD}}\right)$$

$$\cdot \prod_{m=1}^{L} Q\left(\sqrt{2g_{PSK}R_{C_1}d_1\gamma_{SR_m}}\right)$$

$$+ \sum_{L'=1}^{L-1}\sum_{\Omega}\left[\prod_{j\notin\Omega} Q\left(\sqrt{2g_{PSK}R_{C_1}d_1\gamma_{SR_j}}\right)\prod_{j\in\Omega}\left(1 - Q\left(\sqrt{2g_{PSK}R_{C_1}d_1\gamma_{SR_j}}\right)\right)\right.$$

$$\left.\cdot Q\left(\sqrt{2g_{PSK}\left(\left(R_{C_1}d_1 + \frac{R_{C_2}d_2}{(L'+1)}\right)\gamma_{SD} + \frac{R_{C_2}d_2}{(L'+1)}\sum_{j\in\Omega}\gamma_{R_jD}\right)}\right)\right]$$

$$+ \prod_{m=1}^{L} \left(1 - Q\left(\sqrt{2 g_{PSK} R_{C_1} d_1 \gamma_{SR_m}} \right) \right)$$

$$. Q\left(\sqrt{2 g_{PSK} \left(\left(R_{C_1} d_1 + \frac{R_{C_2} d_2}{(L+1)} \right) \gamma_{SD} + \frac{R_{C_2} d_2}{(L+1)} \sum_{m=1}^{L} \gamma_{R_m D} \right)} \right). \qquad (3.18)$$

Now, using (3.10), (3.18) can then be written with the help of [6] as

$$P\left(d | \gamma_{SD}, \gamma_{SR_1}, \cdots, \gamma_{SR_L}, \gamma_{R_1 D}, \cdots, \gamma_{R_L D} \right) = \frac{1}{\pi} \int_0^{\frac{(M-1)\pi}{M}}$$

$$. exp\left(\frac{-g_{PSK} \left(R_{C_1} d_1 + R_{C_2} d_2 \right) \gamma_{SD}}{\sin^2 \theta} \right) d\theta \prod_{m=1}^{L} \frac{1}{\pi} \int_0^{\frac{(M-1)\pi}{M}} exp\left(\frac{-g_{PSK} R_{C_1} d_1 \gamma_{SR_m}}{\sin^2 \theta_m} \right)$$

$$. d\theta_m + \sum_{L'=1}^{L-1} \sum_{\Omega} \left[\prod_{j \notin \Omega} \left(\frac{1}{\pi} \int_0^{\frac{(M-1)\pi}{M}} exp\left(\frac{-g_{PSK} R_{C_1} d_1 \gamma_{SR_j}}{\sin^2 \theta_j} \right) d\theta_j \right) \right.$$

$$. \prod_{j \in \Omega} \left(1 - \frac{1}{\pi} \int_0^{\frac{(M-1)\pi}{M}} exp\left(\frac{-g_{PSK} R_{C_1} d_1 \gamma_{SR_j}}{\sin^2 \theta_j} \right) d\theta_j \right) \frac{1}{\pi} \int_0^{\frac{(M-1)\pi}{M}}$$

$$. exp\left(\frac{-g_{PSK} \left(R_{C_1} d_1 + \frac{R_{C_2} d_2}{(L'+1)} \right) \gamma_{SD}}{\sin^2 \theta} \right) exp\left(\frac{-g_{PSK} R_{C_2} d_2}{(L'+1) \sin^2 \theta} \sum_{j \in \Omega} \gamma_{R_j D} \right) d\theta \right]$$

$$+ \prod_{m=1}^{L} \left(1 - \frac{1}{\pi} \int_0^{\frac{(M-1)\pi}{M}} exp\left(\frac{-g_{PSK} R_{C_1} d_1 \gamma_{SR_m}}{\sin^2 \theta_m} \right) d\theta_m \right) \frac{1}{\pi} \int_0^{\frac{(M-1)\pi}{M}}$$

$$. exp\left(\frac{-g_{PSK} \left(R_{C_1} d_1 + \frac{R_{C_2} d_2}{(L+1)} \right) \gamma_{SD}}{\sin^2 \theta} \right) exp\left(\frac{-g_{PSK} R_{C_2} d_2}{(L+1) \sin^2 \theta} \sum_{m=1}^{L} \gamma_{R_m D} \right) d\theta. \qquad (3.19)$$

Assuming $\bar{\gamma}_{SR_m}$, $\bar{\gamma}_{R_m D}$, and $\bar{\gamma}_{SD}$ to be large and using the results of Appendix A, the average pairwise error probability can be simplified to

$$P(d) \approx \frac{\left(\sin\frac{\pi}{M}\right)^{-2}(\bar{\gamma}_{SD})^{-1}}{\left(R_{C_1}d_1 + R_{C_2}d_2\right)}\frac{1}{\pi}\int_0^{\frac{(M-1)\pi}{M}}\sin^2\theta d\theta$$

$$\cdot \prod_{m=1}^{L}\left(\frac{\left(\sin\frac{\pi}{M}\right)^{-2}(\bar{\gamma}_{SR_m})^{-1}}{R_{C_1}d_1}\frac{1}{\pi}\int_0^{\frac{(M-1)\pi}{M}}\sin^2\theta_m d\theta_m\right)$$

$$+\sum_{L'=1}^{L-1}\sum_{\Omega}\left[\prod_{j\notin\Omega}\left(\frac{\left(\sin\frac{\pi}{M}\right)^{-2}\left(\bar{\gamma}_{SR_j}\right)^{-1}}{R_{C_1}d_1}\frac{1}{\pi}\int_0^{\frac{(M-1)\pi}{M}}\sin^2\theta_j d\theta_j\right)\right.$$

$$\cdot\prod_{j\in\Omega}\left(1-\frac{\left(\sin\frac{\pi}{M}\right)^{-2}\left(\bar{\gamma}_{SR_j}\right)^{-1}}{R_{C_1}d_1}\frac{1}{\pi}\int_0^{\frac{(M-1)\pi}{M}}\sin^2\theta_j d\theta_j\right)\frac{\left(\sin\frac{\pi}{M}\right)^{-2}(\bar{\gamma}_{SD})^{-1}}{\left(R_{C_1}d_1 + \frac{R_{C_2}d_2}{(L'+1)}\right)}$$

$$\cdot\frac{1}{\pi}\int_0^{\frac{(M-1)\pi}{M}}\sin^2\theta\prod_{j\in\Omega}\left(\frac{\left(\sin\frac{\pi}{M}\right)^{-2}(L'+1)\left(\bar{\gamma}_{R_j D}\right)^{-1}}{R_{C_2}d_2}\sin^2\theta\right)d\theta\left.\right]$$

$$+\prod_{m=1}^{L}\left(1-\frac{\left(\sin\frac{\pi}{M}\right)^{-2}\left(\bar{\gamma}_{SR_m}\right)^{-1}}{R_{C_1}d_1}\frac{1}{\pi}\int_0^{\frac{(M-1)\pi}{M}}\sin^2\theta_m d\theta_m\right)\frac{\left(\sin\frac{\pi}{M}\right)^{-2L-2}}{\left(R_{C_1}d_1 + \frac{R_{C_2}d_2}{(L+1)}\right)}$$

$$\cdot\left(\frac{L+1}{R_{C_2}d_2}\right)^{L}(\bar{\gamma}_{SD})^{-1}\prod_{m=1}^{L}\left(\bar{\gamma}_{R_m D}\right)^{-1}\frac{1}{\pi}\int_0^{\frac{(M-1)\pi}{M}}(\sin\theta)^{2L+2}d\theta. \qquad (3.20)$$

When $\bar{\gamma}_{SR_m}$ is very large (i.e., $\bar{\gamma}_{SR_m} \to \infty$), all the relay will have perfect detection, and thus (3.20) will be the same as (3.15). This is true since the first two terms of (3.20) go to zeros. However, it should be noted that when $\bar{\gamma}_{SR_m}$ is

very small, there will be a loss in diversity but the system still offers large coding gains relative to the non-cooperative case. By substituting (3.20) into (3.16), one can obtain an upper bound for the probability of bit error.

3.3   Outage Probability Analysis

The outage probability, P_{out}, is another standard performance criterion for systems operating over slow fading channels [61]. With quasi-static fading, the elements of the sequence $\{\gamma\}$ of block SNRs are exponentially independent and identically distributed (i.i.d.) with average SNR $\bar{\gamma}$. We assume that each codeword is divided into two sub-codewords which may not be of equal length. We denote by β the fraction of time that the source transmits in the first frame and by $(1 - \beta)$ the fraction of time that the relays and source transmit in the second frame. During the first frame, the source transmits with rate $R_{C_1} = R_C/\beta$ code, while during the second frame, the source and relays transmit with rate $R_{C_2} = R_C/(1 - \beta)$ code, where the ratio β $(0 < \beta < 1)$. Therefore, in this section, we derive the outage probability of the proposed scheme for L-relay channels.

First, let us consider non-cooperative direct transmission between the source and destination. During this transmission, the instantaneous capacity $C(\gamma_{SD}) = \log_2(1 + \gamma_{SD})$ [27]. If a rate R_C code is used, then the channel will be in outage whenever $C(\gamma_{SD}) < R_C$, where $\{C(\gamma_{SD}) < R_C\}$ is called the outage event. The outage probability is found by integrating the PDF of γ_{SD} over the outage event region, that is

$$P_{out} = Pr\{C(\gamma_{SD}) < R_C\} = Pr\{\gamma_{SD} < 2^{R_C} - 1\} = \int_0^{2^{R_C}-1} p_{\gamma_{SD}}(\gamma_{SD})d\gamma_{SD}$$

$$= \int_0^{2^{R_C}-1} \frac{1}{\overline{\gamma}_{SD}} exp\left(\frac{-\gamma_{SD}}{\overline{\gamma}_{SD}}\right) d\gamma_{SD} = 1 - exp\left(\frac{1-2^{R_C}}{\overline{\gamma}_{SD}}\right). \tag{3.21}$$

In what follows, we derive the outage probability for both error-free and erroneous detection at the relays.

3.3.1   Distributed Coded Cooperation with Error-Free Relays

If we consider ideal source-relay links, i.e., no errors at the relays, then the destination node will receive a transmission from source and relays. Thus, outage occurs whenever

$$C\left(\gamma_{SD}, \gamma_{R_m D}\right) < R_C, \tag{3.22}$$

Where

$$C\left(\gamma_{SD}, \gamma_{R_m D}\right) = \log_2\left[(1+\gamma_{SD})^\beta \left(1 + \frac{\gamma_{SD}}{(L+1)} + \sum_{m=1}^L \frac{\gamma_{R_m D}}{(L+1)}\right)^{(1-\beta)}\right]. \tag{3.23}$$

The outage probability, P_{out}, can then be evaluated over the outage region in (3.23) as

$$P_{out} = Pr\left\{(1+\gamma_{SD})^\beta \left(1 + \frac{\gamma_{SD}}{(L+1)} + \sum_{m=1}^L \frac{\gamma_{R_m D}}{(L+1)}\right)^{(1-\beta)} < 2^{R_C}\right\}. \tag{3.24}$$

Since $\gamma_{SD}, \gamma_{R_1 D}, \gamma_{R_2 D}, \cdots, \gamma_{R_L D}$ in (3.24) are always greater than or equal zero, then

$$\gamma_{SD} < (2^{R_C} - 1)(L+1) \triangleq A_1, \tag{3.25}$$

$$\gamma_{R_m D} < \left(2^{\left(\frac{R_C}{1-\beta}\right)} - 1\right)(L+1) \triangleq A_2, \tag{3.26}$$

where $m = 1,2,\cdots,L$.

Now using (3.25) and (3.26) in (3.24), the outage probability is given by

$$P_{out} = \int_0^{A_1} \frac{1}{\bar{\gamma}_{SD}} exp\left(\frac{-\gamma_{SD}}{\bar{\gamma}_{SD}}\right) d\gamma_{SD}$$

$$. \int_0^{A_2} \cdots \int_0^{A_2} \prod_{m=1}^{L} \left(\frac{1}{\bar{\gamma}_{R_m D}}\right) exp\left(-\sum_{m=1}^{L} \frac{\gamma_{R_m D}}{\bar{\gamma}_{R_m D}}\right) \prod_{m=1}^{L} d\gamma_{R_m D}$$

$$= \left(1 - exp\left(\frac{-A_1}{\bar{\gamma}_{SD}}\right)\right) \prod_{m=1}^{L} \left(\int_0^{A_2} \frac{1}{\bar{\gamma}_{R_m D}} exp\left(\frac{-\gamma_{R_m D}}{\bar{\gamma}_{R_m D}}\right) d\gamma_{R_m D}\right)$$

$$= \left(1 - exp\left(\frac{-A_1}{\bar{\gamma}_{SD}}\right)\right) \prod_{m=1}^{L} \left(1 - exp\left(\frac{-A_2}{\bar{\gamma}_{R_m D}}\right)\right). \qquad (3.27)$$

To show the diversity in (3.27), we consider Taylor series expansion of exp(x). In particular, we consider the first two terms of this expansion. As such, P_{out}, can be approximated as

$$P_{out} \approx \frac{A_1}{\bar{\gamma}_{SD}} \prod_{m=1}^{L} \frac{A_2}{\bar{\gamma}_{R_m D}}$$

$$\approx (2^{R_C} - 1)(L+1) \left[\left(2^{\left(\frac{R_C}{1-\beta}\right)} - 1\right)(L+1)\right]^L (\bar{\gamma}_{SD})^{-1} \prod_{m=1}^{L}(\bar{\gamma}_{R_m D})^{-1}, \quad (3.28)$$

which suggests that the diversity order is $L+1$ when the channel from S to R_m is error-free.

3.3.2 Distributed Coded Cooperation with Errors at Relays

When a relay is successful in decoding the received message, then that relay will not be in outage, which translates into the following event: $C(\gamma_{SR_m}) = \beta \log_2(1 + \gamma_{SR_m}) > R_C$. Otherwise, the relay will be in outage. Thus, we can write the end-to-end outage probability at the destination given the two phases of transmission as

$$P_{out} = Pr\{(1 + \gamma_{SD})^{\beta}(1 + \gamma_{SD})^{(1-\beta)} < 2^{R_C}\} \prod_{m=1}^{L} Pr\left\{\gamma_{SR_m} < 2^{\frac{R_C}{\beta}} - 1\right\}$$

$$+ \sum_{L=1}^{L-1} \sum_{\Omega} \left[\prod_{j \notin \Omega} Pr\left\{\gamma_{SR_j} < 2^{\frac{R_C}{\beta}} - 1\right\} \prod_{j \in \Omega} Pr\left\{\gamma_{SR_j} > 2^{\frac{R_C}{\beta}} - 1\right\}\right.$$

$$\left. . Pr\left\{(1 + \gamma_{SD})^{\beta}\left(1 + \frac{1}{(L'+1)}\left[\gamma_{SD} + \sum_{j \in \Omega} \gamma_{R_j D}\right]\right)^{(1-\beta)} < 2^{R_C}\right\}\right]$$

$$+ \prod_{m=1}^{L} Pr\left\{\gamma_{SR_m} > 2^{\frac{R_C}{\beta}} - 1\right\}$$

$$. Pr\left\{(1 + \gamma_{SD})^{\beta}\left(1 + \frac{1}{(L+1)}\left[\gamma_{SD} + \sum_{m=1}^{L} \gamma_{R_m D}\right]\right)^{(1-\beta)} < 2^{R_C}\right\}. \quad (3.29)$$

Note that the first term in (3.29) corresponds to the case when all relays are in outage; the second term corresponds to the case when some of the relays are in outage; and the third term corresponds to the case when none of the relays are in outage. It should be clear here that in all three cases the destination is in outage.

The expression in (3.29) can be written in a more compact form as

$$P_{out} = I_1 \prod_{m=1}^{L}\left(1 - exp\left(\frac{1 - 2^{\frac{R_C}{\beta}}}{\bar{\gamma}_{SR_m}}\right)\right) + \sum_{L=1}^{L-1} \sum_{\Omega}\left[\prod_{j \notin \Omega}\left(1 - exp\left(\frac{1 - 2^{\frac{R_C}{\beta}}}{\bar{\gamma}_{SR_j}}\right)\right)\right.$$

$$\left. . \prod_{j \in \Omega} exp\left(\frac{1 - 2^{\frac{R_C}{\beta}}}{\bar{\gamma}_{SR_j}}\right) I_2(j)\right] + I_3 \prod_{m=1}^{L} exp\left(\frac{1 - 2^{\frac{R_C}{\beta}}}{\bar{\gamma}_{SR_m}}\right), \quad (3.30)$$

where I_1, $I_2(j)$, I_3, using Appendix A, are given by

$$I_1 = 1 - exp\left(\frac{(1 - 2^{R_C})}{\bar{\gamma}_{SD}}\right), \quad (3.31)$$

$$I_2(j) = \left(1 - exp\left(\frac{(1 - 2^{R_C})(L' + 1)}{\bar{\gamma}_{SD}}\right)\right)$$

$$\cdot \prod_{j \in \Omega} \left(1 - exp\left(\frac{\left(1 - 2^{\left(\frac{R_C}{1-\beta}\right)}\right)(L'+1)}{\bar{\gamma}_{R_j D}} \right) \right), \tag{3.32}$$

$$I_3 = \left(1 - exp\left(\frac{(1 - 2^{R_C})(L+1)}{\bar{\gamma}_{SD}} \right) \right)$$

$$\cdot \prod_{m=1}^{L} \left(1 - exp\left(\frac{\left(1 - 2^{\left(\frac{R_C}{1-\beta}\right)}\right)(L+1)}{\bar{\gamma}_{R_m D}} \right) \right). \tag{3.33}$$

Upon applying Taylor series expansion of *exp(x)*, and considering only the first two terms of this expansion, the outage probability in (3.30) is given by

$$P_{out} \approx (2^{R_C} - 1)\left(2^{\frac{R_C}{\beta}} - 1 \right)^L (\bar{\gamma}_{SD})^{-1} \prod_{m=1}^{L} \left(\bar{\gamma}_{SR_m} \right)^{-1}$$

$$+ \sum_{L=1}^{L-1} \sum_{\Omega} \left[\prod_{j \notin \Omega} \left(2^{\frac{R_C}{\beta}} - 1 \right) \left(\bar{\gamma}_{SR_j} \right)^{-1} \prod_{j \in \Omega} \left(1 + \frac{\left(1 - 2^{\frac{R_C}{\beta}}\right)}{\bar{\gamma}_{SR_j}} \right) (2^{R_C} - 1)(L'+1) \right.$$

$$\left. \cdot (\bar{\gamma}_{SD})^{-1} \prod_{j \in \Omega} \left(\left(2^{\left(\frac{R_C}{1-\beta}\right)} - 1 \right)(L'+1) \left(\bar{\gamma}_{R_j D} \right)^{-1} \right) \right] + \prod_{m=1}^{L} \left(1 + \frac{\left(1 - 2^{\frac{R_C}{\beta}}\right)}{\bar{\gamma}_{SR_m}} \right)$$

$$(2^{R_C} - 1)(L+1)\left(\left(2^{\left(\frac{R_C}{1-\beta}\right)} - 1 \right)(L+1) \right)^L (\bar{\gamma}_{SD})^{-1} \prod_{m=1}^{L} \left(\bar{\gamma}_{R_m D} \right)^{-1}. \tag{3.34}$$

Similar to the argument used for (3.20), when $\bar{\gamma}_{SR_m}$ are very large, (3.34) reduces to (3.28), which proves that the diversity is $L + 1$ with perfect detection at the relays. When $\bar{\gamma}_{SR_m}$ are very small, however, the diversity gain diminishes and the system will only offer SNR gains relative to the non-cooperative case.

3.4　Simulation Results

In our simulations, we assume that the relay nodes operate in the DF mode. For simplicity, BPSK and quadrature phase shift keying (QPSK) modulations are assumed. The different sub-channels between the source, relays and destination are assumed to be independent flat Rayleigh fading channels. Also, we consider a quasi-static fading channel where the channel coefficients are fixed for the duration of the frame and change independently from one frame to another. In all simulations, otherwise mentioned, the transmitted frame size is equal to $n_1 = n_2 = 130$ coded bits.

The convolutional code used is of constraint length four and generator polynomials $(13, 15, 15, 17)_{octal}$ [44]. When the relays cooperate with the source node, the source transmits the codewords corresponding to rate 1/2, $(13, 15)_{octal}$ convolutional code to the relay and destination nodes in the first frame. The relay nodes receive this codeword and decoding is performed to obtain an estimate of the source information bits. In the second frame, the relay and source nodes transmit the codewords on orthogonal channels corresponding to rate 1/2, $(15, 17)_{octal}$ convolutional code to the destination node.

In the analysis, we assume different SNRs between the source and the relay nodes, which is the most general case. This incorporates different network topologies and distances between the source and relay nodes. However, for simplicity, we assume in the simulations that the average SNRs for all sub-channels between the source and relay nodes are equal $(\bar{\gamma}_{SR_1} = \bar{\gamma}_{SR_2} = \cdots = \bar{\gamma}_{SR_L} = \bar{\gamma}_{SR} = \bar{\gamma}_{RD})$. Also we assume that the *R-D* and *S-D* channels have equal SNRs, i.e., $\bar{\gamma}_{SD} = \bar{\gamma}_{RD} = E_b/N_0$, but the *S-R* SNR, $\bar{\gamma}_{SR}$, can be different.

The union upper bounds on the average bit error probability of the proposed coding scheme operating in the error-free DF mode at relay node for different values of d_{max} are shown in Figure 3.3. The code polynomials $(13, 15, 15, 17)_{octal}$ and the free distance of this code is $d_{free} = 13$. We also include in the figure, for comparison, the simulated BER results of the proposed coding scheme operating in the error-free DF mode.
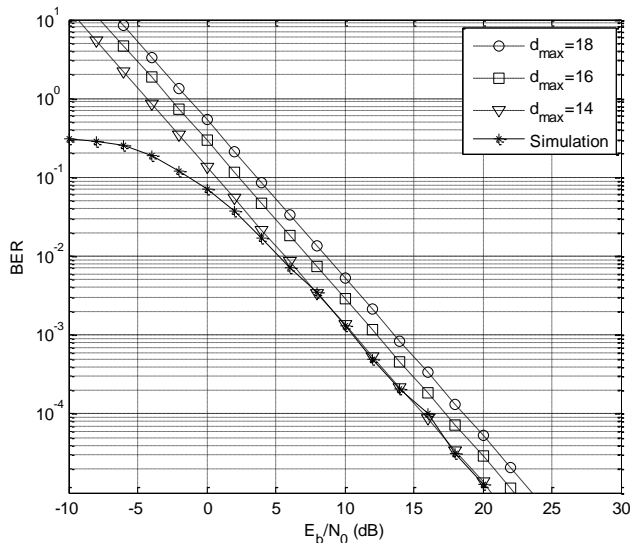

Figure 3.3 *Comparison of analysis and simulated BER with error-free detection at relay node for different values of d_{max}; code $(13, 15, 15, 17)_{octal}$ with $R_{C_1} = R_{C_2} = 0.5$.*

Figure 3.4 shows a comparison of the simulated BER and the analysis in (3.15) and (3.16) for L = 1, 2 relay channels, and M = 2 (BPSK) operating in the error-free DF mode at all relay nodes. In the figure, we include the performance of non-cooperative system as a reference. In non-cooperative case, the source uses convolutional code $(13, 15, 15, 17)_{octal}$ of rate 1/4. As shown from these results, for SNR values as high as 10 dB, the analysis is quite tight when compared to simulated results. Also, the diversity gain achieved using different number of relays is evident from these results.

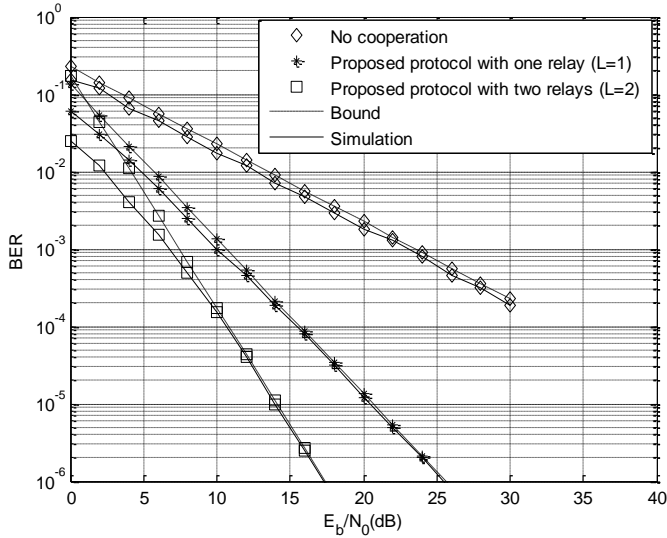**Figure 3.4** *Comparison of the simulated BER and analysis for the proposed coding scheme for L = 1, 2 relay channels, and M = 2 (BPSK) with error-free detection at relay nodes.*

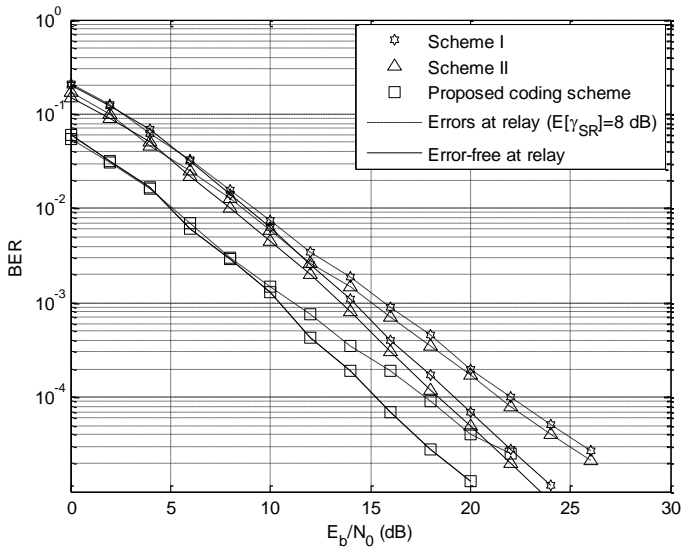**Figure 3.5** *The BER performance comparison of proposed coding scheme and the schemes I, II in section 2.2 for L = 1 relay, M = 2 (BPSK) with error-free detection at relay node, and $\bar{\gamma}_{SR} = 8\ dB$ with relay errors.*

Figure 3.5 shows the BER performance comparison of the proposed coding scheme and the schemes I, II in section 2.2 for both erroneous and error-free detection at the relays. In this figure, we assume $L=1$ and $M=2$ (BPSK). To maintain the same average power in the second frame, the source and relay nodes divide their power according to the ratio $1/(L+1)=1/2$. As shown in the figure, the performance of the proposed coding scheme is *3 dB* better than the scheme II. The performance of the scheme II is *0.5 dB* better than the scheme I. The *0.5-dB* penalty incurred is due to the use of RCPC code.

Intuitively, when the links between the source and relays are error-free, the system mimics a MIMO system with $L+1$ transmit antennas where full diversity is always achieved (assuming independent fading channels). On the contrary, when the transmissions from the source to the relays are subject to channel errors, the loss in diversity is mainly a function of $\bar{\gamma}_{SR}$. This is clear from Figure 3.6, where we show the same performance plots as a function of $\bar{\gamma}_{SR}$ with equal transmit power from the relay and source nodes (i.e., in the second frame). The BER curve when the relay is error-free, having diversity order two, is also shown for comparison. The loss of diversity can be clearly observed when the relay is relatively far from the source, resulting in a low $\bar{\gamma}_{SR}$.

Figure 3.7 shows a comparison between the simulated and the BER upper bound corresponding to (3.16) and (3.20) for $L=2$ relay channels, and $M=4$ (QPSK) as a function of $\bar{\gamma}_{SR}$ with equal transmit power from the relay and source nodes (i.e., in the second frame).

Figure 3.8 shows the outage probability in (3.28) for the proposed transmission scheme (see Figure 3.2) for $L=1, 2, 3$ relay channels. In this figure, we consider error-free recovery at the relays. As shown, the diversity gain achieved using

different number of relays is evident from these results.
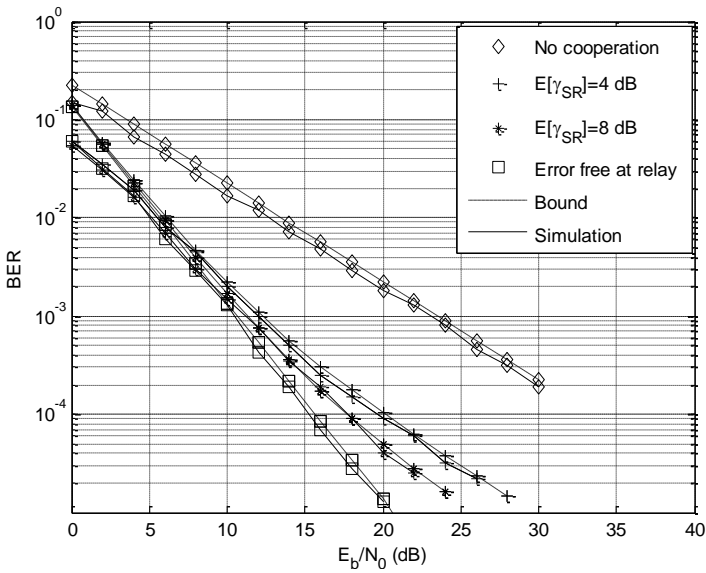
Figure 3.6 *Comparison of analysis and simulated BER for slow Rayleigh fading,*
L=1 (one relay), M=2 (BPSK), and different $\bar{\gamma}_{SR}$ with relay errors.
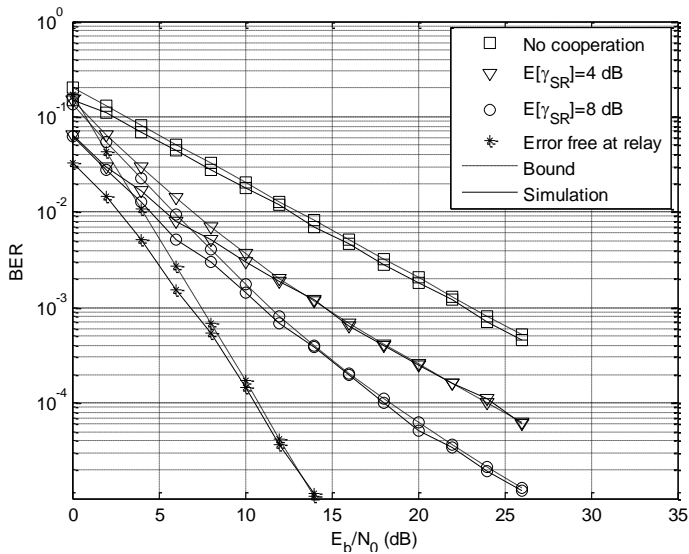
Figure 3.7 *Comparison of analysis and simulated BER for slow Rayleigh fading,*
L=2 (two relays), M=4 (QPSK), and different $\bar{\gamma}_{SR}$ with relay errors.
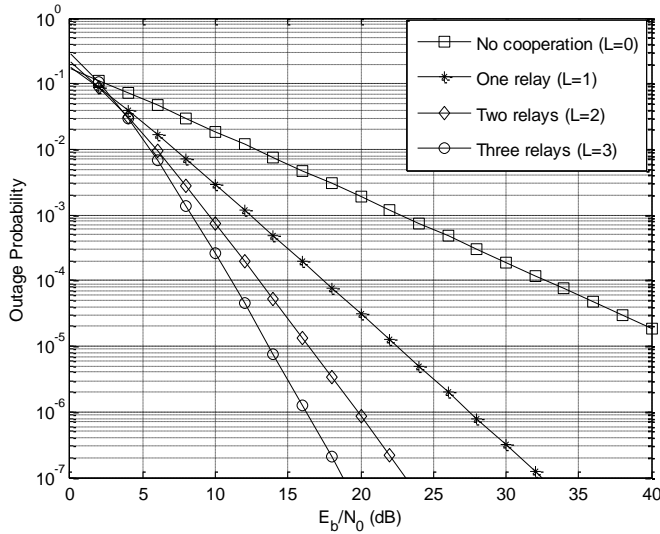
Figure 3.8 *Outage probability for slow Rayleigh fading for L = 1, 2, and 3 relay channels with error-free detection at relay nodes, $\bar{\gamma}_{SD} = \bar{\gamma}_{RD} = \frac{E_b}{N_0}$.*
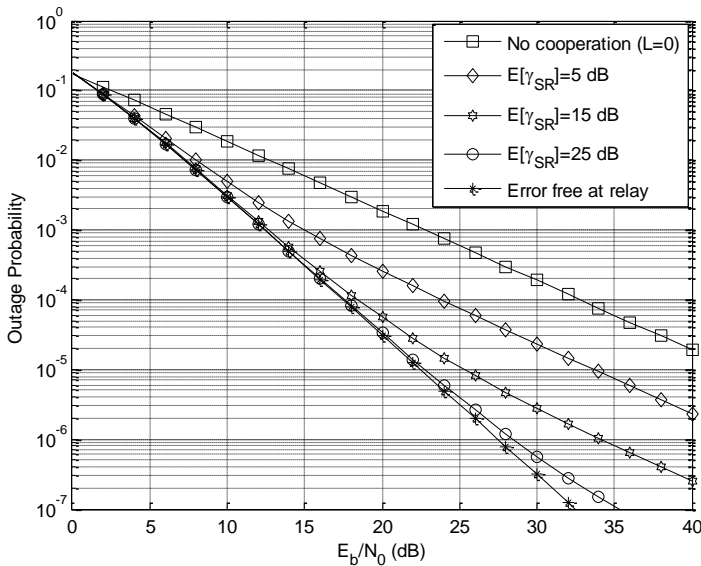
Figure 3.9 *Outage probability for slow Rayleigh fading, L = 1 (one relay), β = 0.5, and different $\bar{\gamma}_{SR}$ with relay errors.*

Finally in Figure 3.9, we present the outage probability in (3.34) when the

effect of channel errors at the relay is considered. In this figure, we assume $L=1$ relay), and $\beta = 0.5$. It is clear from this figure that $\bar{\gamma}_{SR}$ as gets larger, the performance converges to the ideal error-free case. We noted that for $\bar{\gamma}_{SR} > 25\ dB$ the diversity order is approximately two. However, for $\bar{\gamma}_{SR} = 25\ dB$ this diversity order is slightly reduced. Also when $\bar{\gamma}_{SR}$ decreases to $5\ dB$, the overall diversity order drops to one.

4

Antenna/Relay for Coded Cooperative Networks

In this chapter, we analyze the impact of antenna/relay selection on the performance of cooperative networks in conjunction with the distributed coding scheme introduced in Chapter 3. Of course, antenna/relay selection can be used with any other coding scheme and any relay configuration. For simplicity, we assume that there is a single relay that is equipped with n_R antennas and only the best antenna is selected. The selection criterion is based on selecting the best source-relay sub-channel (out of the n_R sub-channels at the relay). The latter assumption is needed essentially to preserve the original structure of distributed MIMO systems where each relay node is assumed to be equipped with one antenna and one RF chain. For this scenario, assuming DF and AF relaying, we derive upper bounds on the BER for M−PSK transmission. Our analytical results show that the proposed scheme achieves full diversity for the entire range of bit error rate of interest, unlike the case without antenna selection.

As for relay selection, in terms of performance analysis, it is exactly the same as the case for antenna selection provided that the receive antennas see independent fades. A main difference between the two cases is that, with relay selection, the relays need to feedback their reliabilities to the source to decide on what relay to use, whereas this feedback is not required for antenna selection. On the other hand, with relay selection, the problem of spatial correlation that arises from collocated antennas can be avoided when the relays are equipped with single antennas. One can also consider multiple antennas and multiple relay selection.

4.1 System Model and Preliminaries

The system model considered in this section is the same one considered in Chapter 3 except that the relay node here is assumed to be equipped with n_R antennas. As shown in Figure 4.1, for simplicity, there are three nodes: source,

relay and destination. The transmitter is equipped with two recursive systematic convolutional (RSC) encoders, denoted by E_1 and E_2, whose rates are $R_{C_1} = K/N_1$ and $R_{C_2} = K/N_2$, respectively, where K is the information sequence length, N_1 is the codeword length at the output of E_1, and N_2 is the codeword length at the output of E_2. The information sequence b is encoded by E_1, resulting in X_1. Assuming M$-$PSK, X_1 is then modulated, resulting in a modulated sequence, C_1, denoted as Frame 1. The length of this sequence is $n_1 = N_1/\log_2 M$. C_1 is then broadcasted from the source to the relay and destination nodes. At the relay, the signal corresponding to the best source-relay sub-channel (out of the n_R received signals) is selected.

4.1.1 Decode-and-Forward Relaying

The system model considered, depicted in Figure 4.1, is the same one considered in Chapter 3 except that the relay node here is assumed to be equipped with n_R antennas.
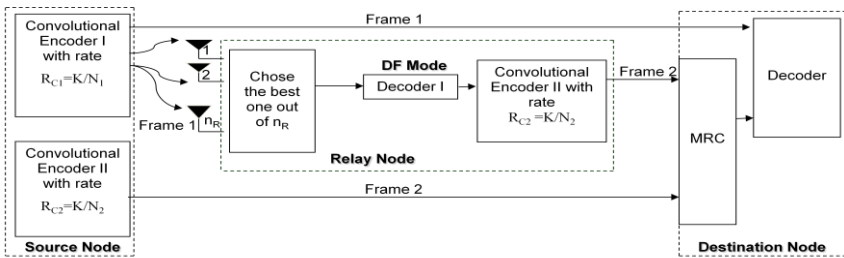

Figure 4.1 *Distributed coded transmission scheme in the DF mode with receive antenna selection at the relay node.*

Therefore, the signals received at the relay and the destination nodes at time t, in the first frame, are respectively given by

$$y_{SR_j}(t) = \sqrt{R_{C_1} E_{SR}} h_{SR_j}(t)s(t) + w_{SR_j}(t), t = 1,2,\cdots,n_1; j = 1,2,\cdots,n_R, \quad (4.1)$$

$$y_{SD}(t) = \sqrt{R_{C_1}E_{SD}}h_{SD}(t)s(t) + w_{SD}(t), \ t = 1,2,\cdots,n_1 \tag{4.2}$$

where $s(t)$ is the output of the modulator of the source node at time t, $h_{SR_j}(t)$ is the fading coefficient between the source transmit antenna and the jth receive antenna at the relay, $h_{SD}(t)$ is the fading coefficient for the $S \to D$ link, E_{SR} and E_{SD} represent the transmitted signal energies for the corresponding link, $w_{SR_j}(t)$ and $w_{SD}(t)$ are AWGN samples with zero mean and variance $N_0/2$ per dimension, and R_{C_1} is the code rate of convolutional encoder I.

In the second frame, If the relay correctly decodes the message it received from the source, the destination receives two versions of C_2, one directly from the source and the other from the relay. MRC combining is performed at the destination. In this case, the received signals at the destination node at time t are given by

$$y_{RD}(t) = \sqrt{R_{C_2}\alpha E_{RD}}h_{RD}(t)\hat{s}(t) + w_{RD}(t), t = n_1 + 1, n_1 + 2, \cdots, n_1 + n_2, \tag{4.3}$$

$$y_{SD}(t) = \sqrt{R_{C_2}(1-\alpha)E_{SD}}h_{SD}(t)s(t) + w_{SD}(t), t = n_1 + 1, n_1 + 2, \cdots, n_1 + n_2 \tag{4.4}$$

where $\hat{s}(t)$ is the output of the modulator of the relay node at time t, $h_{RD}(t)$ is the fading coefficient of the R-D link, E_{RD} represents the transmitted signal energy for the R-D link, $w_{RD}(t)$ is an AWGN noise sample with zero mean and variance $N_0/2$ per dimension, and $0 \le \alpha \le 1$ is the fraction of power transmitted from the relay node during the second frame. For example, when $\alpha = 0$, the relay node does not transmit (no cooperation); whereas when $\alpha = 1$, the source node does not transmit. That is the relay node transmits with energy αE_{RD}, and the source node transmits with energy $(1 - \alpha)E_{SD}$.

4.1.2 Amplify-and-Forward Relaying

The system model for the AF mode is depicted in Figure 4.2. Let $h_{SR}(t)$ be a vector representing the fading coefficients between the source and the n_R antennas at the relay node, that is,

$$\mathbf{h}_{SR}(t) = \left[h_{SR}^1(t), h_{SR}^2(t), \cdots, h_{SR}^{n_R}(t) \right].$$

Also let $h_{SR}^{max}(t)$ denote the fading coefficient in $\mathbf{h}_{SR}(t)$ that has the *largest norm*. As such, the signals received at the destination and the relay (after antenna selection) during the first frame are respectively given by

$$y_{SR}(t) = \sqrt{R_{C_1} E_{SR}} h_{SR}^{max}(t) s(t) + w_{SR}(t), \quad t = 1,2,\cdots,n_1, \tag{4.5}$$

$$y_{SD}(t) = \sqrt{R_{C_1} E_{SD}} h_{SD}(t) s(t) + w_{SD}(t), \quad t = 1,2,\cdots,n_1, \tag{4.6}$$

where s(t) is the output of the modulator of the source node at time t.
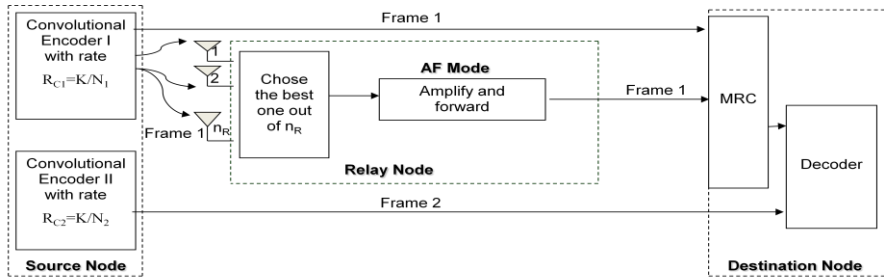
Figure 4.2 *Distributed coded transmission scheme in the AF mode with receive antenna selection at the relay node.*

In the second frame, the destination receives a copy of Frame 1 (i.e., a copy of C_1) from the relay after amplification, as well as Frame 2 directly from the source.

The latter frame is the output of E_2, denoted as X_2, after being modulated to result in a modulated sequence denoted by C_2 of length $n_2 = N_2 / log_2 M$. These two frames are assumed to be transmitted on orthogonal sub-channels. Thus,

assuming negligible delay at the relay, the signals received at the destination during the second frame are then given by

$$y_{RD}(t) = A_{RD}(t)h_{RD}(t)y_{SR}(t) + w_{RD}(t), \quad t = 1,2,\cdots,n_1, \qquad (4.7)$$

$$y_{SD}(t) = \sqrt{R_{C_2}(1-\alpha)E_{SD}}h_{SD}(t)s(t) + w_{SD}(t), \quad t = n_1+1, n_1+2,\cdots,n_1+n_2 \quad (4.8)$$

Where $A_{RD}(t)$ is the amplification factor at the relay. One choice for the gain that we use in this book is [22]

$$A_{RD}(t) = \sqrt{\frac{R_{C_1}\alpha E_{RD}}{R_{C_1}E_{SR}\left|h_{SR}^{max}(t)\right|^2 + \frac{N_0}{2}}}. \qquad (4.9)$$

The two received copies of C_1 are combined at the receiver via MRC, and the resulting frame is augmented with the received version of C_2. The augmented codeword is then fed into a Viterbi decoder matched to both encoders at the source to recover the information bits.

4.2 Decode-and-Forward Relaying: Performance Analysis with Selection

In this section, we evaluate the performance of the above scheme with antenna selection in terms of the average BER at the destination. To derive a closed form expression for the upper bound on the pairwise error probability (PEP) with receive antenna selection at the relay node, we first consider the performance with perfect detection at the relay. We understand that this is rather optimistic and can only be justified under special conditions (i.e., high SNR or un-faded channel between the source and relay), but we use it here as a benchmark for the more realistic case, that is, with decoded errors at the relay. If a relay correctly decodes the message it received from the source node using CRC code, re-encode it with a different code and send it to the destination node, which is more realistic to apply.

4.2.1 Decode-and-Forward with Error-Free Relaying

Under the assumption of error free reception at the relay node, the instantaneous received SNR for the channel from S to D for the first frame is given by

$$\gamma_D(t) = 2R_{C_1} \frac{E_{RD}}{N_0} |h_{SD}(t)|^2 = 2R_{C_1}\gamma_{SD}(t), \quad t = 1,2,\cdots,n_1, \qquad (4.10)$$

and the instantaneous received SNR for the channels from S to D and R to D for the second frame is given by

$$\gamma_D(t) = 2R_{C_2} \left(\frac{(1-\alpha)E_{SD}}{N_0} |h_{SD}(t)|^2 + \frac{\alpha E_{RD}}{N_0} |h_{RD}(t)|^2 \right)$$

$$= 2R_{C_2}\big((1-\alpha)\gamma_{SD}(t) + \alpha\gamma_{RD}(t)\big), \quad t = n_1 + 1, n_1 + 2, \cdots, n_1 + n_2, (4.11)$$

where $\gamma_{SD}(t) = \frac{E_{SD}}{N_0} |h_{SD}(t)|^2, \gamma_{RD}(t) = \frac{E_{RD}}{N_0} |h_{RD}(t)|^2$. To maintain the same average power in the second frame, the relay and source nodes split their powers according to the ratio α.

When the fading coefficients h_{SD}, and h_{RD} are constant over the codeword, the conditional pairwise error probability is given by

$$P(d|\gamma_{SD},\gamma_{RD}) = Q\left(\sqrt{2g_{PSK}\big([R_{C_1}d_1 + (1-\alpha)R_{C_2}d_2]\gamma_{SD} + \alpha R_{C_2}d_2\gamma_{RD}\big)} \right), (4.12)$$

where d_1 and d_2 are the Hamming distances corresponding to E_1 and E_2, respectively, where $d = d_1 + d_2$. Using (3.10), we can rewrite (4.12) as

$$P(d|\gamma_{SD},\gamma_{RD}) = \frac{1}{\pi} \int_0^{\frac{(M-1)\pi}{M}} exp\left(\frac{-g_{PSK}\big(R_{C_1}d_1 + (1-\alpha)R_{C_2}d_2\big)\gamma_{SD}}{\sin^2\theta} \right)$$

$$. exp\left(\frac{-g_{PSK}\, \alpha R_{C_2}d_2\gamma_{RD}}{\sin^2\theta} \right) d\theta. \qquad (4.13)$$

The average PEP is then given by

$$P(d) = \frac{1}{\pi} \int_{0}^{\frac{(M-1)\pi}{M}} \int_{0}^{\infty} \int_{0}^{0} exp\left(\frac{-g_{PSK}\left(R_{C_1}d_1 + (1-\alpha)R_{C_2}d_2\right)\gamma_{SD}}{\sin^2\theta}\right)$$

$$. exp\left(\frac{-g_{PSK}\,\alpha R_{C_2}d_2\gamma_{RD}}{\sin^2\theta}\right)p_{\gamma_{RD}}(\gamma_{RD})p_{\gamma_{SD}}(\gamma_{SD})d\gamma_{RD}d\gamma_{SD}d\theta \qquad (4.14)$$

Using (3.13), one can show that (4.14) can be expressed as

$$P(d) = \frac{1}{\pi} \int_{0}^{\frac{(M-1)\pi}{M}} \left(1 + \frac{g_{PSK}\left(R_{C_1}d_1 + (1-\alpha)R_{C_2}d_2\right)\bar{\gamma}_{SD}}{\sin^2\theta}\right)^{-1}$$

$$\left(1 + \frac{g_{PSK}\,\alpha R_{C_2}d_2\bar{\gamma}_{RD}}{\sin^2\theta}\right)^{-1} d\theta, \qquad (4.15)$$

where $\bar{\gamma}_{SD} = \frac{E_{SD}}{N_0}E[|h_{SD}|^2]$, $\bar{\gamma}_{RD} = \frac{E_{RD}}{N_0}E[|h_{RD}|^2]$ are the average SNRs.

Noting that when the average SNRs $\bar{\gamma}_{SD}$ and $\bar{\gamma}_{RD}$ are relatively high, (4.15) can be approximated as

$$P(d) \approx \left(\sin\frac{\pi}{M}\right)^{-4} \left(\alpha R_{C_2}d_2\bar{\gamma}_{RD}\right)^{-1} \left(\left(R_{C_1}d_1 + (1-\alpha)R_{C_2}d_2\right)\bar{\gamma}_{SD}\right)^{-1}$$

$$.\frac{1}{\pi}\int_{0}^{\frac{(M-1)\pi}{M}} \sin^4\theta d\theta, \qquad (4.16)$$

which suggests that the diversity order achieved is two when the $S-R$ is error-free. Having obtained the PEP in (4.16), the BER probability can be upper bounded using (3.16).

4.2.2 Decode-and-Forward with Relay Errors

In this section, we consider the realistic scenario in which the relay may fail to correctly decode the message it received from the source, that is, when it's CRC dose not check. As mentioned before, we assume that the relay is equipped with

n_R antennas and only the best antenna is selected. Without loss of generality, we can assume that [44]

$$\gamma_{SR_1}(t) \leq \gamma_{SR_2}(t) \leq \cdots \leq \gamma_{SR_{n_R}}(t), \tag{4.17}$$

where $\gamma_{SR_j}(t) = \frac{E_{SR}}{N_0}\left|h_{SR_j}(t)\right|^2$ and $j = 1,2,\cdots,n_R$. Knowing that the largest number out of n_R nonnegative numbers is always greater than or equal to the average of these n_R numbers, we have [44]

$$\frac{1}{n_R}\sum_{j=1}^{n_R}\gamma_{SR_j}(t) \leq \gamma_{SR_{n_R}}(t). \tag{4.18}$$

Using (4.17) and (4.18), when the fading coefficients h_{SR_j}, h_{SD}, and h_{RD} are constant over the codeword, the conditional PEP is given by

$$P\left(d|\gamma_{SD},\gamma_{RD},\gamma_{SR_j}\right) = \left[1 - Q\left(\sqrt{\frac{2g_{PSK}R_{C_1}d_1}{n_R}\sum_{j=1}^{n_R}\gamma_{SR_j}}\right)\right]$$

$$\cdot Q\left(\sqrt{2g_{PSK}\left(\left[R_{C_1}d_1 + (1-\alpha)R_{C_2}d_2\right]\gamma_{SD} + \alpha R_{C_2}d_2\gamma_{RD}\right)}\right)$$

$$+ Q\left(\sqrt{\frac{2g_{PSK}R_{C_1}d_1}{n_R}\sum_{j=1}^{n_R}\gamma_{SR_j}}\right)Q\left(\sqrt{2g_{PSK}\left[R_{C_1}d_1 + R_{C_2}d_2\right]\gamma_{SD}}\right). \tag{4.19}$$

Using (3.10), we can rewrite (4.19) as

$$P\left(d|\gamma_{SD},\gamma_{RD},\gamma_{SR_j}\right) = \frac{1}{\pi^2}\int_0^{\frac{(M-1)\pi}{M}}\int_0^{\frac{(M-1)\pi}{M}} exp\left(\frac{-g_{PSK}R_{C_1}d_1}{n_R\sin^2\theta_1}\sum_{j=1}^{n_R}\gamma_{SR_j}\right)$$

$$\cdot exp\left(\frac{-g_{PSK}\left[R_{C_1}d_1 + R_{C_2}d_2\right]\gamma_{SD}}{\sin^2\theta_2}\right)d\theta_1 d\theta_2 + \frac{1}{\pi}\int_0^{\frac{(M-1)\pi}{M}}$$

$$\cdot exp\left(\frac{-g_{PSK}\alpha R_{C_2}d_2\gamma_{RD}}{\sin^2\theta}\right)exp\left(\frac{-g_{PSK}\left[R_{C_1}d_1 + (1-\alpha)R_{C_2}d_2\right]\gamma_{SD}}{\sin^2\theta}\right)d\theta$$

$$-\frac{1}{\pi^2} \int\limits_{0}^{\frac{(M-1)\pi}{M}} \int\limits_{0}^{\frac{(M-1)\pi}{M}} exp\left(\frac{-g_{PSK}R_{C_1}d_1}{n_R \sin^2\theta_1}\sum_{j=1}^{n_R}\gamma_{SR_j}\right) exp\left(\frac{-g_{PSK}\alpha R_{C_2}d_2\gamma_{RD}}{\sin^2\theta_2}\right)$$

$$.exp\left(\frac{-g_{PSK}\left[R_{C_1}d_1+(1-\alpha)R_{C_2}d_2\right]\gamma_{SD}}{\sin^2\theta_2}\right)d\theta_1 d\theta_2. \qquad (4.20)$$

Using (3.13), the average PEP can then be expressed as

$$P(d) = \frac{1}{\pi^2} \int\limits_{0}^{\frac{(M-1)\pi}{M}} \int\limits_{0}^{\frac{(M-1)\pi}{M}} \prod_{j=1}^{n_R}\left(1+\frac{g_{PSK}R_{C_1}d_1\bar{\gamma}_{SR_j}}{n_R\sin^2\theta_1}\right)^{-1}$$

$$\left(1+\frac{g_{PSK}\left[R_{C_1}d_1+R_{C_2}d_2\right]\bar{\gamma}_{SD}}{\sin^2\theta_2}\right)^{-1} d\theta_1 d\theta_2 + \frac{1}{\pi}\int\limits_{0}^{\frac{(M-1)\pi}{M}}$$

$$\left(1+\frac{g_{PSK}\alpha R_{C_2}d_2\bar{\gamma}_{SD}}{\sin^2\theta}\right)^{-1}\left(1+\frac{g_{PSK}\left[R_{C_1}d_1+(1-\alpha)R_{C_2}d_2\right]\bar{\gamma}_{SD}}{\sin^2\theta}\right)^{-1} d\theta$$

$$-\frac{1}{\pi^2}\int\limits_{0}^{\frac{(M-1)\pi}{M}}\int\limits_{0}^{\frac{(M-1)\pi}{M}}\prod_{j=1}^{n_R}\left(1+\frac{g_{PSK}R_{C_1}d_1\bar{\gamma}_{SR_j}}{n_R\sin^2\theta_1}\right)^{-1}$$

$$.\left(1+\frac{g_{PSK}\ \alpha R_{C_2}d_2\bar{\gamma}_{RD}}{\sin^2\theta_2}\right)^{-1}\left(1+\frac{g_{PSK}\left[R_{C_1}d_1+(1-\alpha)R_{C_2}d_2\right]\bar{\gamma}_{SD}}{\sin^2\theta_2}\right)^{-1}d\theta_1 d\theta_2, \quad (4.21)$$

where $\bar{\gamma}_{SR_j} = \frac{E_{SR_j}}{N_0}E\left[\left|h_{SR_j}\right|^2\right]$. If we assume $\bar{\gamma}_{SD}$, $\bar{\gamma}_{RD}$, and $\bar{\gamma}_{SR_j} = \bar{\gamma}_{SR}$ to be large, then (4.21) can be approximated as

$$P(d) \approx \left(\sin\frac{\pi}{M}\right)^{-2n_R-2}\left(\frac{R_{C_1}d_1\bar{\gamma}_{SR}}{n_R}\right)^{-n_R}\left(\left[R_{C_1}d_1+R_{C_2}d_2\right]\bar{\gamma}_{SD}\right)^{-1}$$

$$.\frac{1}{\pi^2}\int\limits_{0}^{\frac{(M-1)\pi}{M}}\int\limits_{0}^{\frac{(M-1)\pi}{M}}\sin^{2n_R}\theta_1\sin^2\theta_2\ d\theta_1 d\theta_2 + \left(\sin\frac{\pi}{M}\right)^{-4}$$

$$. \left(\alpha R_{C_2} d_2 \bar{\gamma}_{RD} \right)^{-1} \left([R_{C_1} d_1 + (1 - \alpha) R_{C_2} d_2] \bar{\gamma}_{SD} \right)^{-1} \frac{1}{\pi} \int_0^{\frac{(M-1)\pi}{M}} \sin^4 \theta \, d\theta$$

$$- \left(\sin \frac{\pi}{M} \right)^{-2n_R - 4} \left(\frac{R_{C_1} d_1 \bar{\gamma}_{SR}}{n_R} \right)^{-n_R} \left([R_{C_1} d_1 + (1 - \alpha) R_{C_2} d_2] \bar{\gamma}_{SD} \right)^{-1}$$

$$. \left(\alpha R_{C_2} d_2 \bar{\gamma}_{RD} \right)^{-1} \frac{1}{\pi^2} \int_0^{\frac{(M-1)\pi}{M}} \int_0^{\frac{(M-1)\pi}{M}} \sin^{2n_R} \theta_1 \sin^4 \theta_2 \, d\theta_1 d\theta_2 \qquad (4.22)$$

By substituting (4.22) into (3.16), one can obtain an upper bound on the probability of bit error.

If we assume $\bar{\gamma}_{SD} = \bar{\gamma}_{RD} = \frac{E_b}{N_0}$, and $\bar{\gamma}_{SR}$ to be large, then $P(d)$ in (4.22) is the same as $P(d)$ given in (4.16), which proves that the diversity order is two. However, it should be noted that when $\bar{\gamma}_{SR}$ is very small, many decoding errors will be seen at the relay, leading to possible loss in diversity in the SNR range of interest. However, with antenna selection, the value $\bar{\gamma}_{SR}$ of below which the diversity is lost in much smaller than that without antenna selection, as will be demonstrated in the simulation results section.

4.3 Amplify-and-Forward Relaying: Performance Analysis with Selection

As mentioned before, another relaying method is AF, which is a low-complexity alternative to DF relaying. In this section, we derive the BER performance of the underlying system with antenna selection when the relay node operates in the AF mode. The received SNR for one relay node can be obtained by weighting the combination with the respective powers. From Figure 4.2, the instantaneous received SNR for the channels from *S* to *D* and *R* to *D* for the two frames are given by

$$\gamma_Z(t) = |h_{SD}(t)|^2 \frac{R_{C_1} E_{SD}}{\sigma_{SD}^2} + |h_{SR}^{max}(t) A_{RD}(t) h_{RD}(t)|^2 \frac{R_{C_1} E_{SR}}{\sigma_{SRD}^2(t)},$$
$$t = 1, 2, \cdots, n_1, \tag{4.23}$$

$$\gamma_Z(t) = |h_{SD}(t)|^2 \frac{R_{C_2}(1-\alpha) E_{SD}}{\sigma_{SD}^2}, \quad t = n_1 + 1, n_1 + 2, \cdots, n_1 + n_2 \tag{4.24}$$

where $\sigma_{SRD}^2(t) = \sigma_{RD}^2 + |A_{RD}(t) h_{RD}(t)|^2 \sigma_{SR}^2$. In this case, substituting (4.9) in (4.23) leads to

$$\gamma_Z(t) = 2 \left(R_{C_1} \gamma_{SD}(t) + \frac{R_{C_1} \gamma_{SR}^{max}(t) R_{C_1} \alpha \gamma_{RD}(t)}{0.5 + R_{C_1} \gamma_{SR}^{max}(t) + R_{C_1} \alpha \gamma_{RD}(t)} \right), \quad t = 1, 2, \cdots, n_1, \tag{4.25}$$

where $\gamma_{SR}^{max}(t) = |h_{SR}^{max}(t)|^2 \frac{E_{SR}}{N_0}$. At high SNR, (4.25) reduces to

$$\gamma_Z(t) = 2 \left(R_{C_1} \gamma_{SD}(t) + R_{C_1} \frac{\gamma_{SR}^{max}(t) \alpha \gamma_{RD}(t)}{\gamma_{SR}^{max}(t) + \alpha \gamma_{RD}(t)} \right), \quad t = 1, 2, \cdots, n_1. \tag{4.26}$$

Using (4.24) and (4.26), when the fading coefficients h_{SD}, and h_{RD} are constant over the codeword, the conditional PEP is then given by

$$P(d | \gamma_{SD}, \gamma_{RD}, \gamma_{SR}^{max})$$

$$= Q \left(\sqrt{2 g_{PSK} \left([R_{C_1} d_1 + (1-\alpha) R_{C_2} d_2] \gamma_{SD} + R_{C_1} d_1 \frac{\gamma_{SR}^{max} \alpha \gamma_{RD}}{\gamma_{SR}^{max} + \alpha \gamma_{RD}} \right)} \right)$$

$$= Q \left(\sqrt{2 g_{PSK} \left([R_{C_1} d_1 + (1-\alpha) R_{C_2} d_2] \gamma_{SD} + R_{C_1} d_1 \gamma_{SRD} \right)} \right)$$

$$= Q \left(\sqrt{2 g_{PSK} \gamma_D} \right), \tag{4.27}$$

where

$$\gamma_D = [R_{C_1} d_1 + (1-\alpha) R_{C_2} d_2] \gamma_{SD} + R_{C_1} d_1 \gamma_{SRD}, \text{ and} \tag{4.28}$$

$$\gamma_{SRD} = \frac{\gamma_{SR}^{max} \alpha \gamma_{RD}}{\gamma_{SR}^{max} + \alpha \gamma_{RD}}. \tag{4.29}$$

Using the MGF-based approach, the average PEP is given by [59]

$P(d)$

$$= \frac{1}{\pi} \int_0^{\frac{(M-1)\pi}{M}} \Psi_{\gamma_{SD}} \left(\frac{-g_{PSK}\left[R_{C_1}d_1 + (1-\alpha)R_{C_2}d_2\right]}{\sin^2\varphi} \right) \Psi_{\gamma_{SRD}} \left(\frac{-g_{PSK}R_{C_1}d_1}{\sin^2\varphi} \right)$$

$$= \frac{1}{\pi} \int_0^{\frac{(M-1)\pi}{M}} \left(1 + \frac{g_{PSK}\left[R_{C_1}d_1 + (1-\alpha)R_{C_2}d_2\right]\bar{\gamma}_{SD}}{\sin^2\varphi} \right)^{-1}$$

$$\cdot \Psi_{\gamma_{SRD}} \left(\frac{-g_{PSK}R_{C_1}d_1}{\sin^2\varphi} \right) d\varphi. \tag{4.30}$$

In order to find $P(d)$ in (4.30), one has to find a closed form expression for the MGF of γ_{SRD}.

We define random variable (RV) Z as

$$Z \triangleq Z_1 + Z_2 = \frac{1}{\gamma_{SRD}}, \tag{4.31}$$

where $Z_1 = \frac{1}{\gamma_{SR}^{max}}$, and $Z_1 = \frac{1}{\alpha\gamma_{RD}}$, γ_{SR}^{max} and γ_{RD} are independent exponential RVs. Now, we recall some definitions that will be used later to evaluate (4.30).

Definition 1 (PDF and MGF of $Z_1 = 1/\gamma_{SR}^{max}$): Let $\mathbf{h}_{SR}$ be a $1 \times n_R$ channel matrix whose elements are i.i.d complex Gaussian random with mean zero and unit variance. Then the PDF of $Z_1 = 1/\gamma_{SR}^{max}$ can be evaluated with the help of [62] to yield

$$p_{Z_1}(z_1) = \sum_{i=0}^{n_R-1} \frac{n_R}{\bar{\gamma}_{SR} z_1^2} \binom{n_R-1}{i} (-1)^{n_R-1-i} exp\left(-\frac{n_R-i}{\bar{\gamma}_{SR} z_1} \right) U(z_1), \tag{4.32}$$

and its MGF is given by

$$\Psi_{Z_1}(-s) = \int_0^\infty p_{Z_1}(z_1) \exp(-sz_1) \, dz_1$$

$$= \frac{2n_R\sqrt{s}}{\sqrt{\bar{\gamma}_{SR}}} \sum_{i=0}^{n_R-1} \binom{n_R-1}{i} \frac{(-1)^{n_R-1-i}}{\sqrt{n_R-i}} K_1\left(\sqrt{\frac{4s(n_R-i)}{\bar{\gamma}_{SR}}}\right), \tag{4.33}$$

where $K_1(\cdot)$ is the first order modified Bessel function of the second kind.

Definition 2 (PDF and MGF of $Z_2 = 1/\alpha\gamma_{RD}$): Given an exponential RV γ_{RD}, the PDF of $Z_2 = 1/\alpha\gamma_{RD}$ can be shown as

$$p_{Z_2}(z_2) = \frac{1}{\alpha\bar{\gamma}_{RD}\,z_2^2} exp\left(-\frac{1}{\alpha\bar{\gamma}_{RD}\,z_2}\right) U(z_2) \tag{4.34}$$

and its MGF is given by

$$\Psi_{Z_2}(-s) = \int_0^\infty p_{Z_2}(z_2)\exp(-sz_2)\,dz_2$$

$$= \sqrt{\frac{4s}{\alpha\bar{\gamma}_{RD}}}K_1\left(\sqrt{\frac{4s}{\alpha\bar{\gamma}_{RD}}}\right). \tag{4.35}$$

Definition 3 (MGF, CDF, and PDF of Z): The MGF of $Z = Z_1 + Z_2$, $\Psi_Z(-s)$, is given by

$$\Psi_Z(-s) = \Psi_{Z_1}(-s)\Psi_{Z_2}(-s)$$

$$= \frac{4n_R s}{\sqrt{\alpha\bar{\gamma}_{SR}\bar{\gamma}_{RD}}}K_1\left(\sqrt{\frac{4s}{\alpha\bar{\gamma}_{RD}}}\right)\sum_{i=0}^{n_R-1}\binom{n_R-1}{i}\frac{(-1)^{n_R-1-i}}{\sqrt{n_R-i}}K_1\left(\sqrt{\frac{4s(n_R-i)}{\bar{\gamma}_{SR}}}\right). \tag{4.36}$$

The cumulative distribution function (CDF) of Z, $P_Z(z)$, can be shown with the help of [63] as

$$P_Z(z) = l^{-1}\left[\frac{\Psi_Z(-s)}{s}\right] =$$

$$l^{-1}\left[\left[\frac{4n_R}{\sqrt{\alpha\bar{\gamma}_{SR}\bar{\gamma}_{RD}}}K_1\left(\sqrt{\frac{4s}{\alpha\bar{\gamma}_{RD}}}\right)\sum_{i=0}^{n_R-1}\binom{n_R-1}{i}\frac{(-1)^{n_R-1-i}}{\sqrt{n_R-i}}K_1\left(\sqrt{\frac{4s(n_R-i)}{\bar{\gamma}_{SR}}}\right)\right]\right]$$

$$= \frac{2n_R}{z\sqrt{\alpha\bar{\gamma}_{SR}\bar{\gamma}_{RD}}}\sum_{i=0}^{n_R-1}\binom{n_R-1}{i}\frac{(-1)^{n_R-1-i}}{\sqrt{n_R-i}}exp\left(-\left[\frac{(n_R-i)}{\bar{\gamma}_{SR}}+\frac{1}{\alpha\bar{\gamma}_{RD}}\right]\frac{1}{z}\right)$$

$$. K_1 \left(\frac{1}{z} \sqrt{\frac{4(n_R - i)}{\alpha \bar{\gamma}_{SR} \bar{\gamma}_{RD}}} \right), \tag{4.37}$$

where $l^{-1}(\cdot)$ denotes the inverse Laplace transform.

Then, the PDF of Z, $p_Z(z)$, using Appendix B, is given by

$$p_Z(z) = \frac{2 n_R}{z \sqrt{\alpha \bar{\gamma}_{SR} \bar{\gamma}_{RD}}} \sum_{i=0}^{n_R - 1} \binom{n_R - 1}{i} \frac{(-1)^{n_R - 1 - i}}{\sqrt{n_R - i}}$$

$$. \exp \left(- \left[\frac{(n_R - i)}{\bar{\gamma}_{SR}} + \frac{1}{\alpha \bar{\gamma}_{RD}} \right] \frac{1}{z} \right) \left\{ \left[\frac{(n_R - i)}{\bar{\gamma}_{SR}} + \frac{1}{\alpha \bar{\gamma}_{RD}} \right] K_1 \left(\frac{1}{z} \sqrt{\frac{4(n_R - i)}{\alpha \bar{\gamma}_{SR} \bar{\gamma}_{RD}}} \right) \right.$$

$$\left. + \sqrt{\frac{4(n_R - i)}{\alpha \bar{\gamma}_{SR} \bar{\gamma}_{RD}}} K_0 \left(\frac{1}{z} \sqrt{\frac{4(n_R - i)}{\alpha \bar{\gamma}_{SR} \bar{\gamma}_{RD}}} \right) \right\}, \tag{4.38}$$

where $K_0(\cdot)$ is the zeroth-order modified Bessel function of the second kind.

From the definition of the RV Z presented in (4.31), we note that $\gamma_{SRD} = 1/Z$.

Then, the PDF of γ_{SRD}, $p_{\gamma_{SRD}}(\gamma_{SRD})$, is given by

$$p_{\gamma_{SRD}}(\gamma_{SRD}) = p_Z(z) z^2 \big|_{z = \frac{1}{\gamma_{SRD}}}$$

$$= \frac{2 \gamma_{SRD} n_R}{\sqrt{\alpha \bar{\gamma}_{SR} \bar{\gamma}_{RD}}} \sum_{i=0}^{n_R - 1} \binom{n_R - 1}{i} \frac{(-1)^{n_R - 1 - i}}{\sqrt{n_R - i}} \exp \left(- \left[\frac{(n_R - i)}{\bar{\gamma}_{SR}} + \frac{1}{\alpha \bar{\gamma}_{RD}} \right] \gamma_{SRD} \right)$$

$$. \left\{ \left[\frac{(n_R - i)}{\bar{\gamma}_{SR}} + \frac{1}{\alpha \bar{\gamma}_{RD}} \right] K_1 \left(\gamma_{SRD} \sqrt{\frac{4(n_R - i)}{\alpha \bar{\gamma}_{SR} \bar{\gamma}_{RD}}} \right) \right.$$

$$\left. + \sqrt{\frac{4(n_R - i)}{\alpha \bar{\gamma}_{SR} \bar{\gamma}_{RD}}} K_0 \left(\gamma_{SRD} \sqrt{\frac{4(n_R - i)}{\alpha \bar{\gamma}_{SR} \bar{\gamma}_{RD}}} \right) \right\}. \tag{4.39}$$

The MGF of γ_{SRD}, $\Psi_{\gamma_{SRD}}(-s)$, using Appendix B, can be shown to be

$$\Psi_{\gamma_{SRD}}(-s) = \int\limits_{0}^{\infty} p_{\gamma_{SRD}}(\gamma_{SRD}) exp(-s\gamma_{SRD})d\gamma_{SRD}$$

$$= \frac{4n_R}{\sqrt{\alpha\bar{\gamma}_{SR}\bar{\gamma}_{RD}}} \sum_{i=0}^{n_R-1} \binom{n_R-1}{i} \frac{(-1)^{n_R-1-i}}{\sqrt{n_R-i}}$$

$$\cdot \left\{ \sqrt{\frac{(n_R-i)}{\alpha\bar{\gamma}_{SR}\bar{\gamma}_{RD}}} f_1(s,i) + \frac{1}{2}\left[\frac{(n_R-i)}{\bar{\gamma}_{SR}} + \frac{1}{\alpha\bar{\gamma}_{RD}}\right] f_2(s,i) \right\}, \tag{4.40}$$

where

$$f_1(s,i) = \frac{4}{3}\left(\frac{(n_R-i)}{\bar{\gamma}_{SR}} + \frac{1}{\alpha\bar{\gamma}_{RD}} + s + \sqrt{\frac{4(n_R-i)}{\alpha\bar{\gamma}_{SR}\bar{\gamma}_{RD}}}\right)^{-2}$$

$$\cdot F\left(2,\frac{1}{2};\frac{5}{2}; \frac{\left(\frac{(n_R-i)}{\bar{\gamma}_{SR}}+\frac{1}{\alpha\bar{\gamma}_{RD}}+s-\sqrt{\frac{4(n_R-i)}{\alpha\bar{\gamma}_{SR}\bar{\gamma}_{RD}}}\right)}{\left(\frac{(n_R-i)}{\bar{\gamma}_{SR}}+\frac{1}{\alpha\bar{\gamma}_{RD}}+s+\sqrt{\frac{4(n_R-i)}{\alpha\bar{\gamma}_{SR}\bar{\gamma}_{RD}}}\right)}\right), \text{ and} \tag{4.41}$$

$$f_2(s,i) = \frac{32}{3}\sqrt{\frac{(n_R-i)}{\alpha\bar{\gamma}_{SR}\bar{\gamma}_{RD}}}\left(\frac{(n_R-i)}{\bar{\gamma}_{SR}} + \frac{1}{\alpha\bar{\gamma}_{RD}} + s + \sqrt{\frac{4(n_R-i)}{\alpha\bar{\gamma}_{SR}\bar{\gamma}_{RD}}}\right)^{-3}$$

$$\cdot F\left(3,\frac{3}{2};\frac{5}{2}; \frac{\left(\frac{(n_R-i)}{\bar{\gamma}_{SR}}+\frac{1}{\alpha\bar{\gamma}_{RD}}+s-\sqrt{\frac{4(n_R-i)}{\alpha\bar{\gamma}_{SR}\bar{\gamma}_{RD}}}\right)}{\left(\frac{(n_R-i)}{\bar{\gamma}_{SR}}+\frac{1}{\alpha\bar{\gamma}_{RD}}+s+\sqrt{\frac{4(n_R-i)}{\alpha\bar{\gamma}_{SR}\bar{\gamma}_{RD}}}\right)}\right), \tag{4.42}$$

where $F(\cdot,\cdot\,;\cdot\,;\cdot)$ is Gauss hypergeometric series.

Substituting (4.40) in (4.30), and assuming that $\bar{\gamma}_{SD}$, $\bar{\gamma}_{RD}$, $\bar{\gamma}_{SR}$ are relatively large, we can approximate (4.30) as

$$P(d) \approx$$

$$\left(g_{PSK}\left[R_{C_1}d_1 + (1-\alpha)R_{C_2}d_2\right]\bar{\gamma}_{SD}\right)^{-1} \frac{4I(M)n_R}{\sqrt{\alpha\bar{\gamma}_{SR}\bar{\gamma}_{RD}}} \sum_{i=0}^{n_R-1}\binom{n_R-1}{i}\frac{(-1)^{n_R-1-i}}{\sqrt{n_R-i}}$$

$$\left\{ \sqrt{\frac{(n_R - i)}{\alpha \bar{\gamma}_{SR} \bar{\gamma}_{RD}}} f_1\left(-g_{PSK} R_{C_1} d_1, i\right) + \frac{1}{2}\left[\frac{(n_R - i)}{\bar{\gamma}_{SR}} + \frac{1}{\alpha \bar{\gamma}_{RD}}\right] f_2\left(-g_{PSK} R_{C_1} d_1, i\right) \right\}, \quad (4.43)$$

where $I(M) = \frac{1}{\pi} \int_0^{(M-1)\pi/M} \sin^2 \varphi \, d\varphi$. Note that $I(M)$ is a constant that depends on the type of modulation M. By substituting (4.43) into (3.16), we can get the upper bound.

In the case $\bar{\gamma}_{SD} = \bar{\gamma}_{RD} = \bar{\gamma}_{SR} = E_b/N_0$, (4.43) simplifies to

$$P(d) \approx \left(g_{PSK}\left[R_{C_1} d_1 + (1 - \alpha) R_{C_2} d_2\right]\right)^{-1} \left(\frac{E_b}{N_0}\right)^{-2} \frac{4 I(M) n_R}{\sqrt{\alpha}}$$

$$\cdot \sum_{i=0}^{n_R - 1} \binom{n_R - 1}{i} \frac{(-1)^{n_R - 1 - i}}{\sqrt{n_R - i}}$$

$$\left\{ \sqrt{\frac{(n_R - i)}{\alpha \left(\frac{E_b}{N_0}\right)^2}} f_1\left(-g_{PSK} R_{C_1} d_1, i\right) + \frac{0.5}{\frac{E_b}{N_0}}\left[(n_R - i) + \frac{1}{\alpha}\right] f_2\left(-g_{PSK} R_{C_1} d_1, i\right) \right\}, \quad (4.44)$$

which shows that the diversity order is two. However, it should be noted that when $\bar{\gamma}_{SR}$ is very small, there will be a loss in diversity but the system still offers large coding gains relative to the non-cooperative case.

4.4 Relay Selection

In the above analysis, we focused on antenna selection where we assumed only one relay node is present. A natural extension of antenna selection would be relay selection. That is, in case there are several relay nodes present in the network, one can use the best nodes to relay the information to the destination. This alternative may be preferred over antenna selection since it may not always be possible to mount multiple antennas on a single relay node, especially for hand-held wireless devices.

From the relay selection point of view, another advantage is that one need not account for spatial correlation that may arise with collocated antennas. Furthermore, to accomplish relay selection, there should be some form of feedback from the relay nodes to the source to decide on which relay(s) to select, which is not a problem since such information is feedback anyway for other purposes. Further extension would be to perform joint antenna/relay selection.

In terms of performance analysis, assuming perfect feedback information at the source, the analytical results obtained above apply to relay selection in a straight-forward manner. Specifically, when there are L relays available and the best relay is selected, the same BER upper bounds derived above apply to relay selection with n_R replaced by L. Another scenario where these results also apply is that when there are L relay nodes with a total of $n_R \geq L$ antennas mounted on all of the relays while only the best antenna is used. With a little bit of more work, one may also extend these results to the case of multiple relay selection in conjunction with antenna selection.

4.5   Simulation Results

In our simulations, we assume that all sub-channels are independent and quasi-static fading. Only one relay node is assumed which can operate in the DF mode or AF mode. BPSK and QPSK modulations are used. In all simulations, the transmitted frame size is equal to $n_1=n_2=130$ coded bits. We also assume that the $R-D$ and $S-D$ channels have equal SNRs, i.e., $\bar{\gamma}_{SD} = \bar{\gamma}_{RD} = E_b/N_0$, but the $S-R$ SNR, $\bar{\gamma}_{SR}$, can be different. We consider two different convolutional codes, whose generator polynomials in octal form are generally given by $(c_1, c_2, c_3, c_4)_{\text{octal}}$. In our context, this implies that E_1 employs $(c_1, c_2)_{\text{octal}}$ and E_2 employs $(c_3, c_4)_{\text{octal}}$. Specifically we use $(13, 15, 15, 17)_{\text{octal}}$ and $(5, 7, 5, 7)_{\text{octal}}$ [44].

For the former code, RSC E_1 employs $(13, 15)_{\text{octal}}$ and E_2 employs $(15, 17)_{\text{octal}}$. The same holds for $(5, 7, 5, 7)_{\text{octal}}$.

Figure 4.3 shows a comparison between the simulated and analytical BER results using (4.16), (3.16), and (4.22) for the two cases of $\bar{\gamma}_{SR} = 3$ and 7 dB. Code $(13, 15, 15, 17)_{\text{octal}}$ is used with $R_{C_1} = R_{C_2} = 0.5$. To maintain the same average power in the second frame, the source and relay nodes divide their power according to the ratio $\alpha = 0.5$. We also include results for the $n_R = 1$ case (i.e., no antenna selection) (Chapter 3). In addition, we include in the figure, for comparison, results for the non- cooperative case (no relaying) as well as for the error-free DF relaying case. These two cases achieve a diversity of one and two, respectively. As shown in the figure, the diversity degrades due to errors at the relay. The interesting observation here is that the loss in diversity starts to become clear when the $S-R$ channel is less reliable than the $S-D$ and $R-D$ channels. As a matter of fact, under the hypothetical scenario when all channels have equal SNRs, the diversity order is maintained for all range of SNR.

In Figure 4.4, we show a comparison of the simulated and analytical BER results based on the expressions given in (4.16), (3.16), and (4.22) for the two cases of $\bar{\gamma}_{SR} = 3$ and 7 dB. Code $(13, 15, 15, 17)_{\text{octal}}$ is used with $R_{C_1} = R_{C_2} = 0.5$ and $\alpha = 0.5$. In this case, we assume $n_R = 1$ where the best antenna is selected. In contrast with the results shown in Figure 4.3, we can clearly see the positive impact of antenna selection. For example, when $\bar{\gamma}_{SR} = 7$ dB, we see that the diversity is maintained until bit error rate 10^{-5} which provides a gain of more than 5 dB over the case without antenna selection. The same is true for the $\bar{\gamma}_{SR} = 3$ dB where the divergence of the curve from the error-free curve occurs a few decibels later. This clearly demonstrates the importance of using antenna selection.
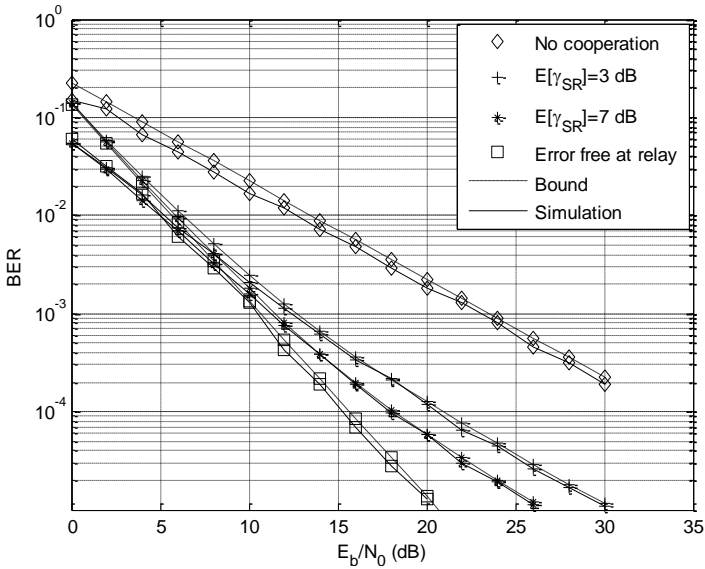
Figure 4.3 *Comparison of analysis and simulated BER for DF relaying over quasi-static fading; $\bar{\gamma}_{SD} = \bar{\gamma}_{RD} = E_b/N_0$, $\bar{\gamma}_{SR} = 3$ and 7 dB; $(13, 15, 15, 17)_{octal}$ with $R_{C_1} = R_{C_2} = 0.5$; $\alpha = 0.5$; $n_R = 1$, i.e., no antenna selection.*
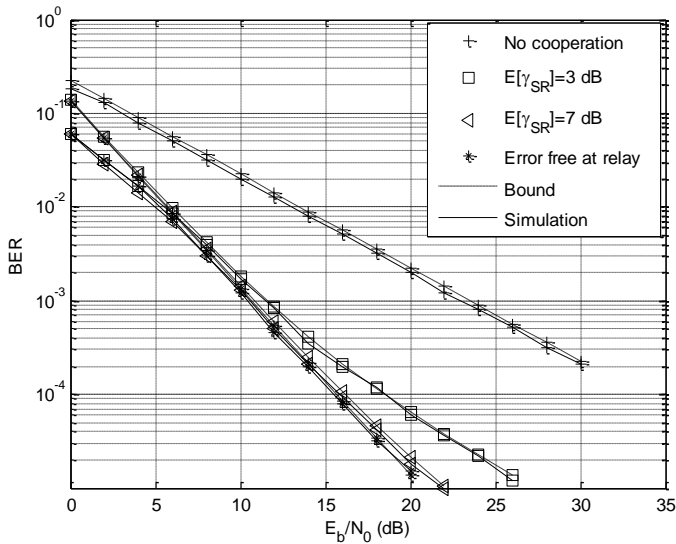

Figure 4.4 *Comparison of analysis and simulated BER for DF relaying over quasi-static fading; $\bar{\gamma}_{SD} = \bar{\gamma}_{RD} = E_b/N_0$, $\bar{\gamma}_{SR} = 3$ and 7 dB; $(13, 15, 15, 17)_{octal}$ with $R_{C_1} = R_{C_2} = 0.5$; $\alpha = 0.5$; $n_R = 2$ and the best antenna is selected.*

Figure 4.5 shows a comparison between the simulated and the bit error rate upper bound corresponding to the expressions given in (3.16), and (4.43) for the two cases of $\bar{\gamma}_{SR} = 3$ and 7 dB. Code $(5, 7, 5, 7)_{\text{octal}}$ is used with $R_{C_1} = R_{C_2} = 0.5$ and $\alpha = 0.5$. We also assume that $n_R = 1$ (no antenna selection). We observe from the figure that the diversity is maintained when all channels ($S-R$, $S-D$, and $R-D$) have equal SNRs, i.e., $\bar{\gamma}_{SR} = \bar{\gamma}_{SD} = \bar{\gamma}_{RD}$. However, the diversity degrades when $\bar{\gamma}_{SR}$ is smaller than the other SNRs, which is similar to the DF relaying case.

To assess the efficacy of antenna selection, we plot in Figure 4.6 the performance of the system corresponding to Figure 4.5 but now with antenna selection. We assume that $n_R = 2$ and the best antenna is used. Similar to the DF case, we observe from the figure that antenna selection preserves the diversity order for a wider range of SNR, which in turns provides substantial coding gains. For instance, for the $\bar{\gamma}_{SR} = 7$ dB and at bit error rate 10^{-5}, there is a gain of about 7 dB when antenna selection is used. Similar favorable results are expected for relay selection, as mentioned before.

Figure 4.7 shows a comparison between the simulated and theoretical BER performance for the two cases of $\bar{\gamma}_{SR} = 4$ and 8 dB , and $M=4$ (QPSK). Code $(5, 7, 5, 7)_{\text{octal}}$ is used with $R_{C_1} = R_{C_2} = 0.5$ and $\alpha = 0.5$. We also assume that $n_R = 2$ and the best antenna is selected. The BER curve when the relay is error-free, having diversity order two is also shown for comparison. It is clear from this figure that as $\bar{\gamma}_{SR}$ gets larger, the performance converges to the ideal error-free case.

Figure 4.5 *Comparison of analysis and simulated BER for AF relaying over quasi-static fading;* $\overline{\gamma}_{SR} = 3$ *and 7 dB; code (5, 7, 5, 7)$_{octal}$;* $n_R = 1$, *i.e., no antenna selection.*
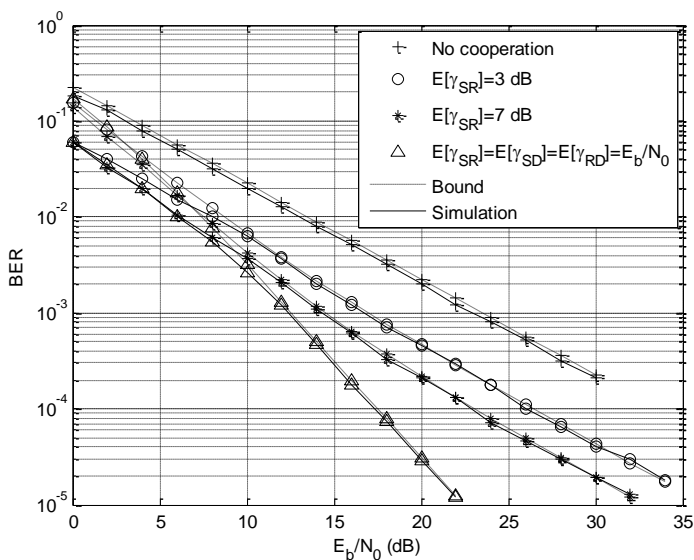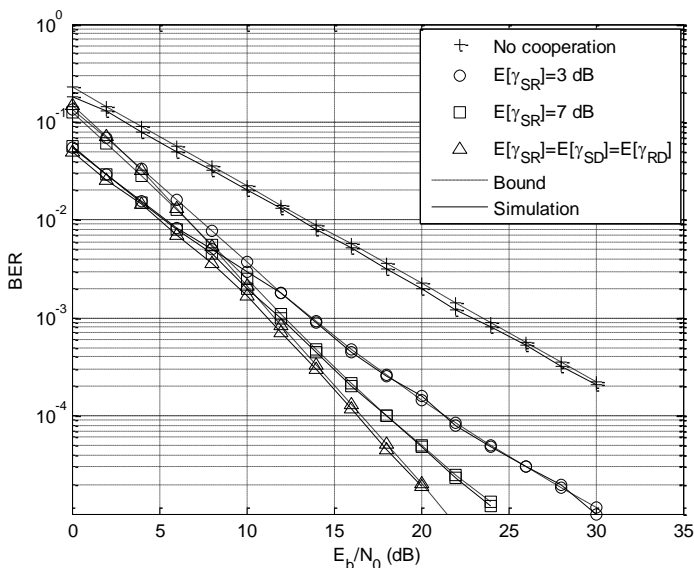

Figure 4.6 *Comparison of analysis and simulated BER for AF relaying over quasi-static fading;* $\overline{\gamma}_{SR} = 3$ *and 7 dB; code (5, 7, 5, 7)$_{octal}$;* $n_R = 2$ *and the best antenna is selected.*

Figure 4.7 *Comparison between the simulated and theoretical BER for QPSK over quasi-static fading, $\bar{\gamma}_{SD} = \bar{\gamma}_{RD} = E_b/N_0$, $\bar{\gamma}_{SR} = 4$ and 8 dB; code $(5, 7, 5, 7)_{octal}$; $n_R = 2$ and the best antenna is selected.*

5

Coded Cooperative
Communications with System
Non-idealities

In the previous chapters, we assumed perfect knowledge of the CSI at all network nodes. However, this is an idealistic assumption since such nod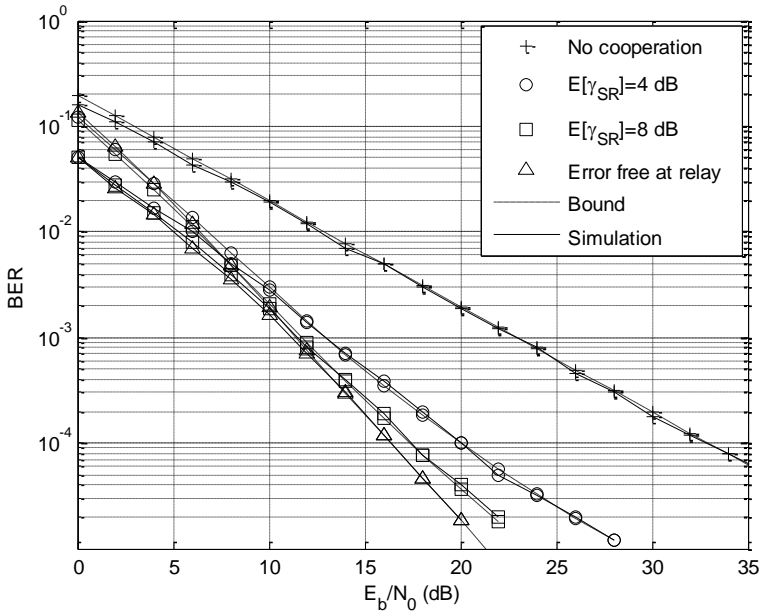es will have to estimate the CSI. The channel estimation technique requires known pilot symbols to be transmitted at the beginning of each data frame. Since pilot symbols reduce spectral efficiency; therefore, it is desirable to use as few as possible. The ultimate objective here in is to achieve performance close to the perfect channel case by using only k pilot symbols.

5.1 Channel Estimation

An important issue affecting the design and analysis of relay transmission protocols is channel state information, i.e., how much radios know about each channel realization throughout the network. For example, using training signals, e.g., pilot tones or symbols, the receivers may estimate the multipath coefficients affecting their respective received signals. Once channel state information is acquired at the distributed radio receivers, protocol designs can feed this information back to the transmitters. This feedback allows the transmitters to adapt their transmissions to the realized channel in effect, often leading to performance improvements when accurate channel state information is obtainable.

5.2 Distributed Coding with MRC Channel Estimation

Recall from Chapters 3 and 4 that we assumed the second frame was transmitted on orthogonal sub-channels (e.g., TDMA, CDMA, or FDMA) from the source and relay nodes to the destination. Also, the detection at the relay and destination nodes was based on perfect channel knowledge. In this chapter, we use the same coding scheme introduced in Chapter 3 with a distributed combining based on Alamouti scheme [9]. For simplicity, we assume that there is

one relay. All the nodes are assumed to be equipped with one antenna and one RF chain. Recall that the coding scheme described earlier in Chapter 3, assumes that the source is equipped with two encoders, where the output of the first encoder is referred to as the first frame (of length N_1 bits) and the output of the second encoder is referred to as the second frame (of length N_2 bits). Also, each relay is equipped with an encoder similar to the second encoder at the source. First, at the beginning of each frame transmitted from *S* to *R*, from *R* to *D*, and from *S* to *D*, a pilot sequence *P* consisting of k_p symbols is sent to estimate all the channels. Then, these channel estimates are used to detect the data.

In the following sections, we describe and analyze the pilot-assisted channel estimation technique when employed in the distributed space-time coding scheme in Chapter 3.

5.2.1   System Model

In this section, we introduce the system model of the distributed space-time coding cooperation scheme when employing channel estimation using pilot signals.

Conventional Pilot Mode

In The block diagram with conventional pilot (CP) channel estimation is shown in Figure 5.1. At the beginning of each frame transmitted from *S* to *R*, from *R* to *D*, and from *S* to *D*, a pilot sequence *P* consisting of k_p symbols [45]

$$P = \left(P_1, P_1, \cdots, P_{k_p} \right) \tag{5.1}$$

is appended to the data sequence. A block diagram of the source, relay and destination when employing channel estimation is shown in Figure 5.2.
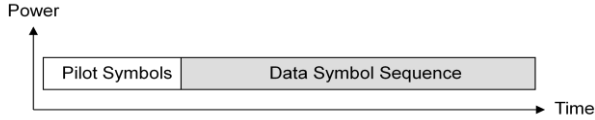
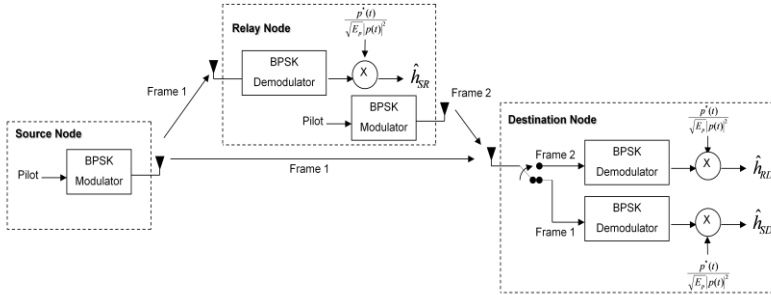**Figure 5.1**   *Symbol block with conventional pilot channel estimation.*

Figure 5.2   *The channel estimation for all the channels for the proposed scheme.*

First Frame: During the first frame transmission, the signals received at the relay and the destination nodes at time t are given respectively by

$$y_{SR}(t) = \sqrt{E_p}\,h_{SR}\,p(t) + n_{SR}(t), \tag{5.2}$$

$$y_{SD}(t) = \sqrt{E_p}\,h_{SD}\,p(t) + n_{SD}(t), \tag{5.3}$$

where p(t) is the pilot sequence transmitted from the source at time slot *t* $(t = 1,2,\cdots,k_p)$, E_p is the transmitted signal energy for the pilot sequence, and the rest of the parameters are defined as in Chapter 3.

The receivers at the relay and the destination estimate the channel fading coefficients h_{SR} and h_{SD} by using the observed sequences $y_{SR}(t)$ and $y_{SD}(t)$. The estimates of h_{SR} and h_{SD} are given by [45]

$$\hat{h}_{SR} = \frac{y_{SR}(t)p^*(t)}{\sqrt{E_p}|p(t)|^2} = h_{SR} + \frac{n_{SR}(t)p^*(t)}{\sqrt{E_p}|p(t)|^2} = h_{SR} + \Delta h_{SR}, \tag{5.4}$$

$$\hat{h}_{SD} = \frac{y_{SD}(t)p^*(t)}{\sqrt{E_p}|p(t)|^2} = h_{SD} + \frac{n_{SD}(t)p^*(t)}{\sqrt{E_p}|p(t)|^2} = h_{SD} + \Delta h_{SD}, \tag{5.5}$$

where Δh_{SR} and Δh_{SD} are the estimation errors due to the noise, given by

$$\Delta h_{SR} = \frac{n_{SR}(t)p^*(t)}{\sqrt{E_p}|p(t)|^2}, \tag{5.6}$$

$$\Delta h_{SD} = \frac{n_{SD}(t)p^*(t)}{\sqrt{E_p}|p(t)|^2}. \tag{5.7}$$

Since $n_{SR}(t)$ and $n_{SD}(t)$ are complex AWGN on the $S{-}R$ and $S{-}D$ links, with zero mean and one-dimensional variance $N_0/2$, the estimation errors Δh_{SR} and Δh_{SD} have a zero mean and one-dimensional variance $N_0/(2k_p E_p)$.

Second Frame: During the second frame transmission, the received signal at the destination node is given by

$$y_{RD}(t) = \sqrt{E_p}h_{RD}p(t) + n_{RD}(t), \tag{5.8}$$

where h_{RD} is modeled as complex Gaussian distributed with zero mean and unit variance, representing the fading channel from R to D, $n_{RD}(t)$ is the AWGN on the $R{-}D$ link with zero mean and one-dimensional variance $N_0/2$.

The receiver at the destination estimates the channel fading coefficient h_{RD} by using the observed sequence $y_{RD}(t)$. The estimate of h_{RD} is then given by

$$\hat{h}_{RD} = \frac{y_{RD}(t)p^*(t)}{\sqrt{E_p}|p(t)|^2} = h_{RD} + \frac{n_{RD}(t)p^*(t)}{\sqrt{E_p}|p(t)|^2} = h_{RD} + \Delta h_{RD}, \tag{5.9}$$

where Δh_{RD} is the estimation error due to the noise, given by

$$\Delta h_{RD} = \frac{n_{RD}(t)p^*(t)}{\sqrt{E_p}|p(t)|^2}. \tag{5.10}$$

Since $n_{RD}(t)$ is complex AWGN, with zero mean and one-dimensional variance $N_0/2$, the estimation error Δh_{RD} has a zero mean and one-dimensional variance $N_0/(2k_p E_p)$.

Data Mode

Having obtained the channel estimates as described earlier, the data mode starts where these estimates are used to detect the transmitted data.

The system model for the proposed system in the first and second frame using Alamouti scheme is depicted in Figure 5.3; 5.4. As shown in the figure, the transmitter is equipped with two RSC encoders, denoted by E_1 and E_2, whose rates are R_{C_1} and R_{C_2}, respectively. The relay is also equipped with E_2. The information sequence b is encoded by E_1, resulting in C_1, which is denoted as *Frame 1*. This frame is broadcasted from the source to the relay and destination nodes. If the relay correctly decodes the message it received from the source, it re-encode it by E_2 and transmitted to the destination as *Frame 2* with rate $R_{C_2} = K/n_2$. At the same time, b is encoded at the source by E_2, resulting in C_2 (denoted as *Frame 2*) which in turn is transmitted from the source to the destination. These two copies (of *Frame 2*) of the source and relay whose CRC check transmit the second frame to the destination. The received copies of the second frame are combined using Alamouti scheme and the information bits are detected via a Viterbi decoder based on the two frames $N = N_1 + N_2$. The combiner output is then augmented with *Frame 1* to form a noisy version of *C*, which is detected at the destination via a Viterbi decoder.

In what follows we mathematically describe the underlying scheme.

First Frame: During the first frame transmission, the signals received at the relay and the destination nodes at time *t* are given by

$$r_{SR}(t) = \sqrt{R_{C_1}E_{SR}}\,h_{SR}x(t) + n_{SR}(t), \tag{5.11}$$

$$r_{SD}(t) = \sqrt{R_{C_1}E_{SD}}\,h_{SD}x(t) + n_{SD}(t), \tag{5.12}$$

where $x(t)$ is the output of the source modulator at time slot t ($t = 1,2,\cdots,n_1$), E_{SR} and E_{SD} are the transmitted signal energies for the corresponding link, R_{C_1} is the code rate of convolutional *encoder I*.
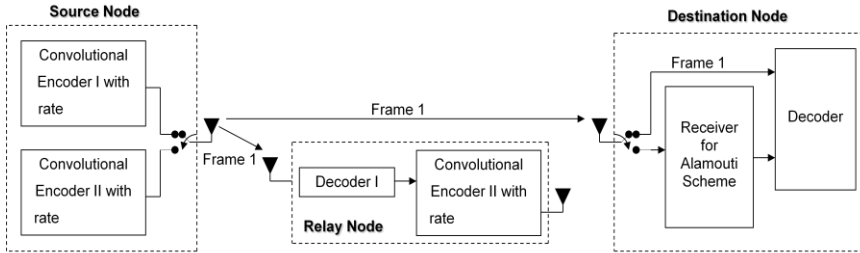

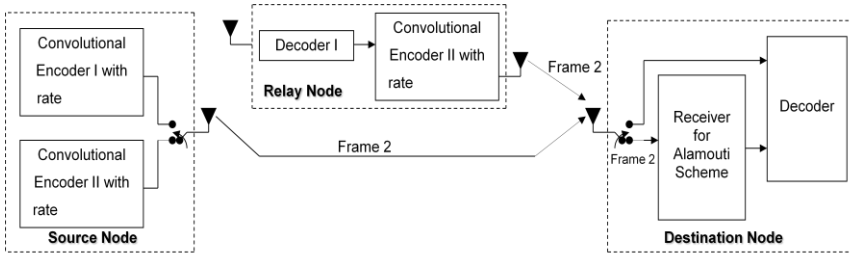**Figure 5.3** *Transmission protocol for the first frame.*

Figure 5.4 *Transmission protocol for the second frame using Alamouti scheme.*

From (5.11) and (5.12), the decision statistics for the channels from *S* to *R* and from *S* to *D* for the first frame are given respectively, by

$$\tilde{x}_{R,1}(t) = \hat{h}_{SR}^* r_{SR}(t) = (h_{SR}^* + \Delta h_{SR}^*)r_{SR}(t)$$

$$= |h_{SR}|^2\sqrt{R_{C_1}E_{SR}}x(t) + h_{SR}^* n_{SR}(t) + \Delta h_{SR}^* h_{SR}\sqrt{R_{C_1}E_{SR}}x(t) + \Delta h_{SR}^* n_{SR}(t), \quad (5.13)$$

$$\tilde{x}_{D,1}(t) = \hat{h}_{SD}^* r_{SD}(t) = (h_{SD}^* + \Delta h_{SD}^*)r_{SD}(t)$$

$$= |h_{SD}|^2\sqrt{R_{C_1}E_{SD}}x(t) + h_{SD}^* n_{SD}(t) + \Delta h_{SD}^* h_{SD}\sqrt{R_{C_1}E_{SD}}x(t) + \Delta h_{SD}^* n_{SD}(t), \quad (5.14)$$

where $t = 1,2,\cdots,n_1$. Since the powers of Δh_{SR} and Δh_{SD} in (5.6) and (5.7), respectively, are relatively small (assuming small errors), the powers of $\Delta h_{SR}^* n_{SR}(t)$ and $\Delta h_{SD}^* n_{SD}(t)$ can be neglected.

Second Frame Using Alamouti Scheme: During the second frame transmission, the received signals at the destination node at time t and $t + 1$ are given by [9]

$$r_D(t) = \sqrt{R_{C_2}\alpha E_{RD}}h_{RD}\hat{x}(t) + \sqrt{R_{C_2}(1-\alpha)E_{SD}}h_{SD}x(t+1) + n_D(t), \quad (5.15)$$

$$r_D(t+1) = -\sqrt{R_{C_2}\alpha E_{RD}}h_{RD}\hat{x}^*(t) + \sqrt{R_{C_2}(1-\alpha)E_{SD}}h_{SD}x^*(t) + n_D(t+1), \quad (5.16)$$

where $\hat{x}(t)$ and $\hat{x}(t+1)$ are the outputs of the relay modulators at time slot t and $t+1$ ($t = n_1 + 1, n_1 + 3, \cdots, n_1 + n_2 - 1$), respectively, the rest of the parameters are defined as before (see Chapter 3).

Using Alamouti's combining scheme [9], from (5.15) and (5.16), the decision statistics for the channels from R to D and S to D for the second frame are given respectively by

$$\tilde{x}_{D,2}(t) = \hat{h}_{RD}^* r_D(t) + \hat{h}_{SD} r_D^*(t+1)$$

$$= |h_{RD}|^2\sqrt{R_{C_2}\alpha E_{RD}}\hat{x}(t) + h_{RD}^* h_{SD}\sqrt{R_{C_2}(1-\alpha)E_{SD}}x(t+1) + h_{RD}^* n_D(t)$$

$$-h_{SD}h_{RD}^*\sqrt{R_{C_2}\alpha E_{RD}}\hat{x}(t+1) + |h_{SD}|^2\sqrt{R_{C_2}(1-\alpha)E_{SD}}x(t) + h_{SD}n_D^*(t+1)$$

$$+\Delta h_{RD}^* h_{SD}\sqrt{R_{C_2}(1-\alpha)E_{SD}}x(t+1) + \Delta h_{RD}^* h_{RD}\sqrt{R_{C_2}\alpha E_{RD}}\hat{x}(t)$$

$$+\Delta h_{RD}^* n_D(t) - \Delta h_{SD}h_{RD}^*\sqrt{R_{C_2}\alpha E_{RD}}\hat{x}(t+1)$$

$$+\Delta h_{SD}h_{SD}^*\sqrt{R_{C_2}(1-\alpha)E_{SD}}x(t) + \Delta h_{SD}n_D^*(t+1), \quad (5.17)$$

$$\tilde{x}_{D,2}(t+1) = \hat{h}_{SD}^* r_D(t) - \hat{h}_{RD}r_D^*(t+1)$$

$$= h_{SD}^* h_{RD}\sqrt{R_{C_2}\alpha E_{RD}}\hat{x}(t) + |h_{SD}|^2\sqrt{R_{C_2}(1-\alpha)E_{SD}}x(t+1) + h_{SD}^* n_D(t)$$

$$+|h_{RD}|^2\sqrt{R_{C_2}\alpha E_{RD}}\hat{x}(t+1) - h_{RD}h_{SD}^*\sqrt{R_{C_2}(1-\alpha)E_{SD}}x(t) - h_{RD}n_D^*(t+1)$$

$$+\Delta h_{SD}^* h_{SD}\sqrt{R_{C_2}(1-\alpha)E_{SD}}x(t+1) + \Delta h_{SD}^* n_D(t)$$

$$+\Delta h_{SD}^* h_{RD} \sqrt{R_{C_2}\alpha E_{RD}}\,\hat{x}(t) + \Delta h_{RD} h_{RD}^* \sqrt{R_{C_2}\alpha E_{RD}}\,\hat{x}(t+1)$$

$$-\Delta h_{RD} h_{SD}^* \sqrt{R_{C_2}(1-\alpha)E_{SD}}\,x(t) - \Delta h_{RD} n_D^*(t+1), \qquad (5.18)$$

where $t = n_1 + 1, n_1 + 3, \cdots, n_1 + n_2 - 1$. Since the powers of Δh_{SD} and Δh_{RD} in (5.7) and (5.10), respectively, are relatively small, the powers of $h_{RD}^* n_D(t)$, $\Delta h_{SD} n_D^*(t+1)$, $\Delta h_{SD}^* n_D(t)$, and $\Delta h_{RD} n_D^*(t+1)$ can be neglected.

5.2.2 Performance Analysis

In this section, we evaluate the performance of our proposed estimation scheme for one relay channel in terms of the average BER at the destination. In our analysis, we consider M-PSK modulation. We first consider error-free recovery at the relay. Then we consider the effect of channel errors at the relay.

The end-to-end conditional pairwise error probability for a coded system is the probability of detecting an erroneous codeword $\hat{\mathbf{x}} = [\hat{x}_1, \hat{x}_2, \cdots, \hat{x}_n]$, when in fact $\mathbf{x} = [x_1, x_2, \cdots, x_n]$ is transmitted. The instantaneous received SNR for non-cooperative transmission from S to D, $\gamma_D(t) = \frac{2R_C E_{SD}|h_{SD}(t)|^2}{N_0\left(1+\frac{R_C E_{SD}}{k_p E_p}\right)}$. There, for non-cooperative transmission, the conditional pairwise error probability from S to D is given by

$$P(\mathbf{x}\rightarrow\hat{\mathbf{x}}|\gamma_{SD}) = Q\left(\sqrt{\frac{2g_{PSK}R_c E_{SD}}{N_0\left(1+\frac{R_C E_{SD}}{k_p E_p}\right)}\sum_{t\in\eta}|h_{SD}(t)|^2}\right)$$

$$= Q\left(\sqrt{\frac{2g_{PSK}R_c}{\left(1+\frac{R_C E_{SD}}{k_p E_p}\right)}\sum_{t\in\eta}\gamma_{SD}(t)}\right). \qquad (5.19)$$

Under slow fading, $h_{SD}(t) = h_{SD}$ for all t and consequently (5.19) can be

written as

$$P(d|\gamma_{SD}) = Q\left(\sqrt{\frac{2g_{PSK}\,R_c}{\left(1+\frac{R_C E_{SD}}{k_p E_p}\right)}\gamma_{SD}}\right). \tag{5.20}$$

In what follows, we derive an upper bound on the probability of bit error for distributed space-time coding using one relay channel. First, we consider the case of error-free relay then, the case of erroneous relay.

DF with Error-Free Relay

Under the assumption of free errors at the relay node, the instantaneous received SNR for the channel from *S* to *D* for the first frame is given by

$$\gamma_{D_1}(t) = \frac{2R_{C_1}E_{SD}|h_{SD}(t)|^2}{N_0\left(1+\frac{R_{C_1}E_{SD}}{k_p E_p}\right)} = \frac{2R_{C_1}\gamma_{SD}(t)}{\left(1+\frac{R_{C_1}E_{SD}}{k_p E_p}\right)}, \quad t = 1,2,\cdots,n_1 \tag{5.21}$$

and the instantaneous received SNR for the channels from *S* to *D* and *R* to *D* for the second frame is given by

$$\gamma_{D_2}(t) = \frac{2R_{C_2}}{N_0}\left(\frac{(1-\alpha)E_{SD}|h_{SD}(t)|^2}{\left(1+\frac{R_{C_2}[(1-\alpha)E_{SD}+\alpha E_{RD}]}{k_p E_p}\right)} + \frac{\alpha E_{RD}|h_{RD}(t)|^2}{\left(1+\frac{R_{C_2}[(1-\alpha)E_{SD}+\alpha E_{RD}]}{k_p E_p}\right)}\right)$$

$$= 2R_{C_2}\left(\frac{(1-\alpha)\gamma_{SD}(t)}{\left(1+\frac{R_{C_2}[(1-\alpha)E_{SD}+\alpha E_{RD}]}{k_p E_p}\right)} + \frac{\alpha\gamma_{RD}(t)}{\left(1+\frac{R_{C_2}[(1-\alpha)E_{SD}+\alpha E_{RD}]}{k_p E_p}\right)}\right)$$

$$t = n_1+1, n_1+2,\cdots,n_1+n_2. \tag{5.22}$$

From (5.21) and (5.22), when the fading coefficients h_{SD}, and h_{RD} are constant over the codeword, the conditional pairwise error probability is given by

$$P(d|\gamma_{SD},\gamma_{RD}) =$$

$$Q\left(\sqrt{2g_{PSK}\left(\frac{R_{C_1}d_1\gamma_{SD}(t)}{\left(1+\frac{R_{C_1}E_{SD}}{k_pE_p}\right)} + \frac{\left[R_{C_2}d_2(1-\alpha)E_{SD}+R_{C_2}d_2\alpha E_{RD}\right]}{1+\frac{R_{C_2}\left[(1-\alpha)E_{SD}+\alpha E_{RD}\right]}{k_pE_p}}\right)}\right). \qquad (5.23)$$

Using (3.10), we can rewrite (5.23) as

$$P(d|\gamma_{SD},\gamma_{RD}) = \frac{1}{\pi}\int\limits_{0}^{\frac{(M-1)\pi}{M}}$$

$$.\,exp\left(-g_{PSK}\left(\frac{R_{C_1}d_1}{\left(1+\frac{R_{C_1}E_{SD}}{k_pE_p}\right)} + \frac{R_{C_2}d_2(1-\alpha)}{1+\frac{R_{C_2}\left[(1-\alpha)E_{SD}+\alpha E_{RD}\right]}{k_pE_p}}\right)\frac{\gamma_{SD}}{\sin^2\theta}\right)$$

$$.\,exp\left(-g_{PSK}\left(\frac{R_{C_2}d_2\alpha}{1+\frac{R_{C_2}\left[(1-\alpha)E_{SD}+\alpha E_{RD}\right]}{k_pE_p}}\right)\frac{\gamma_{RD}}{\sin^2\theta}\right)d\theta. \qquad (5.24)$$

The average pairwise error probability is then given by

$$P(d|\gamma_{SD},\gamma_{RD}) = \frac{1}{\pi}\int\limits_{0}^{\frac{(M-1)\pi}{M}}$$

$$.\int_0^\infty exp\left(-g_{PSK}\left(\frac{R_{C_1}d_1}{\left(1+\frac{R_{C_1}E_{SD}}{k_pE_p}\right)} + \frac{R_{C_2}d_2(1-\alpha)}{1+\frac{R_{C_2}\left[(1-\alpha)E_{SD}+\alpha E_{RD}\right]}{k_pE_p}}\right)\frac{\gamma_{SD}}{\sin^2\theta}\right)p_{\gamma_{SD}}(\gamma_{SD})d\gamma_{SD}$$

$$.\int_0^\infty exp\left(-g_{PSK}\left(\frac{R_{C_2}d_2\alpha}{1+\frac{R_{C_2}\left[(1-\alpha)E_{SD}+\alpha E_{RD}\right]}{k_pE_p}}\right)\frac{\gamma_{RD}}{\sin^2\theta}\right)p_{\gamma_{RD}}(\gamma_{RD})d\gamma_{RD}d\theta. \quad (5.25)$$

Using (3.13), one can show that (5.25) can be expressed as

$$P(d) = \frac{1}{\pi} \int_{0}^{\frac{(M-1)\pi}{M}} \left(1 + \frac{g_{PSK}}{\sin^2\theta} \left(\frac{R_{C_2} d_2 \alpha \bar{\gamma}_{RD}}{1 + \frac{R_{C_2}[(1-\alpha)\bar{\gamma}_{SD} + \alpha\bar{\gamma}_{RD}]}{k_p\left(\frac{E_p}{N_0}\right)}} \right) \right)^{-1}$$

$$\cdot \left(1 + \frac{g_{PSK}}{\sin^2\theta} \left(\frac{R_{C_1} d_1 \bar{\gamma}_{SD}}{\left(1 + \frac{R_{C_1}\bar{\gamma}_{SD}}{k_p\left(\frac{E_p}{N_0}\right)}\right)} + \frac{R_{C_2} d_2 (1-\alpha)\bar{\gamma}_{SD}}{1 + \frac{R_{C_2}[(1-\alpha)\bar{\gamma}_{SD} + \alpha\bar{\gamma}_{RD}]}{k_p\left(\frac{E_p}{N_0}\right)}} \right) \right)^{-1} d\theta, \qquad (5.26)$$

where $E[|h_{SD}|^2] = 1$, and $E[|h_{RD}|^2] = 1$, are the averages of $|h_{SD}|^2$ and $|h_{RD}|^2$, respectively. Using the results of Appendix C, the average pairwise error probability can be shown as

$$P(d) = \frac{(M-1)}{M} + \frac{A(d)}{(B(d)-A(d))\pi} \sqrt{\frac{A(d)}{1+A(d)}} \tan^{-1}\left(\sqrt{\frac{1+A(d)}{A(d)}} \tan\left(\frac{(M-1)\pi}{M}\right) \right)$$

$$+ \frac{B(d)}{(A(d)-B(d))\pi} \sqrt{\frac{B(d)}{1+B(d)}} \tan^{-1}\left(\sqrt{\frac{1+B(d)}{B(d)}} \tan\left(\frac{(M-1)\pi}{M}\right) \right), \qquad (5.27)$$

where

$$A(d) = g_{PSK} \left(\frac{R_{C_1} d_1 \bar{\gamma}_{SD}}{\left(1 + \frac{R_{C_1}\bar{\gamma}_{SD}}{k_p\left(\frac{E_p}{N_0}\right)}\right)} + \frac{R_{C_2} d_2 (1-\alpha)\bar{\gamma}_{SD}}{1 + \frac{R_{C_2}[(1-\alpha)\bar{\gamma}_{SD} + \alpha\bar{\gamma}_{RD}]}{k_p\left(\frac{E_p}{N_0}\right)}} \right), \qquad (5.28)$$

and

$$B(d) = g_{PSK} \left(\frac{R_{C_2} d_2 \alpha \bar{\gamma}_{RD}}{1 + \frac{R_{C_2}[(1-\alpha)\bar{\gamma}_{SD} + \alpha\bar{\gamma}_{RD}]}{k_p\left(\frac{E_p}{N_0}\right)}} \right). \qquad (5.29)$$

Having obtained the pairwise error probability in (5.27), the BER probability

can be upper bounded using (3.16).

Noting that if we assume $\bar{\gamma}_{SD} = \bar{\gamma}_{RD} = E_p/N_0 = E_b/N_0$ to be sufficiently large, the average pairwise error probability can be approximated as

$$P(d) \approx \frac{3(M-1)}{8M} \left(\sin\frac{\pi}{M}\right)^{-4} \left(\frac{R_{C_2} d_2 \alpha}{\left(1+\frac{R_{C_2}}{k_p}\right)}\right)^{-1} \left(\frac{R_{C_1} d_1}{\left(1+\frac{R_{C_1}}{k_p}\right)} + \frac{R_{C_2} d_2 (1-\alpha)}{\left(1+\frac{R_{C_2}}{k_p}\right)}\right)^{-1} \left(\frac{E_b}{N_0}\right)^{-2}, \quad (5.30)$$

which suggests that the diversity order achieved is two when the channel from S to R is error-free, and the k_p symbols of each pilot sequence or the pilot to noise ratio (PNR), (E_p/N_0) increases.

DF with Errors at Relay

The instantaneous received SNR for the channel from S to R for the first frame is given by

$$\gamma_{D_3}(t) = \frac{2R_{C_1} E_{SR} |h_{SR}(t)|^2}{N_0 \left(1+\frac{R_{C_1} E_{SR}}{k_p E_p}\right)} = \frac{2R_{C_1} \gamma_{SR}(t)}{\left(1+\frac{R_{C_1} E_{SR}}{k_p E_p}\right)}, \quad t = 1,2,\cdots,n_1 \quad (5.31)$$

From (5.21), (5.22), and (5.31), when the fading coefficients h_{SD}, h_{RD}, and h_{SR} are constant over the codeword, the conditional pairwise error probability is given by

$$P(d|\gamma_{SD},\gamma_{SR},\gamma_{RD}) = Q\left(\sqrt{2g_{PSK}\left(\frac{R_{C_1} d_1 \gamma_{SD}}{\left(1+\frac{R_{C_1} E_{SD}}{k_p E_p}\right)} + \frac{R_{C_2} d_2 \gamma_{SD}}{\left(1+\frac{R_{C_2} E_{SD}}{k_p E_p}\right)}\right)}\right)$$

$$\cdot Q\left(\sqrt{2g_{PSK}\frac{R_{C_1} d_1 \gamma_{SR}}{\left(1+\frac{R_{C_1} E_{SR}}{k_p E_p}\right)}}\right) + \left(1 - Q\left(\sqrt{2g_{PSK}\frac{R_{C_1} d_1 \gamma_{SR}}{\left(1+\frac{R_{C_1} E_{SR}}{k_p E_p}\right)}}\right)\right)$$

$$Q\left(\sqrt{2g_{PSK}\left(\frac{R_{C_1}d_1\gamma_{SD}}{\left(1+\frac{R_{C_1}E_{SD}}{k_pE_p}\right)}+\frac{[R_{C_2}d_2(1-\alpha)\gamma_{SD}+R_{C_2}d_2\alpha\gamma_{RD}]}{\left(1+\frac{R_{C_2}[(1-\alpha)E_{SD}+\alpha E_{RD}]}{k_pE_p}\right)}\right)}\right). \tag{5.32}$$

Now, using (3.10), (5.32) can be written as

$$P(d|\gamma_{SD},\gamma_{SR},\gamma_{RD}) =$$

$$\frac{1}{\pi}\int_0^{\frac{(M-1)\pi}{M}} exp\left(-g_{PSK}\left(\frac{R_{C_1}d_1}{\left(1+\frac{R_{C_1}E_{SD}}{k_pE_p}\right)}+\frac{R_{C_2}d_2}{\left(1+\frac{R_{C_2}E_{SD}}{k_pE_p}\right)}\right)\frac{\gamma_{SD}}{\sin^2\theta_1}\right)d\theta_1$$

$$\cdot\frac{1}{\pi}\int_0^{\frac{(M-1)\pi}{M}} exp\left(-g_{PSK}\left(\frac{R_{C_1}d_1}{\left(1+\frac{R_{C_1}E_{SR}}{k_pE_p}\right)}\right)\frac{\gamma_{SR}}{\sin^2\theta_2}\right)d\theta_2$$

$$+\left(1-\frac{1}{\pi}\int_0^{\frac{(M-1)\pi}{M}} exp\left(-g_{PSK}\left(\frac{R_{C_1}d_1}{\left(1+\frac{R_{C_1}E_{SR}}{k_pE_p}\right)}\right)\frac{\gamma_{SR}}{\sin^2\theta_1}\right)d\theta_1\right)$$

$$\cdot\frac{1}{\pi}\int_0^{\frac{(M-1)\pi}{M}} exp\left(-g_{PSK}\left(\frac{R_{C_1}d_1}{\left(1+\frac{R_{C_1}E_{SD}}{k_pE_p}\right)}+\frac{R_{C_2}d_2(1-\alpha)}{\left(1+\frac{R_{C_2}[(1-\alpha)E_{SD}+\alpha E_{RD}]}{k_pE_p}\right)}\right)\frac{\gamma_{SD}}{\sin^2\theta_2}\right)$$

$$\cdot exp\left(-g_{PSK}\left(\frac{R_{C_2}d_2\alpha}{\left(1+\frac{R_{C_2}[(1-\alpha)E_{SD}+\alpha E_{RD}]}{k_pE_p}\right)}\right)\frac{\gamma_{RD}}{\sin^2\theta_2}\right)d\theta_2. \tag{5.33}$$

Using (3.13), the average pairwise error probability can then be shown as

$$P(d)=\frac{1}{\pi}\int_0^{\frac{(M-1)\pi}{M}}\left(1+\frac{g_{PSK}}{\sin^2\theta_1}\left(\frac{R_{C_1}d_1\bar{\gamma}_{SD}}{\left(1+\frac{R_{C_1}\bar{\gamma}_{SD}}{k_p\left(\frac{E_p}{N_0}\right)}\right)}+\frac{R_{C_2}d_2\bar{\gamma}_{SD}}{1+\frac{R_{C_2}\bar{\gamma}_{SD}}{k_p\left(\frac{E_p}{N_0}\right)}}\right)\right)^{-1}d\theta_1$$

$$\cdot \frac{1}{\pi} \int_{0}^{\frac{(M-1)\pi}{M}} \left(1 + \frac{g_{PSK}}{\sin^2\theta_2} \left(\frac{R_{C_1} d_1 \bar{\gamma}_{SR}}{\left(1 + \frac{R_{C_1} \bar{\gamma}_{SR}}{k_p \left(\frac{E_p}{N_0} \right)} \right)} \right) \right)^{-1} d\theta_2$$

$$+ \left(1 - \frac{1}{\pi} \int_{0}^{\frac{(M-1)\pi}{M}} \left(1 + \frac{g_{PSK}}{\sin^2\theta_1} \left(\frac{R_{C_1} d_1 \bar{\gamma}_{SR}}{\left(1 + \frac{R_{C_1} \bar{\gamma}_{SR}}{k_p \left(\frac{E_p}{N_0} \right)} \right)} \right) \right)^{-1} d\theta_1 \right)$$

$$\frac{1}{\pi} \int_{0}^{\frac{(M-1)\pi}{M}} \left(1 + \frac{g_{PSK}}{\sin^2\theta_2} \left(\frac{R_{C_1} d_1 \bar{\gamma}_{SD}}{\left(1 + \frac{R_{C_1} \bar{\gamma}_{SD}}{k_p \left(\frac{E_p}{N_0} \right)} \right)} + \frac{R_{C_2} d_2 (1-\alpha) \bar{\gamma}_{SD}}{\left(1 + \frac{R_{C_2} [(1-\alpha)\bar{\gamma}_{SD} + \alpha\bar{\gamma}_{RD}]}{k_p \left(\frac{E_p}{N_0} \right)} \right)} \right) \right)^{-1}$$

$$\cdot \left(1 + \frac{g_{PSK}}{\sin^2\theta_2} \left(\frac{R_{C_2} d_2 \alpha \bar{\gamma}_{RD}}{\left(1 + \frac{R_{C_2} [(1-\alpha)\bar{\gamma}_{SD} + \alpha\bar{\gamma}_{RD}]}{k_p \left(\frac{E_p}{N_0} \right)} \right)} \right) \right)^{-1} d\theta_2, \qquad (5.34)$$

where $E[|h_{SR}|^2] = 1$ is the average of $|h_{SR}|^2$. Using the results of Appendix C, the average pairwise error probability can be shown as

$$P(d) = \left[\frac{(M-1)}{M} - \frac{1}{\pi} \sqrt{\frac{C(d)}{1+C(d)}} \tan^{-1} \left(\sqrt{\frac{1+C(d)}{C(d)}} \tan \left(\frac{(M-1)\pi}{M} \right) \right) \right]$$

$$\cdot \left[\frac{(M-1)}{M} - \frac{1}{\pi} \sqrt{\frac{D(d)}{1+D(d)}} \tan^{-1} \left(\sqrt{\frac{1+D(d)}{D(d)}} \tan \left(\frac{(M-1)\pi}{M} \right) \right) \right]$$

$$+\left[1-\frac{(M-1)}{M}+\frac{1}{\pi}\sqrt{\frac{D(d)}{1+D(d)}}\tan^{-1}\left(\sqrt{\frac{1+D(d)}{D(d)}}\tan\left(\frac{(M-1)\pi}{M}\right)\right)\right]$$

$$\cdot\left[\frac{(M-1)}{M}+\frac{A(d)}{(B(d)-A(d))\pi}\sqrt{\frac{A(d)}{1+A(d)}}\tan^{-1}\left(\sqrt{\frac{1+A(d)}{A(d)}}\tan\left(\frac{(M-1)\pi}{M}\right)\right)\right.$$

$$\left.+\frac{B(d)}{(A(d)-B(d))\pi}\sqrt{\frac{B(d)}{1+B(d)}}\tan^{-1}\left(\sqrt{\frac{1+B(d)}{B(d)}}\tan\left(\frac{(M-1)\pi}{M}\right)\right)\right], \qquad (5.35)$$

where $C(d)=g_{PSK}\left(\frac{R_{C_1}d_1\bar{\gamma}_{SD}}{\left(1+\frac{R_{C_1}\bar{\gamma}_{SD}}{k_p(E_p/N_0)}\right)}+\frac{R_{C_2}d_2\bar{\gamma}_{SD}}{1+\frac{R_{C_2}\bar{\gamma}_{SD}}{k_p(E_p/N_0)}}\right)$, $D(d)=\left(\frac{g_{PSK}\,R_{C_1}d_1\bar{\gamma}_{SR}}{\left(1+\frac{R_{C_1}\bar{\gamma}_{SR}}{k_p(E_p/N_0)}\right)}\right)$,

$A(d)$ and $B(d)$ are defined as in (5.28) and (5.29), respectively. When $\bar{\gamma}_{SR}$ is very large (i.e., $\bar{\gamma}_{SR}\rightarrow\infty$), the relay will have perfect detection, and thus (5.35) will be the same as (5.27). Having obtained the pairwise error probability in (5.35), the BER probability can be upper bounded using (3.16).

5.2.3 Simulation Results

In our simulations, we assume that the relay node operates in the DF mode. For simplicity, BPSK modulation is assumed. In all simulations, otherwise mentioned, the transmitted frame size is equal to n1 = n2 = 130 coded bits, and a pilot sequence consisting of kp symbols. The convolutional code used is of constraint length four and generator polynomials (13, 15, 15, 17)$_{octal}$ [44]. When the relays cooperate with the source node, the source transmits the code-words corresponding to rate 1/2, (13, 15)$_{octal}$ convolutional code to the relay and destination nodes in the first frame. The relay node receives this codeword and decoding is performed to obtain an estimate of the source information bits. In the second frame, the relay and source nodes transmit the code-words corresponding to rate 1/2, (15, 17)$_{octal}$ convolutional code using Alamouti scheme to the

destination node. Also we assume that the $S{-}R$, $R{-}D$, and $S{-}D$ channels have equal PNRs (E_p/N_0).

Figure 5.5 shows a comparison between the simulated and the bit error rate upper bound corresponding to the expressions given in (5.27), and (3.16) with $k_p = 10$ symbols for three cases of $E_p/N_0 = 8$, 10, and 14 dB. Code $(13, 15, 15, 17)_{octal}$ is used with $R_{C_1} = R_{C_2} = 0.5$ and $\alpha = 0.5$. In Figure 5.6, we show a comparison of the simulated and analytical BER results based on the expressions given in (3.16), and (5.35) for $\bar{\gamma}_{SR} = 8$ dB with imperfect channel estimation and $k_p = 10$ symbols for three cases $E_p/N_0 = 10$, 12, and 16 dB. In addition, we include, for comparison, the results for the DF relaying with errors and perfect channel estimation. It is clear from these figures that as E_p/N_0 gets larger, the performance converges to the ideal case.
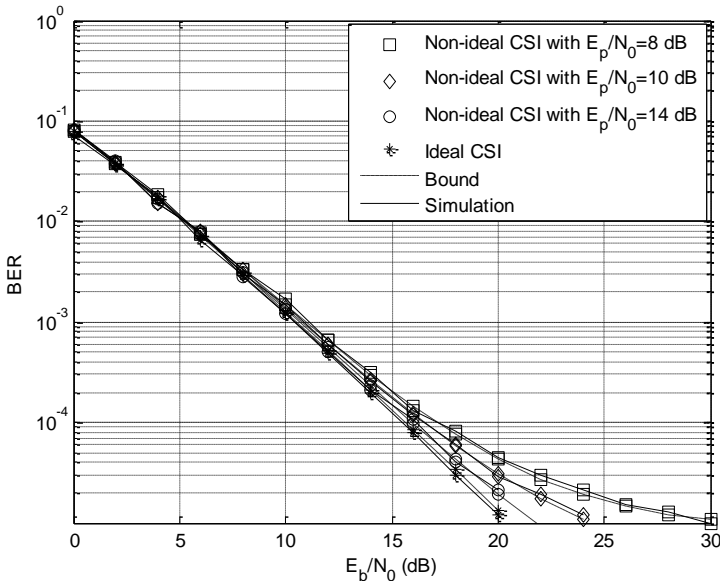

Figure 5.5 *Comparison of analysis and simulated BER with error-free detection at relay node over quasi-static fading; $k_p = 10$ symbols; $E_p/N_0 = 8$, 10, and 14 dB.*
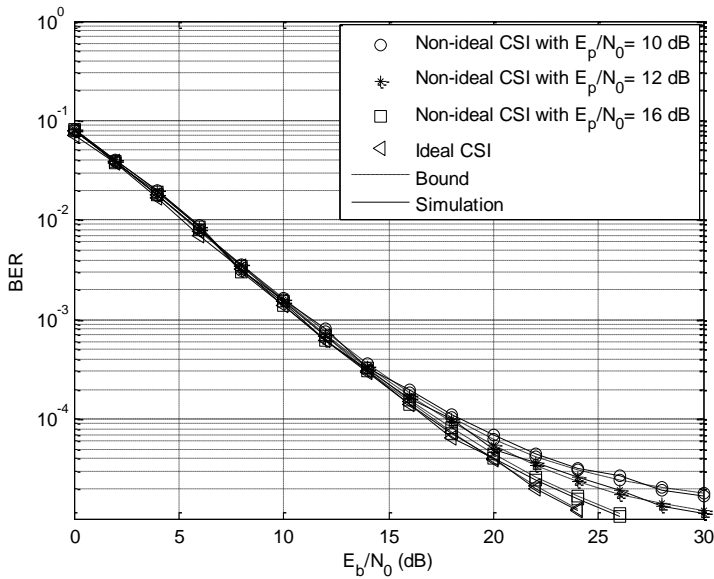
Figure 5.6 *Comparison of analysis and simulated BER for slow Rayleigh fading,*
$\bar{\gamma}_{SR} = 8\ dB$ *with relay errors,* $k_p = 10$ *symbols;* $E_p/N_0 = 10, 12,$ *and 16 dB.*

References

[1] V. Tarokh, N. Seshadri, and A. R. Calderbank, "Space-time codes for high data rate wireless communications: performance criterion and code construction," *IEEE Trans. Inform. Theory*, vol. 44, no. 2, pp. 744-765, Mar. 1998.

[2] A. R. Calderbank, "The art of signaling: Fifty years of coding theory," *IEEE Trans. Info. Theory*, vol. 44, no. 6, pp. 2561-2595, October 1998.

[3] S. Verdu, "Wireless bandwidth in the making," *IEEE Commun. Mag*., vol. 38, no. 7, pp. 53-58, July 2000.

[4] A. F. Naguib, N. Seshadri, and A. R. Calderbank, "Increasing data rate over wireless channels," *IEEE Signal Processing Mag*., vol. 17, no. 3, pp. 76-92, May 2000.

[5] W. C. Jakes, *Microwave Mobile Communication*, 2nd ed. Piscataway, NJ: IEEE Press, 1994.

[6] G. Foschini, "Layered space-time architecture for wireless communication in a fading environment when using multi-element antennas," *Bell Labs Technical Journal*, vol. 1, no. 2, pp. 41-59, 1996.

[7] E. Telatar, "Capacity of multi-antenna Gaussian channels," *Europ. Trans. Telecommu.*, vol. 10, no. 6, pp. 585-595, Nov. 1999.

[8] G. Foschini and M. Gans, "On limits of wireless communications in a fading environment when using multiple antennas," *Wireless Personal Communications*, vol. 6, no. 3, pp. 311-335, Mar. 1998.

[9] S. M. Alamouti, "A simple transmit diversity technique for wireless communications", *IEEE J. Select. Areas Commun*., vol. 16, no. 8, pp.1451-1458, Oct. 1998.

[10] E. Biglieri, J. Proakis, and S. Shamai, "Fading channels: Information-theoretic and communications aspects," *IEEE Trans. Info. Theory*, vol. 44, no. 6, pp. 2619-2692, October 1998.

[11] V. Tarokh, H. Jafarkhani, and A. R. Calderbank, "Space-time block codes from orthogonal designs," *IEEE Trans. Inform. Theory*, vol. 45, no. 5, pp. 1456-1467, July 1999.

[12] S. Baro, G. Bauch and A. Hansmann, "Improved codes for space-time trellis coded modulation," *IEEE Commun. Lett.*, vol. 4, no. 1, pp. 20-22, Jan. 2000.

[13] A. Sendonaris, E. Erkip, and B. Aazhang, "User Cooperation Diversity, Part I: System description," *IEEE Trans. on Commun.*, vol. 51, no. 11, pp. 1927-1938, Nov. 2003.

[14] Sendonaris, E. Erkip, and B. Aazhang, "User Cooperation Diversity, Part II: Implementation Aspects and Performance Analysis," *IEEE Trans. on Commun.*, vol. 51, no. 11, pp. 1939-1948, Nov. 2003.

[15] R. U. Nabar and H. Bolcskei, "Fading relay channels: performance limits and space-time signal design," *IEEE J. on Selected Area in Comm.*, vol. 22, no. 6, pp. 1099-1109, Aug. 2004.

[16] N. Laneman, D. N. C. Tse, and G. W. Wornell, "Cooperative diversity in wireless networks: Efficient protocols and outage behavior," *IEEE Trans. Inform. Theory*, vol. 50, no. 12, pp. 3062-3080, Dec. 2004.

[17] R. U. Nabar and H. Bolcskei, "Space-time signal design for fading relay channels," *IEEE GLOBECOM*, vol. 4, San Francisco, CA, pp. 1952-1956, Dec. 2003.

[18] Chao Wang, John S. Thompson, Yijia Fan, H. Vincent Poor, "On the diversity multiplexing tradeoff of concurrent decode-and-forward relaying," *in Proc. IEEE Wireless Communications and Networking Conference (WCNC)*, pp. 582-587, 2008.

[19] Abdulkareem Adinoyi and Halim Yanikomeroglu, "Cooperative relaying in multi-antenna fixed relay networks," *IEEE Trans. on Wireless Commun.*, vol. 6, no. 2, pp. 533-544, Feb. 2007.

[20] Khuong Ho-Van and Tho Le-Ngoc, "Bandwidth-efficient cooperative relaying schemes with multi-antenna relay," *EURASIP Journal on Advances in Signal Processing, Volume 2008*, Article ID 683105, 11 pages doi: 10.1155/2008/683105.

[21] A. F. Dana and B. Hassibi, "On the power efficiency of sensory and ad hoc wireless networks," *IEEE Trans. Inform. Theory*, vol. 52, no. 7, pp. 2890-2914, July 2006.

[22] N. Laneman and G. W. Wornell, "Distributed space-time-coded protocols for exploiting cooperative diversity in wireless network," *IEEE Trans. Inform. Theory*, vol. 49, no. 10, pp. 2415-2425, Oct. 2003.

[23] J. N. Laneman and G. W. Wornell, "Energy-efficient antenna sharing and relaying for wireless networks," *IEEE Wireless Commun. and Networking Conf.*, vol. 1, Chicago, IL, pp. 7-12, Sep. 2000.

[24] O. Hasna and M. -S. Alouini, "A performance study of dual-hop transmissions with fixed gain relays," *IEEE Trans. on Wireless Commun.*, vol. 3, no. 6, pp. 1963-1968, Nov. 2004.

[25] A. Ribeiro, X. Cai, and G. B. Giannakis, "Symbol error probabilities for general cooperative links," *IEEE Trans. on Wireless Commun.*, vol. 4, no. 3, pp. 1264-1273, May 2005.

[26] A. Zhao and M. C. Valenti, "Distributed turbo coded diversity for the relay channel," *IEE Electronics Letters*, vol. 39, no. 10, pp. 786-787, May 2003.

[27] R. Liu, P. Spasojevic, and E. Soljanin, "Punctured turbo code ensembles," *IEEE Information Theory Workshop (ITW) Conf.*, Paris, France, pp. 249-252, Mar. 2003.

[28] Janani, A. Hedayat, T. E. Hunter, and A. Norsatinia, "Coded cooperation in wireless communications: Space-time transmission and iterative decoding," *IEEE Transaction On Signal Processing,* vol. 52, no. 2, pp. 362-371, Feb. 2004.

[29] A. Wittneben, "A new bandwidth efficient transmit antenna modulation diversity scheme for linear digital modulation," *IEEE International Conf. Comm. (ICC93)*, vol. 3, pp. 1630-1634, May 1993.

[30] Thomas M. Cover and Joy A. Thomas, *Elements of Information Theory*, John Wiley & Sons, Inc., New York, 1991.

[31] E. C. van der Meulen, "Three-terminal communication channels," *Advances in Applied Probability*, vol.3, no. 1, pp. 120-154, 1971.

[32] Edward C. van der Meulen, *Transmission of Information in a T-Terminal Discrete Memory less Channel, Department of Statistics*, University of California, Berkeley, CA, 1968.

[33] Thomas M. Cover and Abbas A. El Gamal, "Capacity theorems for the relay channel," *IEEE Trans. Inform. Theory*, vol. 25, no. 5, pp. 572-584, Sep. 1979.

[34] Schein and R. Gallager, "The Gaussian parallel relay network," *IEEE Int. Symp. Information Theory (ISIT)*, Sorrento, Italy, page 22, June 2000.

[35] T. Hunter and A. Nosratinia, "Cooperation diversity through coding," *IEEE Int. Symp. Information Theory (ISIT)*, Lausanne, Switzerland, page 220, Jun. 2002.

[36] R. Liu, P. Spasojevic, and E. Soljanin, "User cooperation with punctured turbo codes," *in Proc. 41st Allerton Conf. Commun. Control, Comput.*, Monticello, IL, Oct. 2003.

[37] A. Stefanov and E. Erkip, "Cooperative coding for wireless networks," *IEEE Trans. on Commun.*, vol. 52, no. 9, pp. 1470-1476, Sep. 2004.

[38] R. Knopp and P. A. Humblet, "On coding for block fading channels," *IEEE Trans. Inform. Theory*, vol. 46, no. 1, pp. 189-205, Jan. 2000.

[39] A. Stefanov and E. Erkip, "Cooperative space-time coding for wireless networks," *IEEE Trans. on Commun.*, vol. 53, no. 11, pp. 1804-1809, Nov. 2005.

[40] T. E. Hunter and A. Nosratinia, "Diversity through coded cooperation," *IEEE Trans. on Wireless Commun.*, vol. 5, no. 2, pp. 283-289, Feb. 2006.

[41] T. E. Hunter and A. Nosratinia, "Performance analysis of coded cooperation diversity," *ICC 2003*, vol. 4, pp. 2688-2692, 11-15 May 2003.

[42] Erik G. Larsson and Branimir R. Vojcic, "Cooperation transmit diversity based on superposition modulation," *IEEE Commun. Letters*, vol. 9, no. 9, pp. 778-780, Sep. 2005.

[43] Lei Xiao, Thomas E. Fuja, Jorg Kliewer, and Daniel J. Costello, "A network coding approach to cooperative diversity," *IEEE Trans. Inform. Theory*, vol. 53, no. 10, pp. 3714-3722, Oct. 2007.

[44] P. Frenger, P. Orten, and T. Ottosson, "Convolutional codes with optimum distance spectrum," *IEEE Commun. Letters*, vol. 3, no. 11, pp. 317-319, Nov. 1999.

[45] A. Ghrayeb and T. M. Duman, "Performance analysis of MIMO systems with antenna selection over quasi-static fading channels," *IEEE Trans. Veh. Techn.*, vol. 52, no. 2, pp. 281-288, March 2003.

[46] X. Zeng and A. Ghrayeb, "Performance bounds for space-time block codes with antenna selection," *IEEE Trans. Inform. Theory*, vol. 50, no. 9, pp. 2130-2137, Sept. 2004.

[47] W. Hamouda and A. Ghrayeb, "Performance of combined channel coding and space-time block coding systems with antenna selection," *IEEE Veh. Technol. Conf.*

(VTC), Milan, Italy, vol. 2, pp. 623-627, May 2004.

[48] A. Gore and A. Paulraj, "MIMO antenna subset selection with space-time coding," *IEEE Trans. Signal Proc*., vol. 50, no. 10, pp. 2580-2588, Oct. 2002.

[49] Zhuo, Y. Jinhong, B. Vucetic, and Z. Zhendong, "Performance of Alamouti scheme with transmit antenna selection," *IEE Electron. Lett.,* vol. 39, no. 23, pp. 1666-1668, Nov. 2003.

[50] A. F. Naguib, V. Tarokh, N. Seshadri, and A. R. Calderbank, "Space-time coding modem for high data rate wireless communications," *IEEE J. Select. Areas Commun*., vol. 16, no. 8, pp. 1459-1478, Oct. 1998.

[51] A. Fragouli, N. Al-Dhahir, and W. Turin, "Training-based channel estimation for multiple-antenna broadband transmissions," *IEEE Trans. Wireless Commun*., vol. 2, no. 2, pp. 384-391, Mar. 2003.

[52] A. Hassibi and B. M. Hochwald, "How much training is needed in multiple antenna wireless links?" *IEEE Trans. Inform. Theory*, vol. 49, no. 4, pp. 951–963, Apr. 2003.

[53] Y. Jing and B. Hassibi, "Wireless networks, diversity and space-time codes," *IEEE Inform. Theory Workshop*, San Antanio, Texas, pp. 463-468, Oct. 2004.

[54] T. Kiran and B. S. Rajan, "Partially-coherent distributed space-time codes with differential encoder and decoder," *IEEE J. Selected Areas Commun*., vol. 25, no. 2, pp. 426-433, Feb. 2007.

[55] C. S. Patel and G. L. Stuber, "Channel estimation for amplify and forward relay based cooperation diversity systems," *IEEE Trans. on Wireless Commun*., vol. 6, no. 6, pp. 2348-2356, June 2007.

[56] G. S. Rajan and B. S. Rajan, "Leveraging coherent distributed space-time codes for non coherent communication in relay networks via training," *IEEE Trans. on Wireless Commun.,* April 2008.

[57] Feifei Gao, Tao Cui, and A. Nallanathan, "On channel estimation and optimal training design for amplify and forward relay networks*," IEEE Trans. on Wireless Commun.*, vol. 7, no. 5, pp. 1907-1916, May 2008.

[58] Y. Jing and H. Jafarkhani, "Distributed differential space-time coding for wireless relay networks," *IEEE Trans. Commun*., vol. 56, no. 7, pp. 1092-1100, July 2008.

[59] K. Simon and M.-S. Alouini, *Digital Communication over Fading Channels: A Unified Approach to Performance Analysis*, Wiley, New York, 2000.

[60] J. G. Proakis, *Digital Communication*, McGraw-Hill, Inc., 1995.

[61] W. C. Jakes, *Microwave Mobile Communication*, 2nd ed. Piscataway, NJ: IEEE Press, 1994.

[62] S. Gradshteyn and I. M. Ryzhik, *Table of Integrals, Series, and Products*, 5th ed., San Diego, CA: Academic, 1994.

[63] G. E. Roberts and H. Kaufman, *Table of Laplace Transform*, Philadelphia, PA: Saunders, 1966.

[64] Mohamed Elfituri, Walaa Hamouda, and Ali Ghrayeb, "A convolutional-based distributed coded cooperation scheme for relay channels," *IEEE Trans. Veh. Techn.*, vol. 58, no.2, pp. 655-669, Feb. 2009.

[65] Mohamed Elfituri, Walaa Hamouda, and Ali Ghrayeb, "Distributed coded cooperation for relay channels operating in the decode-and-forward mode," *IEEE International Conference on Communications (ICC 2008)*, Beijing, China, pp. 4586-4590, May 2008.

[66] Mohamed Elfituri, Ali Ghrayeb, and Walaa Hamouda, "Antenna/relay selection for coded wireless cooperative networks," *IEEE International Conference on Communications (ICC 2008)*, Beijing, China, pp. 840-844, May 2008.

[67] Mohamed Elfituri, Ali Ghrayeb, and Walaa Hamouda, "Antenna/Relay selection for coded cooperative networks*," IEEE Trans. Commun., accepted for publication*, Mar. 2009.

[68] Mohamed Elfituri, Ali Ghrayeb, and Walaa Hamouda, "Analysis of a distributed coded cooperation scheme for multi-relay channels," *IEEE International Symposium on Signal Processing and Info. Techn. (ISSPIT 2007),* Cairo, Egypt, pp. 454-459, Dec. 2007.

[69] Mohamed Elfituri, Walaa Hamouda, and Ali Ghrayeb, "Outage probability analysis of distributed coded cooperation for relay channels operating in the DF mode," *IEEE International Symposium on Personal Indoor and Mobile Radio Commu. (PIMRC 2007)*, Athens, Greece, pp. 1-5, Sep. 2007.

[70] Mohamed Elfituri, Walaa Hamouda, and Ali Ghrayeb, "Performance analysis of a new transmission scheme for multi-relay channels," *IEEE Workshop on Signal Processing Systems (SiPS 2006),* Banff, Alberta, Canada, pp. 34-38, Oct. 2006.

Appendices

Appendix A: Proof of Equations (3.20) and (3.31)-(3.33)

A.1 Proof of Equation (3.20)

The average pairwise error probability of (3.19), $P(d)$, can then be written as

$$P(d) = \frac{1}{\pi} \int_0^{\frac{(M-1)\pi}{M}} \int_0^\infty exp\left(\frac{-g_{PSK}\left(R_{C_1}d_1 + R_{C_2}d_2\right)\gamma_{SD}}{\sin^2\theta}\right) p_{\gamma_{SD}}(\gamma_{SD}) \, d\gamma_{SD} \, d\theta$$

$$\cdot \prod_{m=1}^{L}\left(\frac{1}{\pi} \int_0^{\frac{(M-1)\pi}{M}} \int_0^\infty exp\left(\frac{-g_{PSK}R_{C_1}d_1\gamma_{SR_m}}{\sin^2\theta_m}\right) p_{\gamma_{SR_m}}(\gamma_{SR_m}) \, d\gamma_{SR_m} \, d\theta_m\right)$$

$$+ \sum_{L'=1}^{L-1}\sum_{\Omega}\left[\prod_{j\notin\Omega}\left(\frac{1}{\pi} \int_0^{\frac{(M-1)\pi}{M}} \int_0^\infty exp\left(\frac{-g_{PSK}R_{C_1}d_1\gamma_{SR_j}}{\sin^2\theta_j}\right) p_{\gamma_{SR_j}}(\gamma_{SR_j}) \, d\gamma_{SR_j} \, d\theta_j\right)\right.$$

$$\cdot \prod_{j\in\Omega}\left(1 - \frac{1}{\pi} \int_0^{\frac{(M-1)\pi}{M}} \int_0^\infty exp\left(\frac{-g_{PSK}R_{C_1}d_1\gamma_{SR_j}}{\sin^2\theta_j}\right) p_{\gamma_{SR_j}}(\gamma_{SR_j}) \, d\gamma_{SR_j} \, d\theta_j\right)$$

$$\cdot \frac{1}{\pi} \int_0^{\frac{(M-1)\pi}{M}} \prod_{j\in\Omega}\int_0^\infty\int_0^\infty exp\left(\frac{-g_{PSK}\left(R_{C_1}d_1 + \frac{R_{C_2}}{(L'+1)}d_2\right)\gamma_{SD}}{\sin^2\theta}\right)$$

$$\left. \cdot exp\left(\frac{-g_{PSK}\left(R_{C_1}d_1 + R_{C_2}d_2\right)\gamma_{SD}}{\sin^2\theta}\right) p_{\gamma_{SD}}(\gamma_{SD}) p_{\gamma_{R_jD}}(\gamma_{R_jD}) \, d\gamma_{SD} \, d\gamma_{R_jD} \, d\theta\right]$$

$$+ \prod_{m=1}^{L}\left(1 - \frac{1}{\pi} \int_0^{\frac{(M-1)\pi}{M}} \int_0^\infty exp\left(\frac{-g_{PSK}R_{C_1}d_1\gamma_{SR_m}}{\sin^2\theta_m}\right) p_{\gamma_{SR_m}}(\gamma_{SR_m}) \, d\gamma_{SR_m} \, d\theta_m\right)$$

$$\cdot \frac{1}{\pi} \int\limits_{0}^{\frac{(M-1)\pi}{M}} \prod_{m=1}^{L} \int\limits_{0}^{\infty} \int\limits_{0}^{\infty} exp \left(\frac{-g_{PSK} \left(R_{C_1} d_1 + \frac{R_{C_2}}{(L'+1)} d_2 \right) \gamma_{SD}}{\sin^2 \theta} \right)$$

$$\cdot exp \left(\frac{-g_{PSK} R_{C_2} d_2 \gamma_{R_m D}}{(L+1)\sin^2 \theta} \right) p_{\gamma_{SD}} (\gamma_{SD}) p_{\gamma_{R_m D}} (\gamma_{R_m D}) d\gamma_{SD} d\gamma_{R_m D} d\theta. \qquad (A.1)$$

Using (3.13), (A.1) can then be written

$$P(d) = \frac{1}{\pi} \int\limits_{0}^{\frac{(M-1)\pi}{M}} \left(1 + \frac{g_{PSK} \left(R_{C_1} d_1 + R_{C_2} d_2 \right) \bar{\gamma}_{SD}}{\sin^2 \theta} \right)^{-1} d\theta$$

$$\cdot \prod_{m=1}^{L} \left(\frac{1}{\pi} \int\limits_{0}^{\frac{(M-1)\pi}{M}} \left(1 + \frac{g_{PSK} R_{C_1} d_1 \bar{\gamma}_{SR_m}}{\sin^2 \theta_m} \right)^{-1} d\theta_m \right)$$

$$+ \sum_{L'=1}^{L-1} \sum_{\Omega} \left[\prod_{j \notin \Omega} \left(\frac{1}{\pi} \int\limits_{0}^{\frac{(M-1)\pi}{M}} \left(1 + \frac{g_{PSK} R_{C_1} d_1 \bar{\gamma}_{SR_j}}{\sin^2 \theta_j} \right)^{-1} d\theta_j \right) \right.$$

$$\cdot \prod_{j \in \Omega} \left(1 - \frac{1}{\pi} \int\limits_{0}^{\frac{(M-1)\pi}{M}} \left(1 + \frac{g_{PSK} R_{C_1} d_1 \bar{\gamma}_{SR_j}}{\sin^2 \theta_j} \right)^{-1} d\theta_j \right) \frac{1}{\pi} \int\limits_{0}^{\frac{(M-1)\pi}{M}}$$

$$\cdot \left(1 + \frac{g_{PSK} \left(R_{C_1} d_1 + \frac{R_{C_2}}{(L'+1)} d_2 \right) \bar{\gamma}_{SD}}{\sin^2 \theta} \right)^{-1} \prod_{j \in \Omega} \left(1 + \frac{g_{PSK} R_{C_2} d_2 \bar{\gamma}_{R_j D}}{(L'+1)\sin^2 \theta} \right)^{-1} d\theta \right]$$

$$+ \prod_{m=1}^{L} \left(1 - \frac{1}{\pi} \int\limits_{0}^{\frac{(M-1)\pi}{M}} \left(1 + \frac{g_{PSK} R_{C_1} d_1 \bar{\gamma}_{SR_m}}{\sin^2 \theta_m} \right)^{-1} d\theta_m \right) \frac{1}{\pi} \int\limits_{0}^{\frac{(M-1)\pi}{M}}$$

$$\cdot \left(1 + \frac{g_{PSK} \left(R_{C_1} d_1 + \frac{R_{C_2}}{(L+1)} d_2 \right) \bar{\gamma}_{SD}}{\sin^2 \theta} \right)^{-1} \prod_{m=1}^{L} \left(1 + \frac{g_{PSK} R_{C_2} d_2 \bar{\gamma}_{R_m D}}{(L+1)\sin^2 \theta} \right)^{-1} d\theta, \ (A.2)$$

where $\bar{\gamma}_{SR_m} = \frac{E_{SR_m}}{N_0} E \left[\left| h_{SR_m} \right|^2 \right]$ is the average SNR.

A.2 Proof of Equation (3.31)-(3.33)

From (3.30), I_1, $I_2(j)$, I_3 can be written as

$$I_1 = Pr\{(1+\gamma_{SD})^\beta (1+\gamma_{SD})^{(1-\beta)} < 2^{R_c}\}$$

$$= \int_0^{2^{R_c}-1} \frac{1}{\overline{\gamma}_{SD}} exp\left(\frac{-\gamma_{SD}}{\overline{\gamma}_{SD}}\right) d\gamma_{SD} = 1 - exp\left(\frac{(1-2^{R_c})}{\overline{\gamma}_{SD}}\right), \qquad (A.3)$$

and

$$I_2(j) = Pr\left\{(1+\gamma_{SD})^\beta \left(1 + \frac{1}{(L'+1)}\left[\gamma_{SD} + \sum_{j\in\Omega} \gamma_{R_j D}\right]\right)^{(1-\beta)} < 2^{R_c}\right\}$$

$$= \int_0^{A_1'} \frac{1}{\overline{\gamma}_{SD}} exp\left(\frac{-\gamma_{SD}}{\overline{\gamma}_{SD}}\right) d\gamma_{SD}$$

$$\cdot \int_0^{A_2} \cdots \int_0^{A_2} \prod_{j\in\Omega}\left(\frac{1}{\overline{\gamma}_{R_j D}}\right) exp\left(-\sum_{j\in\Omega} \frac{\gamma_{R_j D}}{\overline{\gamma}_{R_j D}}\right) \prod_{j\in\Omega} d\gamma_{R_j D}$$

$$= \left(1 - exp\left(\frac{-A_1'}{\overline{\gamma}_{SD}}\right)\right) \prod_{j\in\Omega}\left(\int_0^{A_2'} \frac{1}{\overline{\gamma}_{R_j D}} exp\left(\frac{-\gamma_{R_j D}}{\overline{\gamma}_{R_j D}}\right) d\gamma_{R_j D}\right)$$

$$= \left(1 - exp\left(\frac{-A_1'}{\overline{\gamma}_{SD}}\right)\right) \prod_{j\in\Omega}\left(1 - exp\left(\frac{-A_2'}{\overline{\gamma}_{R_j D}}\right)\right)$$

$$= \left(1 - exp\left(\frac{(1-2^{R_c})(L'+1)}{\overline{\gamma}_{SD}}\right)\right) \prod_{j\in\Omega}\left(1 - exp\left(\frac{\left(1-2^{\left(\frac{R_c}{1-\beta}\right)}\right)(L'+1)}{\overline{\gamma}_{R_j D}}\right)\right), \quad (A.4)$$

and

$$I_3 = Pr\left\{(1+\gamma_{SD})^\beta \left(1 + \frac{1}{(L+1)}\left[\gamma_{SD} + \sum_{m=1}^L \gamma_{R_m D}\right]\right)^{(1-\beta)} < 2^{R_c}\right\}$$

$$= \int_0^{A_1} \frac{1}{\overline{\gamma}_{SD}} exp\left(\frac{-\gamma_{SD}}{\overline{\gamma}_{SD}}\right) d\gamma_{SD}$$

$$\cdot \int_0^{A_2} \cdots \int_0^{A_2} \prod_{m=1}^L \left(\frac{1}{\overline{\gamma}_{R_m D}}\right) exp\left(-\sum_{m=1}^L \frac{\gamma_{R_m D}}{\overline{\gamma}_{R_m D}}\right) \prod_{m=1}^L \gamma_{R_m D}$$

$$= \left(1 - exp\left(\frac{-A_1}{\overline{\gamma}_{SD}}\right)\right) \prod_{m=1}^L \left(\int_0^{A_2} \frac{1}{\overline{\gamma}_{R_m D}} exp\left(\frac{-\gamma_{R_m D}}{\overline{\gamma}_{R_m D}}\right) d\gamma_{R_m D}\right)$$

$$= \left(1 - exp\left(\frac{-A_1}{\overline{\gamma}_{SD}}\right)\right) \prod_{m=1}^L \left(1 - exp\left(\frac{-A_2}{\overline{\gamma}_{R_m D}}\right)\right)$$

$$= \left(1 - exp\left(\frac{(1-2^{R_c})(L+1)}{\overline{\gamma}_{SD}}\right)\right) \prod_{m=1}^L \left(1 - exp\left(\frac{\left(1-2^{\left(\frac{R_c}{1-\beta}\right)}\right)(L+1)}{\overline{\gamma}_{R_m D}}\right)\right), \quad (A.5)$$

Appendix B: Proof of Equations (4.38) and (4.40)

B.1 Proof of Equation (4.38)

From (4.37), the CDF of Z, $P_Z(z)$, is given by

$$P_Z(z) = \frac{2^{n_R}}{z\sqrt{\alpha\overline{\gamma}_{SR}\overline{\gamma}_{RD}}} \sum_{i=0}^{n_R-1} \binom{n_R-1}{i} \frac{(-1)^{n_R-1-i}}{\sqrt{n_R-i}} exp\left(-\left[\frac{(n_R-i)}{\overline{\gamma}_{SR}} + \frac{1}{\alpha\overline{\gamma}_{RD}}\right]\frac{1}{z}\right) K_1\left(\frac{1}{z}\sqrt{\frac{4(n_R-i)}{\alpha\overline{\gamma}_{SR}\overline{\gamma}_{RD}}}\right), (B.1)$$

Taking the derivative of (B.1) with respect to z and using the expression for the derivative of the modified Bessel function, given in [62] as

$$z\frac{d}{dz}K_v(z) + vK_v(z) = -zK_{v-1}(z). \quad (B.2)$$

yields (4.38).

B.2 Proof of Equation (4.40)

From (4.39), the PDF of γ_{SRD} is given by

$$p_{\gamma_{SRD}}(\gamma_{SRD}) = \frac{2\gamma_{SRD}\, n_R}{\sqrt{\alpha\bar{\gamma}_{SR}\bar{\gamma}_{RD}}} \sum_{i=0}^{n_R-1} \binom{n_R-1}{i} \frac{(-1)^{n_R-1-i}}{\sqrt{n_R-i}}$$

$$.\,exp\left(-\left[\frac{(n_R-i)}{\bar{\gamma}_{SR}} + \frac{1}{\alpha\bar{\gamma}_{RD}}\right]\gamma_{SRD}\right)\left\{\left[\frac{(n_R-i)}{\bar{\gamma}_{SR}} + \frac{1}{\alpha\bar{\gamma}_{RD}}\right] K_1\left(\gamma_{SRD}\sqrt{\frac{4(n_R-i)}{\alpha\bar{\gamma}_{SR}\bar{\gamma}_{RD}}}\right)\right.$$

$$\left. + \sqrt{\frac{4(n_R-i)}{\alpha\bar{\gamma}_{SR}\bar{\gamma}_{RD}}} K_0\left(\gamma_{SRD}\sqrt{\frac{4(n_R-i)}{\alpha\bar{\gamma}_{SR}\bar{\gamma}_{RD}}}\right)\right\}. \tag{B.3}$$

The MGF of γ_{SRD}, $\Psi_{\gamma_{SRD}}(-s)$, can be shown as

$$\Psi_{\gamma_{SRD}}(-s) = \int_0^\infty p_{\gamma_{SRD}}(\gamma_{SRD}) exp(-s\gamma_{SRD}) d\gamma_{SRD}$$

$$\Psi_{\gamma_{SRD}}(-s) = \frac{4n_R}{\sqrt{\alpha\bar{\gamma}_{SR}\bar{\gamma}_{RD}}} \sum_{i=0}^{n_R-1} \binom{n_R-1}{i} \frac{(-1)^{n_R-1-i}}{\sqrt{n_R-i}}$$

$$.\left\{\sqrt{\frac{(n_R-i)}{\alpha\bar{\gamma}_{SR}\bar{\gamma}_{RD}}} f_1(s,i) + \frac{1}{2}\left[\frac{(n_R-i)}{\bar{\gamma}_{SR}} + \frac{1}{\alpha\bar{\gamma}_{RD}}\right] f_2(s,i)\right\}, \tag{B.4}$$

where

$$f_1(s,i) = \int_0^\infty \gamma_{SRD}\, exp\left(-\left[\frac{n_R-i}{\bar{\gamma}_{SR}} + \frac{1}{\alpha\bar{\gamma}_{RD}} + s\right]\gamma_{SRD}\right) K_0\left(\gamma_{SRD}\sqrt{\frac{4(n_R-i)}{\alpha\bar{\gamma}_{SR}\bar{\gamma}_{RD}}}\right) d\gamma_{SRD}$$

and

$$f_2(s,i) = \int_0^\infty \gamma_{SRD}\, exp\left(-\left[\frac{n_R-i}{\bar{\gamma}_{SR}} + \frac{1}{\alpha\bar{\gamma}_{RD}} + s\right]\gamma_{SRD}\right) K_1\left(\gamma_{SRD}\sqrt{\frac{4(n_R-i)}{\alpha\bar{\gamma}_{SR}\bar{\gamma}_{RD}}}\right) d\gamma_{SRD}$$

Using [62] we obtain the result in (4.40).

Appendix C: Proof of Equations (5.27) and (5.35)

C.1 Proof of Equation (5.27)

From (5.26), the average pairwise error probability, $P(d)$, is given by

$$
P(d) = \frac{1}{\pi} \int\limits_0^{\frac{(M-1)\pi}{M}} \left(1 + \frac{g_{PSK}}{\sin^2\theta} \left(\frac{R_{C_2} d_2 \alpha \left(\frac{E_{RD}}{N_0} \right)}{1 + \frac{R_{C_2} \left[(1-\alpha) \left(\frac{E_{SD}}{N_0} \right) + \alpha \left(\frac{E_{RD}}{N_0} \right) \right]}{k_p \left(\frac{E_p}{N_0} \right)}} \right) \right)^{-1}
$$

$$
\cdot \left(1 + \frac{g_{PSK}}{\sin^2\theta} \left(\frac{R_{C_1} d_1 \left(\frac{E_{SD}}{N_0} \right)}{\left(1 + \frac{R_{C_1} \left(\frac{E_{SD}}{N_0} \right)}{k_p \left(\frac{E_p}{N_0} \right)} \right)} + \frac{R_{C_2} d_2 (1-\alpha) \left(\frac{E_{SD}}{N_0} \right)}{1 + \frac{R_{C_2} \left[(1-\alpha) \left(\frac{E_{SD}}{N_0} \right) + \alpha \left(\frac{E_{RD}}{N_0} \right) \right]}{k_p \left(\frac{E_p}{N_0} \right)}} \right) \right)^{-1} d\theta. \quad \text{(C.1)}
$$

From (C.1), the average pairwise error probability can be shown as

$$
P(d) = \frac{1}{\pi} \int\limits_0^{\frac{(M-1)\pi}{M}} \left(1 + \frac{A(d)}{\sin^2\theta} \right)^{-1} \left(1 + \frac{B(d)}{\sin^2\theta} \right)^{-1} d\theta
$$

$$
= \frac{1}{\pi} \int\limits_0^{\frac{(M-1)\pi}{M}} \left(\frac{\sin^2\theta}{\sin^2\theta + A(d)} \right) \left(\frac{\sin^2\theta}{\sin^2\theta + B(d)} \right) d\theta
$$

$$
= \frac{1}{\pi} \int\limits_0^{\frac{(M-1)\pi}{M}} \left(1 - \frac{A(d)}{\sin^2\theta + A(d)} \right) \left(1 - \frac{B(d)}{\sin^2\theta + B(d)} \right) d\theta
$$

$$
P(d) = \frac{1}{\pi} \int_0^{\frac{(M-1)\pi}{M}} \left(1 - \frac{A(d)}{\sin^2\theta + A(d)} - \frac{B(d)}{\sin^2\theta + B(d)} + \frac{A(d)B(d)}{(\sin^2\theta + A(d))(\sin^2\theta + B(d))} \right) d\theta, \quad \text{(C.2)}
$$

Applying a partial fraction expansion into the last term of (C.2), the average pairwise error probability, $P(d)$, is given by

$$P(d) = \frac{1}{\pi} \int\limits_{0}^{\frac{(M-1)\pi}{M}} \left(1 - \frac{A(d)}{\left(\sin^2\theta + A(d)\right)} - \frac{B(d)}{\left(\sin^2\theta + B(d)\right)} + \frac{B(d)}{(B(d)-A(d))} \frac{A(d)}{\left(\sin^2\theta + A(d)\right)} \right.$$

$$\left. + \frac{A(d)}{(A(d)-B(d))} \frac{B(d)}{\left(\sin^2\theta + B(d)\right)} \right) d\theta$$

$$= \frac{1}{\pi} \int_{0}^{\frac{(M-1)\pi}{M}} \left(1 + \frac{A(d)}{(B(d)-A(d))} \frac{A(d)}{\left(\sin^2\theta + A(d)\right)} + \frac{B(d)}{(A(d)-B(d))} \frac{B(d)}{\left(\sin^2\theta + B(d)\right)} \right) d\theta. \quad \text{(C.3)}$$

Using [62] we obtain the result in (5.27).

C.2   Proof of Equation (5.35)

From (5.34), the average pairwise error probability is given by

$$P(d) = \left(\frac{1}{\pi} \int\limits_{0}^{\frac{(M-1)\pi}{M}} \left(1 + \frac{C(d)}{\sin^2\theta_1} \right)^{-1} d\theta_1 \right) \left(\frac{1}{\pi} \int\limits_{0}^{\frac{(M-1)\pi}{M}} \left(1 + \frac{D(d)}{\sin^2\theta_2} \right)^{-1} d\theta_2 \right)$$

$$+ \left(1 - \frac{1}{\pi} \int\limits_{0}^{\frac{(M-1)\pi}{M}} \left(1 + \frac{D(d)}{\sin^2\theta_1} \right)^{-1} d\theta_1 \right)$$

$$\cdot \left(\frac{1}{\pi} \int_{0}^{\frac{(M-1)\pi}{M}} \left(1 + \frac{A(d)}{\sin^2\theta_2} \right)^{-1} \left(1 + \frac{B(d)}{\sin^2\theta_2} \right)^{-1} d\theta_2 \right), \quad \text{(C.4)}$$

The average pairwise error probability, P (d), can be written as

$$P(d) = \left(\frac{1}{\pi} \int\limits_{0}^{\frac{(M-1)\pi}{M}} \left(1 - \frac{C(d)}{\sin^2\theta_1 + C(d)} \right) d\theta_1 \right)$$

$$\cdot \left(\frac{1}{\pi} \int\limits_{0}^{\frac{(M-1)\pi}{M}} \left(1 - \frac{D(d)}{\sin^2\theta_2 + D(d)} \right) d\theta_2 \right)$$

$$+\left(1 - \frac{1}{\pi}\int_0^{\frac{(M-1)\pi}{M}}\left(1 - \frac{D(d)}{\sin^2\theta_1 + D(d)}\right)d\theta_1\right)$$

$$\cdot\left(\frac{1}{\pi}\int_0^{\frac{(M-1)\pi}{M}}\left(1 - \frac{A(d)}{\left(\sin^2\theta_2 + A(d)\right)}\right)\left(1 - \frac{B(d)}{\left(\sin^2\theta_2 + B(d)\right)}\right)d\theta_2\right). \quad \text{(C.5)}$$

Applying a partial fraction expansion into the last term of (C.5) and using [62] we obtain the result in (5.35).

Introduction

Whenever size, power, or other constraints preclude the use of multiple-input multiple-output (MIMO) systems, wireless systems cannot benefit from the well-known advantages of space-time coding (STC) methods. Also the complexity (multiple radio-frequency (RF) front ends at both the transmitter and the receiver), channel estimation, and spatial correlation in centralized MIMO systems degrade the performance. In situations like these, the alternative would be to resort to cooperative communications via multiple relay nodes. When these nodes work cooperatively, they form a virtual MIMO system. The destination receives multiple versions of the same message from the source and one or more relays, and combines these to create diversity.

Assistance professor Mohamed Mustafa Mohamed Elfituri is the dean of the College of Electrical and Electronics Technology, Benghazi, Libya since 2011. He received his Ph.D. in Department of Electrical and Computer Engineering, University of Concordia University, Montreal, Canada in May 2009, and his M.Sc. in Department of Electrical and Electronics Engineering, University of Garyounis, Benghazi, Libya in Feb. 1999, and his B.Sc. in Department of Electrical and Electronics Engineering, University of Garyounis, Benghazi, Libya in July 1993. Dr. Mohamed is a lecturer in Department of Electrical and Electronics Engineering, University of Garyounis, Benghazi, Libya from 1999 to 2003; and he has been an assistance professor since 2012. In addition to teaching, Dr. Mohamed worked as RF Designer from 2009 to 2010 at Barrett Broadband Networks Inc., Woodstock, NB, Canada.

ISBN 978-1-940366-40-1

9 781940 366401 >

Price: US $85